INSTITUTO NACIONAL DE PESQUISAS DA AMAZÔNIA - INPA
UNIVERSIDADE DO ESTADO DO AMAZONAS - UEA

CURSO DE PÓS-GRADUAÇÃO EM CLIMA E AMBIENTE

ESTUDO DA ORGANIZAÇÃO DA TURBULÊNCIA NA INTERFACE FLORESTA-ATMOSFERA: ANÁLISES DE DADOS OBSERVACIONAIS E SIMULAÇÃO NUMÉRICA

CLÉO QUARESMA DIAS JÚNIOR

Manaus, Amazonas

Julho, 2015

CLÉO QUARESMA DIAS JÚNIOR

ESTUDO DA ORGANIZAÇÃO DA TURBULÊNCIA NA INTERFACE FLORESTA-ATMOSFERA: ANÁLISES DE DADOS OBSERVACIONAIS E SIMULAÇÃO NUMÉRICA.

DR. EDSON PEREIRA MARQUES FILHO - orientador
DR LEONARDO DEANE DE ABREU SÁ - co-orientador

Tese apresentada ao Instituto Nacional de Pesquisas da Amazônia e Universidade do Estado do Amazonas, como parte dos requisitos para obtenção do título de Doutor em Clima e Ambiente.

Manaus, Amazonas
Julho, 2015

D541 Dias Júnior, Cléo Quaresma
Estudo da organização da turbulência na interface floresta-atmosfera: análises de dados observacionais e simulação numérica / Cléo Quaresma Dias Júnior. --- Manaus: [s.n.], 2015.
107 p. : il.

Tese (Doutorado) --- INPA/UEA, Manaus, 2015.
Orientadores: Edson Pereira Marques Filho.
Coorientador: Leonardo Deane de Abreu Sá.
Área de concentração : Clima e Ambiente.

1. Ventos. 2. Large eddy simulation. 3. Turbulência. I. Título.

CDD 551.518

Sinopse:

Estudaram-se aspectos do arrasto superficial e suas consequências em escoamentos acima de florestas densas, a detecção de estruturas coerentes, a existência de diferentes regimes turbulência noturnos e a simulação do escoamento turbulento através do "Large Eddy Simulation".

Palavras-chave: Floresta Amazônica, Ponto de Inflexão, Perfis de vento, Estruturas Coerentes, LES, Transformada Wavelet.

Manaus, Amazonas

Julho, 2015

Para minha esposa, Mary Barroso Dias, minha princesa Maria Eduarda Barroso Dias e meus queridos pais Cléo Quaresma Dias e Sebastiana do Socorro Almeida.

AGRADECIMENTOS

Ao Dr. Leonardo Deane de Abreu Sá que nestes 10 anos de convivência, além de ter me ensinado valiosos conhecimentos a respeito do "fazer ciência", me mostrou como é ser um cientista e um homem ético, honesto e um servidor público que exerce com extrema probidade sua função.

Ao Dr. Edson Pereira Marques Filho pela paciência nos ensinamentos computacionais, nas orientações, nas motivações científicas. Além do que lhe sou muito grato à logística computacional oferecida para o uso do LES.

Aos professores do CLIAMB, em especial ao Dr. Antônio Manzi, Dra. Rita Valéria e ao Dr. Luiz Candido pela transmissão de valiosos conhecimentos.

Ao Dr. Luiz Candido que sempre se mostrou muito solícito no que se refere ao uso do supercomputador do INPA.

A banca avaliadora que prontamente se dispôs a participar desta defesa.

Ao Instituto Nacional de Pesquisas da Amazônia (INPA) e Universidade do Estado do Amazonas (UEA) através do Programa de Pós-Graduação em Clima e Ambiente (CLIAMB).

A CAPES palas bolsas de doutorado e "Ciência sem Fronteiras" que me permitiram conhecer e interagir com diferentes cientistas de outros países.

Ao Dr. Matthias Mauder pela receptividade quando estive na Alemanha e pela infraestrutura oferecida ao desenvolvimento de parte desta pesquisa.

Ao Projeto LBA pelos dados disponíveis.

A todos os colegas de turma, em especial ao Raoni, Elisa, Paulo Coutinho, Stefan pelo companheirismo durante esses quatro anos.

Aos amigos de residência em Manaus, Francisco, Cledenilson e Claudomiro pelo apoio motivacional.

“Se você encontrar um caminho
sem obstáculos, ele provavelmente
não leva a lugar nenhum.”
(Frank Clark)

RESUMO

Investigou-se a estrutura do escoamento turbulento acima da reserva florestal Rebio-Jarú, localizada no Estado de Rondônia. Para isso, utilizaram-se dados medidos em torre micrometeorológica, coletados durante a estação úmida, em períodos diurnos e noturnos, e também se recorreu à modelagem numérica usando-se Large Eddy Simulation (LES).

Para condições diurnas foram analisados alguns aspectos do perfil vertical do vento médio acima e no interior do dossel florestal. Usou-se satisfatoriamente a função tangente hiperbólica com o objetivo de se obter um ajuste para o perfil vertical do vento acima e no interior do dossel florestal, o qual levou em conta a variabilidade da altura do ponto de inflexão no perfil vertical do vento e o índice de área foliar. Além disso, obteve-se uma relação linear robusta entre a variabilidade da altura do ponto de inflexão e a escala temporal associada à organização das estruturas coerentes existentes imediatamente acima da copa florestal.

Para a camada limite noturna foram analisadas ocorrências de três diferentes regimes turbulentos: regime 1) fraca turbulência e baixa velocidade do vento; regime 2) forte turbulência e alta velocidade do vento e regime 3) eventos turbulentos não estacionários. Notou-se que na camada limite noturna amazônica a maior frequência de ocorrência é do regime 1 (95%), comparada aos regimes 2 e 3 (5% cada). Contudo, para situações do regime 2, observou-se que o fluxo de calor sensível é cerca de 40 vezes maior comparativamente às situações em que o regime 1 é dominante. Além do quê, em situações em que predomina o regime 2, observou-se que a altura do ponto de inflexão, a escala de comprimento de cisalhamento do vento, as escalas temporais das estruturas coerentes e a taxa de dissipação de energia cinética turbulenta foram consideravelmente maiores quando comparados aos respectivos valores obtidos no regime 1, indicando a ocorrência de forte mistura turbulenta na camada limite superficial. Também constatou-se que os episódios classificados como regime 3 foram essencialmente não-estacionários.

Na aplicação do LES foi acrescentada uma força de arrasto no modelo, representativa da floresta amazônica, com o objetivo de se ter simulações o mais próximo da realidade. Seu objetivo foi o de investigar a ocorrência das estruturas coerentes acima da floresta amazônica. Os resultados mostraram que o escoamento turbulento foi sensível à presença do dossel florestal, com um nítido ponto de inflexão no perfil vertical do vento logo acima do dossel. Além disso, os perfis do fluxo de momento e de energia cinética turbulenta foram similares àqueles obtidos com dados experimentais. Na região entre 1h e 4h (onde h corresponde à

altura média do dossel florestal) os valores de várias grandezas aí observadas, tais como pressão, fluxo de momento, skewnesses de componentes de velocidade do vento e vorticidade sugerem que as estruturas coerentes se organizam na forma de rolos, com eixo de simetria perpendicular ao escoamento médio. Os resultados reforçam a importância de se considerar a física do ponto de inflexão no perfil vertical de velocidade do vento nas trocas turbulentas entre floresta e atmosfera.

ABSTRACT

Were investigated the structure of turbulent flow above the Rebio-Jarú forest reserve, located in the state of Rondônia. For this, we used data measured in micrometeorological tower, collected during the wet season, in daytime and nighttime periods, and also performed numerical modeling using Large Eddy Simulation (LES).

For daytime conditions some aspects of the average vertical wind profile above and within the forest canopy were analyzed. It is used the hyperbolic tangent function satisfactorily in order to obtain a functional shape for the vertical wind profile above and inside the canopy, which took into account the variability of the height of the inflection point in the vertical wind profile and the leaf area index, too. Furthermore, we obtained a robust linear relationship between the varying height of the inflection point and the characteristic time scale associated with the coherent organization of existing structures immediately above the forest canopy.For the nocturnal boundary layer situations, three different turbulent regimes were analyzed: regime 1) weak turbulence and low wind speed; regime 2) strong turbulence and high wind speed and regime 3) non-stationary turbulent events. It was noted that in the nocturnal boundary layer the highest frequency of occurrence is related with the first regime (95%), compared to regimes 2 and 3 (5% each). However, for regime-2's situations, it was observed that the sensible heat flux is about 40 times higher compared to situations in which the regime 1 is dominant. Besides, in situations where the regime 2 is predominant, it was observed that the height of the inflection point, the length-scale associated with the wind-shear, the coherent structures' time scale, and the dissipation rate of turbulent kinetic energy were significantly higher when compared to the respective values obtained in the regime 1, indicating the occurrence of strong turbulent mixing in the surface boundary layer in such situations. In addition, it was found that the episodes classified as regime 3 were essentially non-stationary.

In applying LES was added a drag force into the model, representative of the rainforest canopy, in order to obtain simulations closer to reality. Its main goal was to investigate the occurrence of coherent structures above the Amazon rainforest. The results showed that the turbulent flow was sensitive to the presence of the forest canopy, with a well-defined inflection point on the vertical wind profile just above the canopy. Furthermore, the profiles of momentum flux and turbulent kinetic energy were similar to those obtained with experimental data. In the region between 1h and 4h (where h is the average height of the forest canopy) the observed values of several physical variables such as pressure, momentum

fluxes, skewnesses of the wind velocity components, and vorticity are suggesting that coherent structures are organized in form of rolls, with symmetry axis perpendicular to the mean flow. The results reinforce the importance of considering the physical role of the inflection point on the vertical wind speed profile in the turbulent exchanges between forest and atmosphere.

SUMÁRIO

LISTA DE FIGURAS

Capítulo 1

Capítulo 2

Capítulo 3

Capítulo 4

INTRODUÇÃO

Os estudos de escoamentos turbulentos acima de florestas apresenta considerável complexidade quando comparado com aquele da interação entre superfícies "lisas", homogêneas e a atmosfera (Mahrt et al., 1994; Högström e Bergström, 1996; Raupach et al., 1996; Brunet e Irvine, 2000; Kruijt et al., 2000; Mahrt, 2000). Esta complexidade tem estimulado a realização de intensas pesquisas para compreender melhor a dinâmica do escoamento atmosférico acima do dossel florestal e seu grau de acoplamento com o escoamento no interior da cobertura vegetal.

Dentre os principais processos aerodinâmicos presentes acima de florestas pode-se destacar o intenso cisalhamento do vento, que induz o surgimento de um ponto de inflexão no perfil de velocidade do vento (PI), logo acima da altura media da copa (Raupach et al., 1996; Mahrt et al., 2000). O surgimento de um PI é inevitável quando ocorre absorção de momento em um espaço verticalmente estendido, como o que acontece acima de florestas (Finnigan, 2000). Análise de estabilidade linear e não-linear deste PI prevê uma sequência de autovalores instáveis, primeiro em duas e, em seguida, em três dimensões. A instabilidade inicial, linear, é uma onda de Kelvin-Helmholtz, o que pode ser interpretado como regiões de perturbações positivas e negativas na vorticidade, com um comprimento de onda λ que é proporcional à espessura da vorticidade, (Finnigan *et al.*, 2009). A análise não linear mostra que a vorticidade da onda pode evoluir para vórtices de amplitude finita que apresentam eixos de simetria transversais à direção do escoamento médio, com o comprimento de onda original λ (Stewart, 1969).

A existência de um PI gera instabilidades hidrodinâmicas no escoamento turbulento, dificultando sua representação sobre florestas em termos da Teoria da Similaridade de Monin-Obukhov (TSMO) (Brunet e Irvine, 2000). Esta camada turbulenta próxima a superfícies rugosas, conhecida como subcamada rugosa (SR), exige novas interpretações físicas para explicar fenômenos que ai ocorrem, particularmente alguns não lineares (Py et al., 2004; Campanharo *et al.*, 2008; Belusic e Mahrt, 2012). Além disso, na SR, os grandes vórtices turbulentos apresentam uma dinâmica, escala e energia determinadas pela instabilidade do PI (Finnigan, 2000).

Thomas e Foken (2007) procuraram definir uma "altura aerodinâmica do dossel" e consideraram-na como sendo z_x, a altura do ponto de inflexão no perfil do vento médio (API). Para determinar z_x, eles ajustaram os dados dos perfis verticais de vento disponíveis a um polinômio de terceira ordem. Este método, sugerido originalmente por Raupach et al. (1996),

parece razoável e está consistente com a idéia do perfil de vento logarítmico sobre o dossel e exponencial dentro deste, desde que se considere a existência de uma região intermediária, a SR, na qual os perfis de velocidade média do vento apresentam características especiais, muito diferentes daquelas previstas pela TSMO.

Pontos de inflexão no perfil de vento acima da floresta Amazônica, em Rondônia, já foram investigados por diferentes autores (Pachêco, 2001; Sá e Pachêco, 2006; Dias-Júnior *et al*., 2013). Os resultados destes estudos constataram que a altura do ponto de inflexão varia durante o dia e que esta constitui um parâmetro de escala importante na obtenção de relações gerais para o perfil do vento acima e dentro do dossel. Sá e Pachêco (2006) propuseram uma nova relação para o perfil vertical da velocidade do vento acima e no interior da floresta. Eles usaram informações da posição do ponto de inflexão e da velocidade do vento na altura de sua ocorrência, bem como uma escala de comprimento associada ao cisalhamento vertical do vento na altura média da copa florestal. Resultados de Marshall *et al*. (2002), para simulação do escoamento acima de vegetação em túnel de vento, mostraram grande concordância com os resultados de Sá e Pachêco (2006), ainda que eles não tenham levado em conta a possibilidade de variação do API, como estes últimos autores propuseram. Dias-Júnior *et al*. (2013) sugeriram que a variação do API pode trazer como consequência a variação da escala temporal de ocorrência de estruturas coerentes (ECs) no campo térmico, fenômeno extremamente concernente aos fluxos turbulentos de calor sensível (Paw U et al., 1992).

Em relação às ECs, é importante mencionar que vários pesquisadores já mostraram que elas contribuem de forma decisiva para os fluxos turbulentos de calor sensível e de momento (Turner *et al*., 1994; Högström e Bergström, 1996; Thomas e Foken, 2007; Eder et al., 2013). No entanto, poucos estudos abordaram a questões da dinâmica do escoamento nas proximidades do dossel da floresta amazônica, e o impacto delas nos processos de troca em geral. Além disso, na interface floresta-atmosfera algumas características peculiares do escoamento atmosférico podem ser relevantes na formação de tais estruturas, como por exemplo: a instabilidade do ponto de inflexão (Robinson, 1991; Raupach *et al*., 1996; Brunet e Irvine, 2000; Finnigan, 2000), curto-circuito espectral (Cava e Katul, 2008), variabilidade sazonal no índice de área foliar (Doughty *et al*., 2008) com possíveis consequências no arrasto superficial, variabilidade espacial das concentrações de carbono e fluxos de CO_2 ao longo de regiões planas, declives e vales na floresta (Araújo *et al*., 2010).

Para se chegar aos objetivos propostos neste trabalho recorreu-se, além da utilização de dados experimentais, à simulação dos grandes turbilhões (Large Eddy Simulation - LES). É importante mencionar que dentre as muitas vantagens do LES, uma delas é a de permitir

uma melhor compreensão da estrutura da turbulência em alturas não alcançadas pelas torres micrometeorológicas. Além do quê, o LES permite a investigação de características espaciais do escoamento turbulento, o que dificilmente poderia ser realizado apenas com medidas em situ.

As análises dos dados experimentais possibilitaram a melhor compreensão de algumas características do escoamento turbulento, tanto para a camada limite convectiva (CLC) quanto para a camada limite noturna (CLN) amazônicas.

Para a CLC, analisou-se uma escala temporal associada com o API. Observou-se que há uma estreita correlação entre as escalas temporais das ECs e do API. Tal resultado permite a obtenção de novos "insights" sobre a instabilidade do ponto de inflexão, além de proporcionar um melhor entendimento das principais características dos vórtices turbulentos acima de florestas altas. Além disso, usou-se a função tangente hiperbólica para parametrizar o perfil vertical do vento, acima e dentro da floresta, usando-se para tanto alguns parâmetros chaves, tal com o API e o índice de área foliar, como os propostos por Yi (2008).

Para a CLN a complexidade do escoamento turbulento se acentua, uma vez que sob tais situações muitos fenômenos associados à estratificação estável podem tornar o escoamento mais complexo, como é o caso da existência de ondas internas de gravidade (Zeri e Sá, 2011), ventos catabáticos (Princevac *et al.*, 2008), correntes de densidade (Sun *et al.*, 2002), instabilidades de Kelvin-Helmholtz (Zhang *et al.*, 2001), jatos de baixos níveis (Poulos *et al.*, 2002), dentre outros. No caso do escoamento acima de vegetação alta, ainda há o fator complicador associado à existência da SR (Williams *et al.*, 2007).

Outra questão relevante nos estudos da CLN é o da caracterização dos regimes turbulentos noturnos e problemas correlatos (Mahrt, 1998, 1999; Acevedo e Fitzjarrald, 2003; Cava *et al.*, 2004; Van de Wiel *et al.*, 2002a, 2002b, 2003; Acevedo *et al.*, 2009; Sun *et al.*, 2012). Estudos recentes aplicados a sítios experimentais da Amazônia, Uatumã (a nordeste do estado do Amazonas) e da Rebio-Jarú (a nordeste do estado de Rondônia), mostraram diferenças significativas no que concerne: i) à ocorrência de ondas de gravidade, à influência de nuvens nas grandezas escalares do escoamento, à existência de maior ou menor estacionariedade (Zeri *et al.*, 2014) e a existência de diferentes regimes de turbulência noturnos (Cava *et al.*, 2004; Sun *et al.*, 2012); ii) à variabilidade sazonal dos fluxos e concentrações de CO_2 acima da floresta de Uatumã em função do regime de turbulência existente (Mafra, 2014).

Um dos principais objetivos deste trabalho foi investigar aspectos cíclicos da CLN (Van de Wiel *et al.*, 2002a, 2002b, 2003), no que tange a classificação e caracterização de

regimes turbulentos. Contudo, há duas questões importantes abordadas nessa tese: i) a relevância de fenômenos noturnos na atmosfera tropical acima de continente; ii) as características da turbulência acima de uma floresta singular pela sua extensão, povoada por árvores altas como é o caso da floresta amazônica. Nesta condição, em mais de 90 % do tempo os ventos são fracos e o transporte turbulento também é fraco. Contudo, em curtos intervalos de tempo, da ordem de dezenas de minutos, durante os quais aumenta o caráter estacionário das flutuações turbulentas, ocorrem eventos de vento forte com intenso transporte turbulento, o que muda o caráter das trocas turbulentas entre floresta-atmosfera. Pouca atenção tem sido dada aos estudos destes eventos intensos. Os resultados aqui apresentados são contrários a ideia frequentemente difundida de que as noites na floresta tropical são calmas, sem eventos intensos.

As simulações com o LES reproduziram adequadamente várias características observadas no escoamento turbulento na interface vegetação-atmosfera da floresta amazônica e também possibilitaram a melhor compreensão de algumas características da estrutura mecânica da turbulência atmosférica e sua variabilidade horizontal e vertical, tais como: i) altura em que as ECs mecânicas se organizem na forma de "rolos"; ii) variabilidade vertical das fases de "intrusão" e "ejeção"das ECs, do fluxo de momento, das skewness, do coeficiente de correlação, dentre outros.

Esta Tese é composta por quatro manuscritos científicos apresentados como capítulos. Um deles já foi publicado, estando atualmente disponível na versão online. Os outros três artigos foram submetidos, mas ainda estão em processo de revisão. O capítulo 1 refere-se às questões da variabilidade da escala temporal das ECs encontradas nas séries temporais de temperatura acima da Rebio-Jarú e à sua relação com o API. O capítulo 2 está relacionado às questões do arrasto superficial na interface floresta-atmosfera e à possibilidade de obtenção de relação geral para o perfil da velocidade do vento médio acima e dentro da copa florestal, que leva em conta o valor do índice de área de folha e o API. No capítulo 3 analisou-se a estrutura da turbulência atmosférica, baseado na existência de três diferentes regimes turbulentos noturnos acima da floresta amazônica. Tais regimes foram classificados de acordo com metodologia proposto por Sun *et al* (2012), sendo eles: regime 1) turbulência fraca e vento fraco; regime 2) forte turbulência e velocidade do vento alta 3) eventos turbulentos intermitentes. No capítulo 4 usou-se o modelo LES para simular o escoamento turbulento acima da floresta amazônica. Para tanto, foi inserido no modelo uma força de arrasto, representativa de um típico dossel florestal amazônico. Os resultados das simulações

mostraram-se sensíveis a presença do dossel com um nítido ponto de inflexão no perfil vertical do vento.

Elementos Complementares.

Neste tópico irei mencionar algumas etapas importantes vividas por mim, durante o período em que estive cursando o Doutorado em Clima e Ambiente:

- Participei do "São Paulo Spring School on Urban Climate at Tropical Regions", realizado na Universidade de São Paulo (USP), em setembro de 2013. Neste evento apresentei o trabalho "vertical variability of the turbulent flow over rough surfaces", o qual foi escolhido o melhor trabalho apresentado no evento;
- Apresentei o trabalho "A Study of Distinct Turbulence Night-time Regimes above Amazon forest in ATTO-Site" no workshop do ATTO, realizado em abril de 2014 no instituto Max Planck, em Mainz/Alemanha;
- Fiz um estágio sanduíche, pelo Programa Ciência sem Fronteiras, sob supervisão do pesquisador Mathhia Mauder no Karlsruhe Institute of Technology (KIT), Institute of Meteorology and Climate Research Atmospheric Environmental Research (IMK-IFU), Campus Alpin, Garmisch-Partenkirchen/Alemanha, durante os períodos de abril a julho de 2014;
- Também obtive resultados para o sítio experimental do Uatumã que foram publicados no trabalho "Andrea et al. (2015) The Amazon Tall Tower Observatory (ATTO) in the remote Amazon Basin: overview of first results from ecosystem ecology, meteorology, trace gas, and aerosol measurements, Atmos. Chem. Phys. Discuss., 15, 11599-11726, doi:10.5194/acpd-15-11599-2015";
- Apresentei o trabalho "LES Applied to Analyze the Turbulent Flow Organization above Amazon Forest," no GoAmazon2014/15 Science Conference, realizado em maio de 2015, na universidade de Harvard.

OBJETIVO

Investigar, através de dados observacionais e modelagem numérica (LES), a variabilidade vertical da estrutura da turbulência atmosférica na camada limite convectiva e noturna, acima da floresta amazônica, sob diferentes condições de estabilidade atmosférica.

Capítulo 1

Dias-Junior, C.Q. Sá, L.D.A. Pachêco, V.B. de Souza, C.M. 2013. Coherent structures detected in the unstable atmospheric surface layer above the Amazon forest. *Journal of Wind Engineering and Industrial Aerodynamics*, 115:1-8.

Coherent structures detected in the unstable atmospheric surface layer above the Amazon Forest

C.Q. Dias-Junior[a], L.D.A Sá[b], V.B. Pachêco[c], C.M. de Souza[a].

[a] *Instituto Nacional de Pesquisas da Amazônia* (*INPA*) , *Av. André Araújo, nº 2936, Aleixo, Manaus, Amazonas, Brazil*

[b] *Centro Regional da Amazônia (CRA), Instituto Nacional de Pesquisas Espaciais (INPE), Parque de Ciência e Tecnologia do Guamá, Av. Perimetral, nº 2651, Belém, Pará, Brazil,*

[c]*Universidade Federal do Amazonas, Av. General Rodrigo Octávio, nº 6200, Coroado I, Manaus, Amazonas, Brazil.*

Abstract

Some characteristics of the turbulence structure above primary forest localized in the south-western Amazon are analyzed. The data was collected in 60 m height meteorological tower erected in Rebio- Jarú Reserve, Brazil. The Morlet's wavelet is used to detect coherent structures (CS) "ramp" time scales from turbulent virtual temperature data measured above forest, under day-time conditions. It is shown that there is a close relationship between time scale of the coherent structure (TCS) and the height to the inflection point in the mean wind speed profile (IP). A time scale associated with the IP is used to provide useful information on inside canopy penetration flow in order to be compared with the CS time-scale. The results show a very robust correlation between these two time scales (for 144 half - hourly data sets, a correlation coefficient value of 0.9 have been obtained). Such results provide new insights regarding shear instability and turbulent eddy characteristics above tall vegetation, in the surface roughness sub-layer (SRS).

Keywords: Turbulence; Coherent structures; Roughness sub-layer; Wind profile; Shear instability; Time-Scales; Wavelets.

1. Introduction

The first investigations regarding atmospheric flow similarity relationships above forest canopies have pointed out turbulent exchange above and below tall vegetation as scalar diffusivity anomalies (Thom, 1975) and the existence of a roughness transition sub-layer (RTS) associated with turbulent flow above very complex surfaces as forests and the failure

of the familiar Monin-Obukhov Similarity Theory (MOST) which is suitable for smooth and horizontally homogeneous surfaces (Högström and Bergström, 1996; Raupach and Thom, 1981). In the RTS, turbulent exchange processes are strongly influenced by coherent structures generated by shear instability mechanisms associated with the existence of the inflection point in the mean wind profile. Actually strong wind shear in the forest-atmosphere interface creates regions of peculiar coherent "roll" eddies (Gerz et al., 1994; Boldes et al. 2003; Boldes et al., 2007; Raupach et al., 1996; Robinson, 1991) and generates spectral short-circuiting and wake production within the canopy trunk space (Cava and Katul, 2008; Finnigan, 2000). Such features introduce new kind of problems in applying footprint and fetch concepts for measuring meteorological variables (Horst and Weil, 1992; Lee, 2003), and in estimating vertical fluxes (Horst and Weil, 1994; Mahrt, 2010; Sakai et al., 2001).

One important issue associated with the role of Amazonian forest in biosphere-atmosphere exchanges, is the momentum transfer from the atmosphere to the surface. Problems related to the coupling between above canopy flow and below Amazonian forest canopy flow have been discussed by authors as Fitzjarrald et al., (1990), Kruijt et al., (2000), Silva Dias (2002), Viswanadham et al., (1990), among others. Despite much work being developed on this subject, there are few studies relating wind speed profile inflection point occurrence and scalar ramp (CS) characteristics, as time or frequency scales (Raupach et al., 1996; Thomas and Foken, 2005) above tall vegetation. CS are ubiquitous in turbulent flows (Antonia, 1979; Boldes et al., 2007; Gilliam et al., 2000; Jordan et al., 1997; Thomas and Foken, 2007). They are distinct large-scale fluctuation patterns regularly observed in turbulent flows (Wilczak, 1984). Above tall forests CS are linked with inside canopy gust penetration, and present specific frequency or time-scale of occurrence. Two time (or frequency) scales are compared: the time of occurrence of CS based on Gao and Li (1993) procedure of detecting TCS in a T_V (virtual temperature) time-series using wavelet transform, and a time scale related with a gust penetration scale, calculated using inflection point in the mean wind speed profile information, as proposed by Marshall et al. (2002). The gust penetration time scale proposition is based on Robinson (1991) discussion about the consequences of the existence of an inflection point in the wind speed profile above tall vegetation which is capable to generate slow-dissipation rolls-like CS, which are ranged transversally to the mean stream flow. According to Raupach et al. (1996), and their "mixing layer analogy", such CS are related to the creation of an oscillation mode and vorticity generation at the interface

between above and inside canopy flows. It is just this kind of oscillation which is to be detected. To this end analyses are carried out using the proposed time scale.

2. Experimental and methods

2.1. Site and data

The biological forest reserve of Jarú is a 268,000 hectares located in south-western Amazon, (Andreae et al., 2002). It is an area of typical tropical rain forest, between $10^0$05'S and $10^0$19'S and between $61^0$35'W and $61^0$57'W, at approximately 145 m above sea level height. A 60 m height micrometeorological tower with the following coordinates $10^0$4'42.36'' S; $61^0$56'1.62'' W (Zeri and Sá, 2010) was built in the Rebio-Jarú Reserve (Fig. 1), which presents homogeneous fetch conditions from north-west to south-east sides of the tower (in a clockwise sense). At the remaining directions, around 1km homogeneous fetch conditions hold (Sá and Pachêco, 2006). River Machado is approximately 800m at southern side. Culf et al. (1996) present geographical and climatological information concerning this experimental site in which a 60m height meteorological tower has been erected. As mentioned by von Randow et al. (2002), at the top of the tower, a vertical beam was placed in which a 3-D sonic anemometer (CSAT3, Campbell Scientific Inc.), whose specifications are described in the document http://s.campbellsci.com/documents/us/manuals/csat3.pdf (Appendix C), was installed at the height of 67 m above the forest floor, at a sampling rate of 16 Hz. The sonic anemometer has measured the three wind components (u,v,w) and the sonic virtual air temperature (T_v), and it is shown in Fig. 3. According to Andreae et al. (2002) forest canopy height ranges from 30 m to 35 m. Wright et al. (1996) reported a 4.6 value for leaf area index and McWilliam et al. (1996) also present information concerning the tree species found in the Rebio-Jarú Reserve.

The Rebio-Jarú Reserve is one of the several sites in which the Large Scale Biosphere-Atmosphere Experiment in Amazonia (LBA) was carried out (Silva Dias et al., 2002). In the present study 144 fast response virtual temperature half-hourly data sets sampled at 16 Hz have been used, and low response wind profile data sampled at 0.1 Hz, corresponding to day-time periods of the 1999 Julian days 41, 42, 43, 45, 46, 50. As a part of the Rebio-Jarú Reserve scientific activities energy budget components, wind velocity, temperature, humidity data was measured at several heights on a micrometeorological tower. To investigate the relationship between TCS and the IP, data provided by nine cup anemometers (Low Power A100L2, Vector Instruments Inc.) ranged in previously defined heights to give accurate resolution information regarding the inflection point in the mean wind speed profile have been

used, as shown in Fig. 2. Thus, 1 hour averaged wind speed values, which have been measured at heights of 55.00 m, 50.55 m, 47.70 m, 42.90 m, 40.25 m, 37.80 m, 32.8 m, 26.65 m, and 14.30 m above the ground, are available for calculations.

Virtual temperature time series has been obtained with sonic anemometer-thermometer measurements. As the speed of sound varies with temperature and humidity, but is approximately stable with pressure change, sonic anemometers are also used as thermometers. Their basic principle is based upon the measurement of the traveling time of an ultrasound pulse between two transducers. As is presented in the Manufacturer's Manual (CSAT3 Three Dimensional Sonic Anemometer – Instruction Manual, Campbell Scientific, Inc., 1998-2012, Appendix C), (http://s.campbellsci.com/documents/us/manuals/csat3.pdf), the sonic virtual temperature, in degrees Celsius, is given by: $T_s = (c^2 / \gamma_d R_d) - 273.15$, where $\gamma_d = 1.4$ is the ratio of specific heat of dry air at constant pressure to that at constant volume; $R_d = 287.04\ J\ K^{-1}\ kg^{-1}$ is the gas constant for dry air; c is the sound velocity provided by the sonic anemometer. It is important to remember that the effect of humidity on the speed of sound has been included in the sonic virtual temperature T_v, $T_v = T_s + 273.15 = T(1 + 0.61q)$, where T is the air temperature and q is the air specific humidity.

Fig.1: Meteorological tower erected at Rebio-Jarú forest reserve.

Fig.2: Fast response instruments in the meteorological tower at Rebio-Jarú.

Fig. 3: Cup anemometers ranged at different heights in the meteorological tower at Rebio-Jarú

2.2. Meteorological conditions

Several environmental data of the Rebio-Jarú reserve in 1999, during the experimental field campaign (from February 10th to March 08th 1999), are presented by Pachêco (2001) and Table 1 presents some meteorological information such as maximum and minimum values of the atmospheric pressure (to 30 m height), wind speed (to 55.00 m height) and air temperature (to 54.90 m height) measured at the meteorological tower, during the experimental field campaign.

Julian days	Atmosp. pressure (mb) maximum	Atmosp. pressure (mb) minimum	Air temp.(ºC) maximum	Air temp.(ºC) minimum	Wind speed (ms^{-1}) maximum	Wind speed (ms^{-1}) minimum
41	994.8	988.2	30.8	23.2	2.80	0.83
42	994.5	988.0	30.5	24.4	2.95	0.62
43	994.5	987.9	33.2	23.3	2.91	0.61
44	993.8	987.8	32.2	24.3	3.60	1.15
45	995.0	987.7	32.5	23.6	3.72	0.88
46	995.3	988.3	30.6	23.4	3.75	0.96
47	995.0	988.2	30.4	23.9	2.65	0.51
48	994.2	987.8	30.5	24.2	3.14	0.87
49	995.5	989.5	29.4	22.7	3.02	0.82
50	994.5	989.5	30.7	23.6	4.31	0.58
51	994.3	989.0	29.1	23.1	3.55	0.79
55	995.0	990.1	26.4	22.5	3.16	0.65
56	993.6	987.0	29.2	23.1	3.61	0.88
57	994.7	987.5	28.6	23.1	4.36	0.96
58	993.5	987.6	28.3	23.2	2.81	0.69
59	992.4	986.2	28.7	23.8	3.72	0.51
60	990.8	985.0	30.1	23.4	3.83	1.57
61	992.4	987.8	28.5	22.4	3.54	0.64
62	993.5	989.2	30.3	23.7	3.62	0.71
63	993.4	986.0	30.6	22.8	4.37	0.64
64	993.2	986.8	29.4	23.7	4.76	0.64
65	991.8	985.9	29.7	22.9	3.18	0.57
66	990.1	984.5	30.2	23.0	3.25	0.58
67	991.1	985.9	28.3	24.2	3.01	0.91

Table I: Rebio-Jarú meteorological data obtained the 1999 experiment field campaign.

In the Fig. 4.a and 4.b is shown the mean wind direction. The first associated with the day-time, at times when the convective activity generated by surface-heat is greater; there is a clear predominance of northern winds. The second corresponds to the night-time and early morning, there are two preferential directions for the wind: one continues to be of the north, but the other corresponds to the opposite direction. It is possible that the prevalence of southern winds in some periods is associated with the situation in which the wind speed is weak such way to predominate effects linked to local experimental site topography. Effectively, to the southeast of the tower, there were small hills tens of meters high and it is possible that they induce the katabatic wind formation in the northern region. Moreover, the Fig. 5 shows precipitation data, in mm, for each day of the experiment.

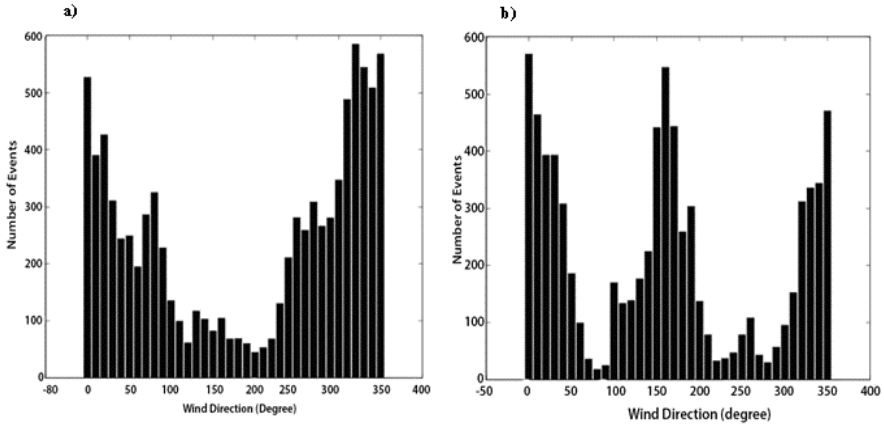

Fig. 4: Histogram of frequency of wind direction for observations of the intervals: (a) from 11:00 to 16:00 local-time and (b) from 20:00 up to 9:00 local-time.

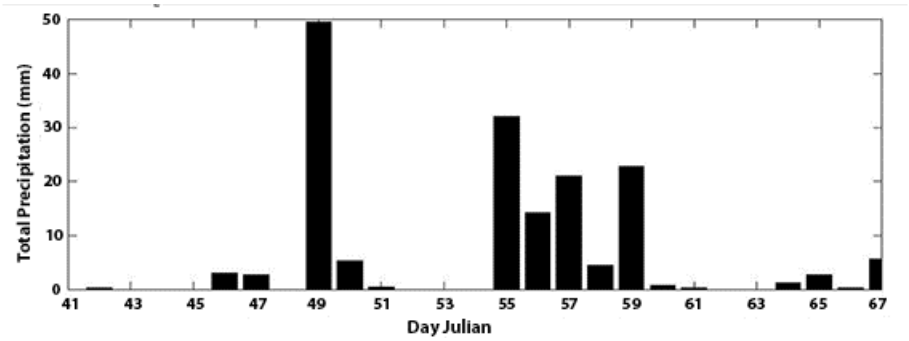

Fig. 5: Total precipitation for Julian days: 41 to 51 and 55-67.

2.3. Data quality control

Before performing the statistical calculations with Rebio-Jarú reserve data, they have been submitted to quality control tests. In a first step of this procedure, a visual inspection of all available meteorological time-series has been performed. In situations in which this procedure did not reveal itself sufficient, a data quality control based on Vickers and Mahrt (1997) has been used. These authors have compiled several methods to assess the quality of turbulent data, proposed by several authors and applied to data obtained at well-known micrometeorological field campaigns such as RASEX, Microfronts95 and BOREAS with satisfactory results.

2.4. Methods

Two kinds of meteorological information have been used in order to compare time scale characteristics of the “ramp” coherent structures and the inflection point in the mean wind speed profile:

i) Vertical mean profiles of the wind speed obtained from cup anemometer data. Based on these profiles, third degree polynomial function fittings have been performed to determine the inflection point height for each data run.

ii) Time series of virtual temperature to detect, the time-scale of coherent structures by means of wavelet transform application as proposed by Gao and Li (1993) and explained as follows.

To detect CS on a virtual temperature time series, sampled at 16 Hz rate, a continuous one-dimensional wavelet transform (Eq.1) has been used, which is defined when applied to a given signal $f(t)$ as:

$$W_{\psi}\, f\,(\mathrm{a},\mathrm{b}) = \frac{1}{\sqrt{\mathrm{a}}} \int_{-\infty}^{+\infty} f\,(\mathrm{t})\, \psi\left(\frac{\mathrm{t}-\mathrm{b}}{\mathrm{a}}\right) dt \qquad (1)$$

Where $a \in \mathcal{R}^{+}$ and $b \in \mathcal{R}$.

The wavelet is a mathematical function which has some special properties (Farge, 1992): i) Admissibility: The analyzing function has to have its average equal to zero; ii) Similarity: The scale decomposition is carried out by translation and dilatation of one only "mother wavelet", is stretched or compressed and displaced along the time to generate a family of "daughter wavelets", which are expressed as function of two parameters: one for the scales (a), and other for the time position (b). With the set of daughter wavelets, a time series can be decomposed at different scales, and thus, it is possible to calculate by-scale statistical relevant information (Furon et al., 2008).

Is used the Morlet's complex function (Eq. 2) which is suitable for coherent structure time scale analysis, as deeply discussed by Thomas and Foken (2005).

$$\psi\,(\eta) = \pi^{-\frac{1}{4}}\, e^{i\,\omega_0\,\eta}\, e^{-\eta^2/2} \qquad (2)$$

where η is the dimensionless parameter of time and ω_0 is the dimensionless frequency. Other types of wavelet functions and their characteristics can be found at Torrence and Compo (1997).

According with Gao and Li (1993), the scale of occurrence of CS in scalar data, such as virtual temperature time-series, may be determined using the scale variance of wavelet coefficients of the available data (Eq. 3). The TCS corresponds to the one in which the wavelet coefficient variances reach its maximum value.

$$\sigma(a,b) = \int \left| T_{\psi} f(a,b) \right|^2 db \tag{3}$$

where $T_{\psi} f(a,b)$ is the Morlet's Wavelet Transform.

As shown in Fig. 6, for a day-time half-hourly data set of Rebio-Jarú reserve (10 February 1999, 09:00 h – 09:30 h, local time), the largest variance corresponds to the time scale of about 78 s. Thus, this value is considered as the TCS for virtual temperature "like-ramp" structures above forest canopy.

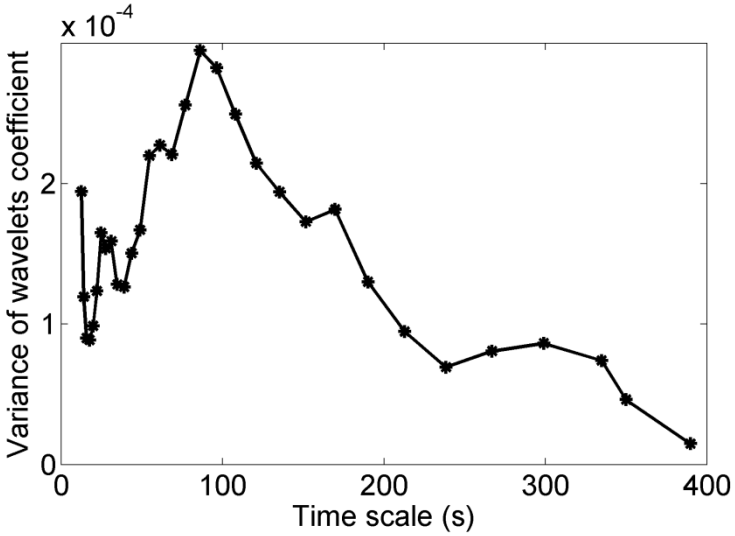

Fig. 6: Scale variance of the wavelets coefficients as a function of the time scale, for virtual temperature time series obtained from 09:00 h - 09:30 h, local time, 10 February , 1999.

To investigate the mechanical turbulent processes observed near the inflection point in the mean wind speed profile, which are dominated by peculiar like-roll coherent structures (Robinson, 1991), is proposed an IP time scale (t_i), based on the vertical wind shear observed in this region, which is defined as:

$$t_i = \left(z_f - z_i\right) \Big/ \left(u_f - u_i\right) \tag{4}$$

Where z_f is the fixed height (67 m) in which the fast response turbulent data has been recorded, z_i is the inflection point height (which changes along the day), and u_f and, u_i are the 30 min wind speed mean values measured at z_f and zi, respectively. Thus, it is a logical assumption to suppose that t_i value contains information concerning the inside canopy penetration capability of a like-roll vortex, or in other words, that it contains some information regarding the rate at which this vortex will be dissipated by the forest canopy.

To investigate wind mean profile characteristics and to calculate the inflection point height in the mean wind speed profile, a third degree polynomial function least square numerical best fit has been done. Once obtained the best fitted function, it was possible to calculate the inflection point height (z_i) as shown in the Fig. 7 (for this data set, a value of 38.36 m for the inflection point height has been found).

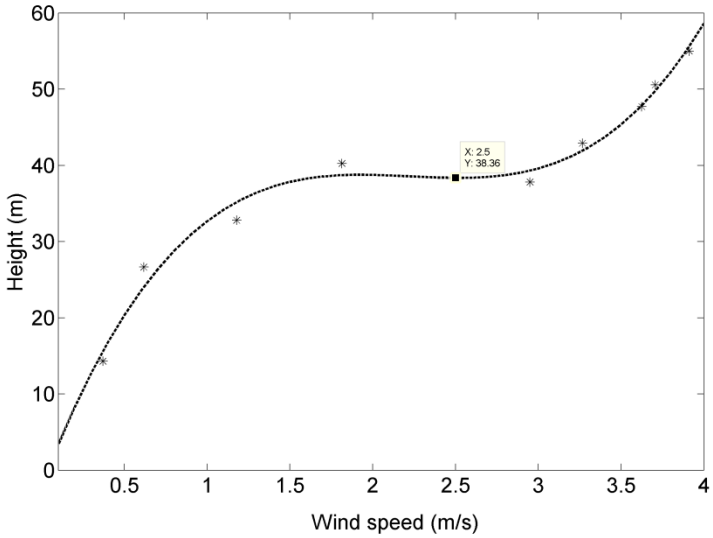

Fig. 7: Third degree polynomial best fitting for the vertical wind speed profile (low response wind speed data measured from 15:30 h -16:00 h, on 19 February, 1999.

Pachêco (2001) calculated the profile of vertical of the dimensionless wind velocity for three different conditions: clear sky, partially covered with sky cloud and overcast. His adjustments polynomials of vertical profiles of wind velocity do not seem to have been influenced by the sky coverage. In the Fig. 8 has been shown a dimensionless vertical wind profile graph provided by Pachêco (2001) for conditions of partially covered sky, situation frequently found in the Amazon. Yet, according to Pacheco (2001), the change of cloud coverage does not generate significant changes in the wind velocity vertical profile.

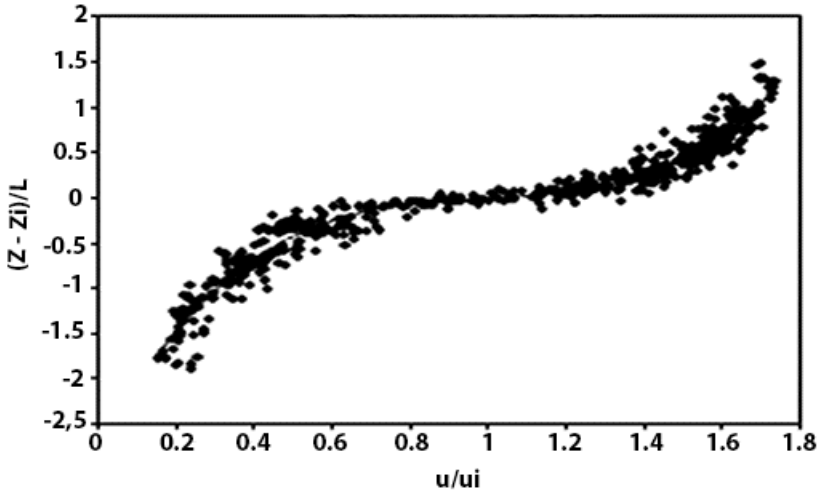

Fig. 8: Vertical profile of dimensionless wind velocity for a partially overcast sky.

3. Results

To emphasize the similar shapes of the curves representing the along day-time variation of the inflection point height, z_i, and of the TCS, Fig. 9 and Fig. 10 are presented, for data collected at the Rebio-Jarú forest reserve. It clearly shows that z_i and TCS ranges from along the day. After 7:00 h there is a decrease tendency in z_i values from around 41 m to 38 m, which remains almost constant between 11:00 h and 13:30 h. After this time, z_i displays a slower but clear increase tendency up to 18:00 h, when it stabilizes around a 41 m height. On the other hand, the TCS value has a slow decrease during the morning: from approximately 75 s at 06:00 h to 50 s at noon. After 13:00 h it depicts a slow increase during afternoon and reaches a value of 75 s at 18:00 h. Regarding the data gathered above the forest, in spite of some uncertainty in the data (concerning z_i and TCS calculations) it is observed a close relationship between the TCS and the height of the inflection point in the mean wind speed profile above forest, z_i.

The suggested assumption is that TCS variation is associated with a “roll-like” vertical displacement in its location above the forest canopy. As reported by Raupach et al. (1996) and Robinson (1991), such eddies, ranged transversally to the wind direction, dissipated kinetic energy in a slower way (time scales of about 60 s) when compared to the turbulent eddies generated above “smooth” surfaces (time scales of about 30 s), ranged along the wind direction. The minimum TCS value corresponds to the minimum inflection-point height and this should be associated to a more effective kinetic energy dissipation when the roll-like eddy approximates of the top canopy region, with its roughness elements acting as wake generators, increasing wind-shear effects and thus, the decreasing the TCS.

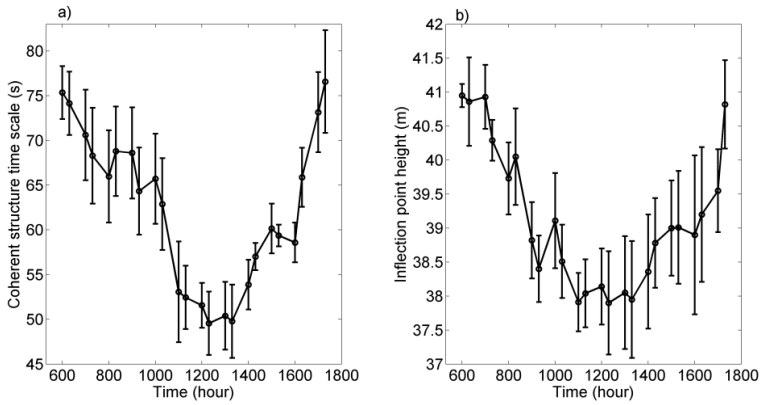

Fig. 9: Evolution of the coherent structures time-scale hourly-mean values (a) and the vertical wind profile inflection point height (b), along with their standard deviations, obtained above Rebio-Jarú forest reserve, for 144 available half-hourly data sets.

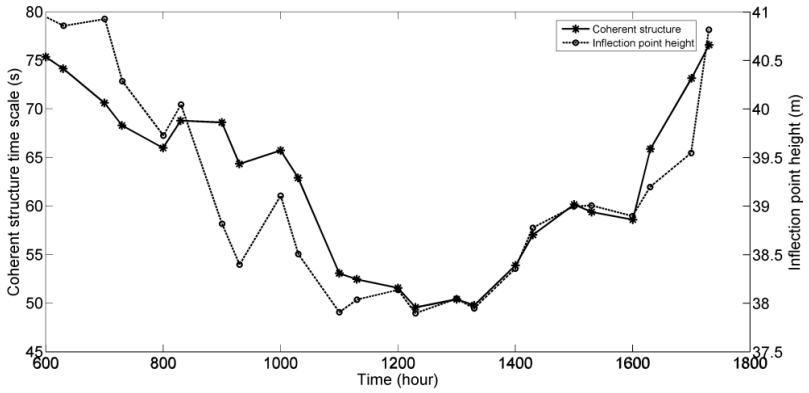

Fig. 10: Comparison of the evolution of the inflection point height and the coherent structures time-scale above Rebio-Jarú forest reserve.

To search more quantitative information concerning the above relationship, a numerical linear fit of the IP height value, z_i, against the TCS has been done, as shown in Fig. 11.

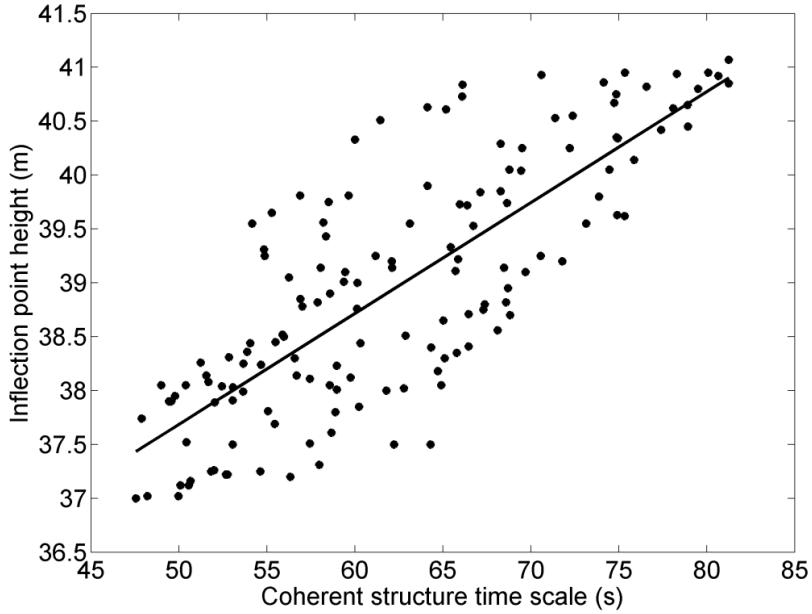

Fig. 11: Comparison between the inflection point height and the coherent structure time-scale for 144 run data for day-time conditions.

Despite the narrow z_i band variation (37 m to 42 m), the linear regression between TCS and z_i presented reasonable least square fit, with a correlation coefficient next to a 0.8 value, for 144 half-hourly data sets. This result reinforce the assumption concerning the existence of a close relationship between two distinct turbulent parameters: a mechanical variable, z_i, associated with the mean wind speed vertical profile and a thermodynamic variable, TCS, associated with virtual temperature coherent structures, whose time scale is detectable by wavelet analysis.

To perform a comparison between inflection point into canopy penetration characteristics and TCS on basis of a same physical fundamental dimension, information provided by an IP time scale is used and expressed in Eq. 4, based on the assumption that it contains physical information about the capability of penetration into canopy of a roll-like vortex. A linear fit regression comparing the two investigated time scales is presented in Fig. 12.

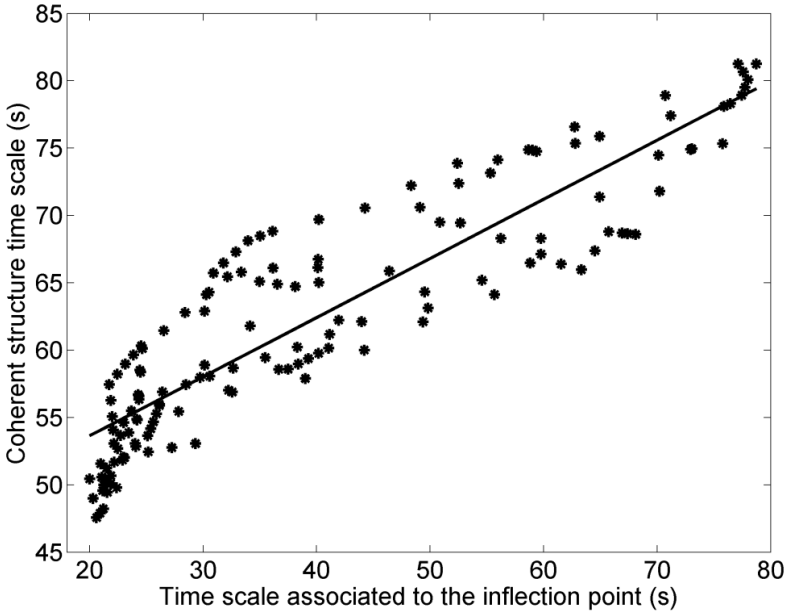

Fig. 12: Comparison of two time-scales: coherent structure time scale (y-axis) and inflection point time-scale (x-axis) for 144 half-hourly data sets.

The results seem to agree with Raupach et al. (1996) findings, in which they argue that active turbulence and coherent motions near the top of a vegetation canopy are patterned on a plane mixing layer as a consequence of instabilities associated with the existence of an "inflection point in the mean wind speed profile". As uttered by Raupach et al. (1996), such "mixing-layer turbulence" analogy formed around an IP would be associated with the existence of two co-flowing streams of distinct velocities, which differ in many ways from classical atmospheric surface layer turbulent structure observed above gentle surfaces. Regarding IP day-time variability assumption, the results corroborate Marshall et al. (2002) findings concerning the choice of new appropriate turbulent scales for obtaining general relationships for near tall vegetation atmospheric flow. The best linear fit comparison of these two time scales (IP and CS) shown in the Fig. 12, has provided a correlation coefficient remarkably good, (approximately *0.9* correlation coefficient for *144* half-hourly data sets) for day-time period. Coherent structure patterns near forest canopy are related to at least two phenomena: vertical wind shear stress near the top of canopy and scalar vertical gradient (Paw U et al., 1992; Warhaft, 2000). Thus, mechanical processes such as role–like vortex might influence near forest canopy ramp-like structures associated with virtual temperature time series. Therefore, the dependence between the frequency of CS and the IP height and even the IP time scales should be explained by this kind of relationship.

In effect, Bolzan and Vieira (2006) have studied some characteristics of atmospheric turbulence on the same experimental site studied by us. They have used an approach of Katul et al. (1995) based on the correlation coefficient calculation among different scales of the turbulent flow and also based on the "cross wavelet power" (CWP) analysis.

Their study focused on interactions among turbulent time series of vertical wind velocity, w, and temperature, *T*, suggested that scale correlations for the *w* data increase considerably when thermal coherent structures are present. These are distinctly shaped "like-ramps "corresponding to time intervals between approximately *1.7* and *3.7* min, which could be related to vertical thermal gradients in the atmosphere. They would promote an increase in the interaction between these variables, *w* and *T*, and also depend on the atmospheric stability conditions.

They also found a characteristic scale for relations among scales, which is probably associated with processes of coalescence of vortices in ABL, as discussed by McNaughton (2004), and the movements in the larger scales of the atmospheric unstable flow show much less coherence for wind field, compared to the thermal field (Belušić and Mahrt, 2012), what reinforces the assumption of Bolzan and Vieira (2006) regarding the probable influence of thermal factors in explaining their results. These authors show that it is clearly observed an increase of correlation among w scales for a scale located around 34s, for both daytime and the nighttime conditions.

It should be emphasized that the results of Bolzan and Vieira (2006) are not necessarily in opposition to the results of this investigation (in which variations were found in the range of occurrence of coherent structures detected in time series of *T*), since the methodology used to detect coherent structures is different from that used by Katul et al. (1995), which is based on correlation among scales.

A good explanation to support this assertion is based on the assumption Belušić and Mahrt (2012), according to which the structure of the turbulent processes in the atmospheric surface boundary layer (ASL) is such that, even when occurring physical processes that act to change the turbulent structure turbulence with time, the relations among scales, surprisingly, appears to remain the same, which led Belušić and Mahrt (2012) to raise the issue according with which "the geometry can be more universal than physics" in atmospheric turbulent processes close to the surface.

That is, the timescale of occurrence of coherent structure above the canopy can change throughout the day, as also changes the height of the inflection point of the profile of average

wind speed. However, the ratios of occurrences between different eddies, should not change significantly.

Campanharo et al. (2008) when using high resolution temperature time series of the in Rebio-Jarú site in Amazon, have obtained very interesting conclusions regarding the chaotic nature of the flow above the forest canopy, with relatively low correlation dimension ($D2 = 3.50 \pm 0.05$) and with the largest Lyapunov exponent $\lambda 1 = 0.050 \pm 0.002$.

These properties, according to them, are related, not to the existence of atmospheric turbulence per se, but the occurrence of coherent structures within the atmospheric surface layer, just above the forest canopy. These would make the atmospheric turbulent flow considerably more "deterministic", despite its expected complexity in the forest-atmosphere interface, as highlighted by Belušić and Mahrt (2012).

They attributed this increasing of "order" in the flow, at least in part, to the occurrence of the inflection point instability of the flow near the top of forest canopy (Raupach et al. 1996).

Chian et al. (2008) have also analyzed the turbulent data measured above the Rebio Jarú site and applying two different nonlinear techniques (kurtosis and phase coherence index) showed that there is a clear increase of the scalar-velocity similarity for the turbulence within the forest canopy when compared to the turbulence above the forest canopy.

They have suggested that the intermittency of turbulence existing within and above the forest canopy of the Amazon rainforest is generated by phase coherence due to nonlinear wave-wave interactions.

These results are obtained for Rebio-Jarú forest reserve. More investigation have to be performed in order to improve our knowledge about mixed-layer analogy processes and also obtain more general information corresponding leading scales on the RTS above tall vegetation canopies.

4. Conclusion

Turbulent coherent structures in the atmospheric flow above Rebio-Jarú forest reserve have been studied. Wind speed slow response data is used to detect inflection point height in vertical wind profile and also an inherent time-scale related to mechanical vortex in the interface forest-atmosphere (and its capability to penetrate into the forest canopy). Fast response virtual temperature time series is used in order to detect ramp-like structures and its associated time-scale using wavelet transform. It is shown that there are statistically robust relationships between the inflection point height in the mean wind speed profile and TCS

associated with virtual temperature time series, which both change along the day with minimum values next to noon time. It has been proposed also a time scale associated with vertical wind shear (TWS) above the inflection point height and its displacement into the forest canopy. These two time scales, TCS and TWS, displayed a very well good correlation. These results are important in order to improve the understanding regarding the roughness transition sub-layer and have implication to amend the parameterization of the exchange processes.

Acknowledgements

The authors would like to thank all people which directly or indirectly contributed to the fulfillment of the 1999 LBA – Intensive wet Campaign, and the support of the university in Ji-Paraná (UNIR), Instituto Brasileiro do Meio Ambiente e dos Recursos Naturais Renováveis (IBAMA) and Instituto Nacional de Colonização e Reforma Agrária (INCRA). This work was done under the LBA project framework, sponsered by the European Union, NASA, and Brazilian Agencies as the Conselho Nacional de Pesquisa e Desenvolvimento Tecnológico (CNPq) and the Fundação de Amparo à Pesquisa do Estado de São Paulo (FAPESP, process 01/06908-7). Leonardo Sá is particularly grateful to CNPq for his research grant (process 303.728/2010-8). We thank Augusto Cesar Oliveira Freire for help with the language

References

Andreae, M.O., Artaxo, P., Brandão, C., Carswell, F.E., Ciccioli, P., Costa, A.L., Culf, A.D., Esteves, J.L., Gash, J.H.C., Grace, J., Kabat, P., Lelieveld, J., Malhi, Y., Manzi, A.O., Meixner, F.X., Nobre, A.D., Nobre, C., Ruivo, M.L.P., Silva Dias, M.A., Stefani, P., Valentini, R., von Jouanne, J., Waterloo, M.J., 2002. Biogeochemical cycling of carbon, water, energy, trace gases, and aerosols in Amazonia: The LBA-EUSTACH experiments. J. Geophys. Res. 33, 1-25.

Antonia, R.A., Chambers, A.J., Phong-Anant, D., Rajagopalan, S., 1979. Properties of spatial temperature derivatives in the atmospheric surface layer. Boundary-Layer Meteorol. 1, 101-118.

Belušić, D., Mahrt, L., 2012. Is geometry more universal than physics in the atmospheric boundary layer flow? J. Geophys. Res. 117, Doi: 10.1029/2011JD016987.

Boldes, U., Scarabino, A., Di Leo, J. M., Colman, J., Gravenhorst, G. 2003. Characteristics of some organized structures in the turbulent wind above and within a spruce forest from field measurements. J. Wind Eng. Ind. Aerodyn. 91, 1253-1269.

Boldes, U., Scarabino, A., Colman, J. 2007. About the three-dimensional behavior of the flow within a forest under unstable conditions. J. Wind Eng. Ind. Aerodyn. 95, 91-112.

Bolzan, M.J.A., Vieira, P.C., 2006. Wavelet analysis of the wind velocity and temperature variability in the Amazon forest. Braz. J. Physics, 36, 1217-1222.

Campanharo, A.S.L.O., Ramos, F.M., Macau, E.E.N., Rosa, R.R., Bolzan, M.J.A., Sá, L.D.A., 2008. Searching chaos and coherent structures in the atmospheric turbulence above amazon forest. Phil. Trans. R. Soc. A, 366, 579-589.

Cava, D., Katul, G.G., 2008. Spectral short-circuiting and wake production within the canopy trunc space of an alpine hardwood forest. Boundary-Layer Meteorol. 126, 415-431.

Chian, A.C.-L., Miranda, R.A., Koga, D., Bolzan, M.J.A., Ramos, F.M., Rempel, E.L., 2008. Analysis of phase coherence in fully developed atmospheric turbulence: Amazon forest canopy. Nonlin. Processes Geophys. 15, 567-573.

Culf, A.D., Esteves, J.L., Marques Filho, A.O., Rocha, H.R., 1996, Radiation, temperature and humidity over forest and pasture in Amazonia, In: Gash, J.H.C., Nobre, C.A., Roberts, J.M., Victoria, R.L. (Eds), Amazonian Deforestation and Climate. John Wiley, Chichester, pp. 175-191.

Farge, M., 1992. The wavelet transform and its applications to turbulence. Annu. Rev. Fluid Mech. 24, 395-457.

Finnigan, J.J., 2000. Turbulence in plant canopies. Annu. Rev. Fluid Mech. 32, 519-571.

Fitzjarrald, D.R., Moore, K.E., Cabral, O.M.R., Scolar, J., Manzi, A.O., Sá, L.D.A., 1990. Daytime turbulent exchange between the Amazon forest and the atmosphere. J. Geophys. Res. 10, 16825-16838.

Furon, A.C., Wagner-Riddle, C., Smith, C.R., Warland, J.S., 2008. Wavelet analysis of wintertime and spring thaw CO_2 and N_2O fluxes from agricultural fields. Agr. Forest Meteorol. 148, 1305-1317.

Gao, W., Li, B.L., 1993., Wavelet analysis of coherent structures at the atmosphere-forest interface. J. Appl. Meteorol. 32, 1717-1725.

Gerz, T., Howell, J., Mahrt, L., 1994. Vortex structures and microfronts. Phys. Fluids, 3, 1242-151.

Gilliam, X., Dunyak, J., Doggett, A. Smith, D. 2000. Coherent structure detection using wavelet analysis in long time-series. J. Wind Eng. Ind. Aerod. 88, 183-195.

Högström, U., Bergström, H., 1996. Organized turbulence in the near-neutral atmospheric surface layer. J. Atmos. Sci. 17, 2452-2464.

Horst, T.W., Weil, J.C., 1992. Footprint estimation for scalar flux measurements in the atmospheric surface layer. Boundary-Layer Meteorol. 59, 279-292.

Horst, T.W., Weil, J.C., 1994. How far is far enough? The fetch requirements for micrometeorological measurement of surface fluxes. J. Atmos. Ocean. Tech. 11, 1018-1025.

Jordan, D.A., Hajj, M.R., Tieleman, H.W. 1997. Characterization of turbulence scales in the atmospheric surface layer with the continuous wavelet transform. J. Wind Eng. Ind. Aerod. 69-71, 709-716.

Katul, G.G., Parlange, M.B., Albertson, J.D., Chu, C.R., 1995. Local Isotropy and Anisotropy in the Sheared and Heated Atmospheric Surface Layer. Boundary-Layer Meteorol. 72, 123-148.

Kruijt, B., Malhi, Y., Lloyd, J., Nobre, A.D., Miranda, A.C., Pereira, M.G.P., Culf, A., Grace, J., 2000. Turbulence statistics above and within two Amazon rain forest canopies. Boundary-Layer Meteorol. 2, 297-331.

Lee, X., 2003. Fetch and footprint of turbulent fluxes over vegetative stands with elevated sources. Boundary-Layer Meteorol. 107, 561-579.

Mahrt, L., 2010. Computing turbulent fluxes near the surface: Needed improvements. Agr. Forest Meteorol. 150, 501-509.

Marshall, B.J., Wood, C.J., Gardiner, B.A., Belcher, B.E., 2002. Conditional sampling of forest canopy gusts. Boundary-Layer Meteorol. 102, 225-251.

McNaughton, K.G., 2004. Turbulence structure of the unstable atmospheric surface layer and transition to the outer layer. Boundary-Layer Meteorol. 112, 199-221.

McWilliam, A.L.C., Cabral, O.M.R., Gomes, B.M., Esteves, J.L., Roberts, J., 1996. Forest and pasture leaf-gas exchange in south-east Amazonia. In: Gash J.H.C., Nobre C.A., Roberts J.M., Victoria R.L. (Eds.), Amazonia Deforestation and Climate. John Wiley, Chichester, pp. 175-191.

Pachêco, V.B., 2001. Algumas Características do Acoplamento Entre o Escoamento Acima e Dentro da Floresta Amazônica'. M.Sc Thesis, National Institute of Space Research, São José dos Campos, Brazil, 98 pp. (in Portuguese).

Paw U, K.T., Brunet, Y., Collineau, S., Shaw, R.H., Maitani, T., Qiu, J., Hipps, L., 1992. On coherent structures in turbulence above and within agricultural plant canopies. Agr. Forest Meteorol. 61, 55-68.

Raupach M.R., Thom A.S. 1981. Turbulence in and above Plant Canopies. Annu. Rev. Fluid Mech. 13: 97-129.

Raupach, M.R., Finnigan, J.J., Brunet, Y., 1996. Coherent eddies and turbulence in vegetation canopies: The mixing-layer analogy. Boundary-Layer Meteorol. 78, 351-382.

Robinson, S.K., 1991. Coherent motions in the turbulent boundary layer. Annu. Rev. Fluid Mech. 23, 601-639.

Sá, L.D.A., Pachêco, V.B., 2006. Wind Velocity Above and Inside Amazonian Rain Forest in Rondônia. Braz. J. Meteorol. 21, 50-58.

Sakai, R.K., Fitzjarrald, D.R., Moore, K.E., 2001. Importance of low-frequency contributions to eddy fluxes observed over rough surfaces. J. Appl. Meteorol. 40, 2178-2192.

Silva Dias, M.A.F.S., Rutledge, S., Kabat, P., Silva Dias, P., Nobre, C., Fisch, G., Dolman, H., Zipser, E., Garstang, M., Manzi, A., Fuentes, J., Rocha, H., Marengo, J., Plana-Fattori, A., Sá, L.D.A., Avalá, R.C.S., Andreae, M., Artaxo, P., Gielow, R., Gatti, L., 2002. Clouds and rain processes in a biosphere atmosphere interaction context in the Amazon Region. J. Geophys. Res. 20, 1-46.

Thom, A.S., 1975. Momentum, mass and heat exchange of plant communities, In: Monteith, J.L., (Eds), Vegetation and the Atmosphere. Academic Press, London, pp. 57-110.

Thomas, C., Foken, T., 2005. Detection of long-term coherent exchange over spruceforest using wavelet analysis. Theor. Appl. Climatol. 80, 91-104.

Thomas, C., Foken, T., 2007. Flux contribution of coherent structures and its implications for the exchange of energy and matter in a tall spruce canopy. Boundary-Layer Meteorol. 123, 317-337.

Torrence, C., Compo, G.P., 1998. A practical guide to wavelet analysis. Bull. Am. Meteorol. Soc. 79, 61–78.

Vickers, D., Mahrt, L., 1997. Quality control and flux sampling problems for tower and aircraft data. J. Atmos. Ocean. Tech. 14, 512-526.

Viswanadham, Y., Molion, L.C.B., Manzi, A.O., Sá, L.D.A., Silva Filho, V.P., André, R.G.B., Nogueira, J.L.M., dos Santos, R.C., 1990. Micrometeorological Measurements in Amazon Forest during GTE/ABLE-2A Mission. J. Geophys. Res. 95: 13669-13682.

von Randow, C., Sá, L.D.A., Prasad, G.S.S.D., Manzi, A.O., Arlino, P.R.A., Kruijt, B. 2002. Scale Variability of Atmospheric Surface Layer Fluxes of Energy and Carbon over a Tropical Rain Forest in Southwest Amazonia. I. Diurnal Conditions. J. Geophys. Res. 107, 8062-8072.

Warhaft, Z., 2000. Passive scalars in turbulent flows. Annu. Rev. Fluid Mech. 32, 203-240.

Wilczak, J.M., 1984. Large-scale eddies in the unstably stratified atmospheric surface layer. Part I: Velocity and temperature structures. J. Atmos. Sci. 41, 3537-3550.

Wright, I.R., Nobre, C.A., Tomasella, J., Rocha, H.R., Roberts, J.M., Vertamatti, E., Culf, A.D., Alvalá, R.C.S., Hodnett, M.G., Ubarana, V.N., 1996. Towards a GCM surface parameterization of Amazonia, In: Gash, J.H.C., Nobre, C.A., Roberts, J.M., Victoria, R.L. (Eds), Amazonian Deforestation and Climate. John Wiley, Chichester, pp. 473-504.

Zeri, M., Sá, L.D.A., 2010. The impact of data gaps and quality control filtering on the balances of energy and carbon for a Southwest Amazon forest. Agr. Forest Meteorol. 150, 1543-1552.

Capítulo 2

---

de Souza, C.M. Dias-Junior, C.Q. Tota, J. Sá, L.D.A. 2015. An empirical-analytic model to describe the vertical wind speed profile above and within amazon forest. *Aceito condicionalmente para Meteorological Applications em 15/06/2015.*

An empirical-analytic model of the vertical wind speed profile above and within an amazon forest site

Cledenilson Mendonça de Souza[a,b], Cléo Quaresma Dias-Júnior[b,e], Júlio Tóta[c], Leonardo Deane de Abreu Sá[d]

[a] Universidade Federal do Amazonas – UFAM/ICSEZ, Parintins, AM, Brasil
[b]Instituto Nacional de Pesquisas da Amazônia- INPA/ CLIAMB , Manaus, AM, Brasil.
[c] Universidade Federal do Oeste do Pará – UFOPA, Santarém, PA, Brasil
[d]Instituto Nacional de Pesquisas Espaciais – INPE/ CRA, Belém, PA, Brasil.
[e]Instituto Federal de Educação Ciência e Tecnologia do Pará- IFPA, Bragança, PA, Brasil.

Abstract

This paper considers mean wind velocity profiles measured on a 60 m high tower in the Rebio-Jarú forest (10° 04.7′ S, 61° 52.0′ W), located in the Brazilian north-western state of Rondônia. The data were collected during the wet season intensive campaign of the LBA (Large Scale Biosphere-Atmosphere Experiment in Amazonia). Nine cup anemometers were vertically placed to provide a good estimate of the inflection point height of the mean velocity wind profile. The resulting data were used to formulate a mean vertical wind speed profile, $\overline{u}(z)$, based on key parameters such as the inflection point height and leaf area index. The modified hyperbolic tangent function was used to provide a more flexible fit to the experimental data. An exponential term was also added to the $\overline{u}(z)$ function, so that it can assume the appropriate 's' shape near the ground. Thus, some parameters were incorporated into the analytical profile function to enable more flexibility. The presented results demonstrate that the profile is a good fit to experimental data measured above and within the Amazon forest canopy.

Keywords: Wind profile; Roughness sub-layer; Modified hyperbolic tangent function; Inflectional point; Amazon forest; Turbulence.

1. Introduction

Previous investigations regarding the validity of the atmospheric flow's similarity relationships above tall forest canopies noted some anomalous aspects of turbulent exchanges at the forest-atmosphere interface (Thom *et al*., 1975). This raised interesting questions concerning

a roughness sub-layer (RSL), which is present above very complex surfaces such as forests (Raupach and Thom 1981; Cellier and Brunet, 1992; Finnigan, 2000). It is difficult to estimate turbulent fluxes under such conditions (Sakai *et al*., 2001; Von Randow *et al*., 2002; Mahrt, 2010) and new similarity relationships are required (Raupach *et al*., 1996; Marshall *et al*., 2002; Sá and Pachêco, 2006). One important feature associated with these discrepancies is the existence of an inflection point in the mean wind profile. This generates a new kind of turbulent instability in the atmospheric flow because of the strong wind shear in the forest/atmosphere interface, which may create regions with 'like-roll' coherent vortices (Robinson, 1991; Raupach *et al*., 1996). These vortices have peculiar spectral characteristics (Campanharo *et al*., 2008, Dias-Júnior *et al*., 2013), which may generate specific local phenomena such as spectral short-circuiting and turbulent wakes caused by the interaction of the canopy forest with the turbulent flow (Finnigan, 2000; Cava and Katul, 2008).

These complex flow characteristics make it difficult to accurately estimate mean turbulent variables in the RSL near tall vegetation like the Amazonian forest (Sakai *et al*., 2001). Thus, it is important to determine the momentum transfer from the atmosphere to the surface when considering the role of the Amazonian forest in biosphere-atmosphere exchanges. Problems related to the coupling between the atmospheric flow above and below the Amazon forest canopy were studied by Fitzjarrald *et al*. (1990), Viswanadham *et al*. (1990), Kruijt *et al*. (2000), Sá and Pachêco (2006) and Zeri *et al*. (2013), among others. Despite this extensive research, there are few systematic studies that associated wind profile shapes with features of the Amazon forest canopy (such as foliage structure), as investigated by Yi (2008) for a forest in a temperate zone. These issues must be considered when developing surface-atmosphere exchange schemes for modelling purposes, which is the focus of this paper.

2. Material and methods

2.1. Experimental site

The Rebio-Jarú forest reserve is located in the southwestern Amazon. It is 2680 km^2 of typical tropical rain forest, and is located between 10° 05' S and 10° 19' S, and 61° 35' W and 61° 57' W, approximately 100–150 m above sea level (Zeri and Sa, 2010). A 60 m height micrometeorological tower was built in the Rebio-Jarú reserve (Figure 1). According to Andreae *et al*. (2002), it 'presents horizontally homogeneous conditions from northwest to southeast, which is the dominant wind direction (in a clockwise sense)'. Mc William *et al*. (1996) presented information concerning the tree species found in this reserve. Culf *et al*. (1996), Andreae *et al*.

(2002) and Dias-Júnior *et al*. (2013) presented several geographical and climatic reviews of this experimental site.

Several studies have considered the leaf area index (LAI) of Amazon forests, to estimate its value in different Amazonia experimental sites. Among them, Moura (2001) proposed an LAI of 6 for the Rebio-Jarú reserve, and Marques Filho *et al*. (2005) found LAI values of 6.4 and 6.1 for the ZF2 at km 14 and km 34 experimental sites, respectively. These sites are both located next to Manaus, in the central Amazon. Roberts *et al*. (1996) used different methods for estimating the LAI, and calculated values between 4.6 and 6 for the Rebio-Jarú reserve. Based on this result, this study used a LAI value of 6.

Figure 1. Micrometeorological tower built on the Jarú Reserve.

Some investigations suggest that there may be a relationship between the vertical wind profile and foliage structure. The findings of Yi (2008) imply that $\overline{u}(z)/\overline{u_h}$, is function of LAI, where $\overline{u}(z)$ is the mean wind vertical profile and $\overline{u_h}$ is the mean wind speed at the top of the canopy. Doughty and Goulden (2008) analysed in situ and satellite data of the Tapajós National Forest in the Amazon, approximately 150 km south of Santarém, Pará, Brazil. Their results showed that the LAI was subject to seasonal variations. According to these researchers, the LAI has a minimum value just over 4 m^2 m^{-2} from December through to April, a period that mostly corresponds to the local wet season. However, according to Doughty and Goulden (2008), leaf production increases from July to September, corresponding to the local dry season. During this period, many trees 'change their old leaves for new leaves', and the LAI may reach 6 m^2 m^{-2}.

2.2. Dataset

The Rebio-Jarú reserve is one of several experimental sites in the LBA (Large Scale Biosphere-Atmosphere Experiment in Amazonia). The extensive LBA experimental campaigns were carried out in two steps: The wet season campaign, from 25 January to 5 March 1999, and the dry-to-wet campaign, from 15 September to 10 November 2002 (Silva Dias *et al*., 2002). As a part of the scientific activities in the Rebio-Jarú reserve, the energy budget components, wind velocity, temperature, and humidity were measured at several heights on a micrometeorological tower. Nine cup anemometers (Low Power A100L2, Vector Instruments Inc.) sampled at 0.1 Hz provided data for the wind profile, as shown in Figure 2. They were placed at previously defined levels to provide accurate information about the inflection point height, and useful information about the atmospheric flow in the forest-atmosphere interface. Thus, the instruments were vertically installed at heights of 55.00 m, 50.55 m, 47.70 m, 42.90 m, 40.25 m, 37.80 m, 32.85 m, 26.65 m and 14.30 m.

We applied some of Vickers and Mahrt's (1997) procedures regarding quality control of the experimental data, to remove spurious spikes, amplitude resolution problems, dropouts and unrealistic data.

Figure 2. Profile of the nine anemometers installed in the Jarú Reserve micrometeorological tower.

2.3. Theoretical elements and methodology

There is some experimental evidence that similarity relationships based on Monin–Obukhov similarity theory (MOST) cannot appropriately describe the atmospheric flow in the RSL above tall vegetation (Thom *et al*., 1975; Cellier and Brunet, 1992; Raupach *et al*., 1996; Finnigan, 2000; Py *et al*., 2004). Many empirical formulations for normalized $\overline{u}(z)$ in the RSL have been proposed, based on roughness parameters distinct of the well-known zero-plane

displacement height (d) and roughness length (z_0). Such relationships can more appropriately express some exchange processes between the biosphere and atmosphere that occur near the top of a tall forest (Raupach *et al*., 1996; Finnigan, 2000; Marshall *et al*., 2002; Py *et al*., 2004; Sá and Pachêco, 2006; Doughty and Goulden, 2008; Tóta *et al*., 2012; Dias-Júnior *et al*., 2013).

Regarding some important issues associated with the wind profile's shape above tall vegetation in the RSL.

i) Fitzjarrald *et al*. (1990) obtained some evidence that suggests that the flow in the canopy top provides information regarding a characteristic length scale (L_h) for the flow at the interface between forest and atmosphere. That is,

$$L_h = \frac{\overline{u}_h}{\left.\frac{d\overline{u}}{dz}\right|_h}, \tag{1}$$

where $\overline{u}_h$ is the mean wind velocity at level h (which corresponds to the mean canopy height) and $\left.\frac{d\overline{u}}{dz}\right|_h$ is the mean velocity gradient at h.

ii) Raupach *et al*. (1996) used L_h to obtain a universal relationship that describes $\overline{u}(z)$ using the hyperbolic tangent function (HTF):

$$\frac{\overline{u}(z)}{\overline{u}_h} = 1 + \tanh\left(\frac{z}{L_h}\right). \tag{2}$$

iii) Marshall *et al*. (2002) used wind tunnel data, and Sá and Pachêco (2006) used experimental data from the Amazon forest to investigate a formulation for $\overline{u}(z)$ that incorporates dynamical information of the inflection point height (z_i) and the wind shear measured at h. They used scaling parameters: u_i (mean wind velocity at z_i) as a characteristic velocity scale, and L_h as defined in Equation (1). Their analyses were extended to both flows, above and within the canopy. With these two characteristic scales, they obtained a general relationship for the vertical profile:

$$\overline{u}/u_i = F[(z - z_i)/L_h], \tag{3}$$

where $\overline{u}$ is the mean wind velocity at z, and F is a function whose mathematical form is determined empirically from experimental data. This fits very well with experimental data measured far above the ground, but does not explain the influence of the canopy's foliage structure on the shape of the wind profile. To overcome this drawback, a new modified HTF formulation was proposed, which was based on earlier models of vertical profiles in the RSL

(Raupach *et al*., 1996; Yi, 2008). A mathematical device was added to the $\overline{u}(z)$ function to obtain a better fit for this curve.

The theoretical bases for this proposition were presented by Raupach *et al*. (1996), who considered an inflection point on the wind vertical profile next to the top of the canopy. They suggested that the HTF can provide a good numerical fit to the wind's vertical profile data. However, a simple HTF cannot generate a good numerical fit, if the actual empirical function for $\overline{u}(z)$ is not exactly symmetrical with respect to z_i. Thus, we propose a modified form of the HTF to improve the fit of $\overline{u}(z)$, which can more flexibly incorporate asymmetric shapes. Our technique can provide: 1) a good analytical model for the wind speed profile, which results in a good experimental fit for regions above and below z_i; and 2) a new formulation for $\overline{u}(z)$, which incorporates some features of the vertical structure of the forest canopy and some aerodynamic characteristics of the coupling between the flows above and within the canopy. The best fitting-curve is not perfectly anti-symmetric with respect to the horizontal axis at z_i. Therefore, to improve this fit, we inserted some flexible features into the best-fitting curve, making it less rigid than the original HTF. For this, we propose a new argument for the HTF. Following on from the HTF model formulations of Raupach *et al*. (1996) and Yi (2008), this leads to a new formulation for $\overline{u}(z)$ above and within the forest canopy:

$$\bar{u}(z) = \overline{u_H}\left\{tanh\left[\beta + \gamma exp\left(-LAI\left(1 - {}^{z}/_{z_i}\right)\right)\right]\right\}, \quad (4)$$

where H is the height of the highest measuring level (55 m, for the Rebio-Jarú experimental site); $\overline{u_H}$ is the mean wind speed at the H; β and γ are fitting parameters; z_i is the inflection point height of the vertical wind profile; z is a measuring height; and $\overline{u}(z)$ is the mean wind speed at z. β and γ are new parameters, which are explained as follows.

β influences the lower wind profile. That is, it can change the wind profile within the forest canopy. This is mainly useful for wind profiles in regions where there is a secondary maximum in the wind profile, due to the trunk spaces of forests (Kaimal and Finnigan, 1994, pp. 77–79). In Amazon forests, such occurrences of secondary maximums in the wind profiles can exist in forests located in slopes or valleys. For example, the forests studied by Araújo *et al*. (2010) and Tóta *et al*. (2012) in their investigations regarding the effects of terrain heterogeneity on atmospheric flows within tall vegetation. The β parameter provides a bet fit to the wind profile in these situations.

γ influences the wind profile in the opposite way to β, that is, it amplifies the upper part of the wind profile without introducing substantial changes to the lower part. The γ

parameter can describe the wind profile's shape over forests located in horizontally homogeneous, smooth areas, where we do not expect drainage flows or secondary maxima. In these situations, the forests' LAI are sufficiently high to hamper momentum transport deep into the canopy.

To improve the profile fit, and to allow for an 's' shape near the ground (as suggested by Yi (2008)), we included an exponential term in the analytical form of $\overline{u}(z)$. That is,

$$\overline{u}(z) = \overline{u}_H \left\{ \left[\frac{-1+\exp(\mu z)}{\exp(\omega z)} \right] \alpha tanh \left[\beta + \gamma \cdot exp\left(-LAI\left(1 - \frac{z}{z_i}\right)\right)\right]\right\}, \quad (5)$$

where $\mu, \alpha, \beta, \gamma$, and ω are fit parameters and LAI=6 for the Rebio-Jarú forest (Moura, 2001). $\alpha, \mu,$ and ω are new parameters, and are described as follows.

α multiplies the entire second part of Equation (5), which describes the dimensionless vertical profile of the wind speed above and within the forest canopy. Thus, it should produce a better fit to the vertical wind profile, covering situations ranging from very light winds to strong winds. In summary, α is strongly correlated with the average wind speed at any time.

μ and ω enable more flexibility in terms of the s-shaped region located below z=20 m. They do not influence the z_i value on the superior part of $\overline{u}(z)$. Thus, these parameters may incorporate some of the mechanical effects of the vegetation roughness and buoyancy effects. They are intended to make z dimensionless within the two arguments of the exponential functions in Equation 5 (but not in Equation (4)). They are generally close to unity (i.e., 1). However, the arguments are within the exponential functions, so they can introduce considerable variations in the dimensionless wind profile. These parameters may be considered as a single constant in this study. Note that in the Rebio-Jarú tower, the wind velocities were recorded down to z=14 m.

3. Results

The first numerical experiment analysed the wind speed profiles provided by Equation (4). The curves generated by this model and by experimental data are presented in Figure 3. They depict shapes that are not fully symmetric with respect to the inflection point. Note that the variables in Figure 3 are not dimensionless. Thus, this model was not built with the aim of obtaining universal relationships, but simply to show the mean shape of the wind field under a wide range of environmental conditions.

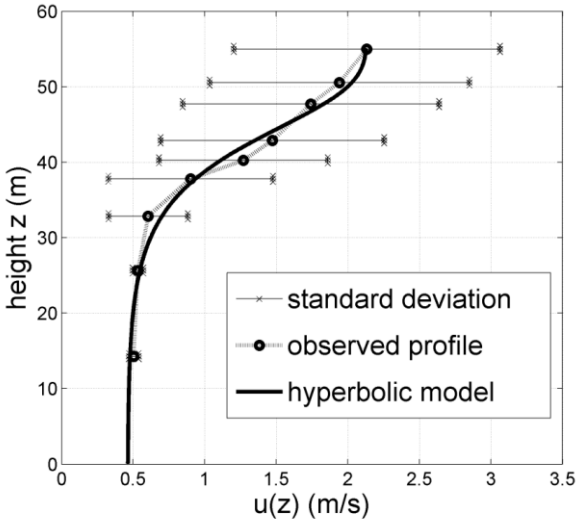

Figure 3. The observed vertical mean wind profile compared with the one provided by the Hyperbolic model (Julian day 46; from 0800 a.m. to 0900 a.m.).

The β and γ parameters in Equation (4) are linked to physical effects acting on and above the inflectional point zone. These parameters are associated with the existence of a roughness sublayer (Finnigan, 2000), its heterogeneous features resulting from the effect of distinct canopy architectures on the turbulence structure (Baldocchi and Meyers (1988), and its prevailing atmospheric stability conditions (Mahrt *et al*., 2001).

Figures 4 and 5 help to explain the physical meanings of β and γ. Figure 4 shows that variations in β change the inferior part of the curve representing the lower canopy region. In contrast, Figure 5 shows how variations in γ change the behaviour of the curve in the region near the canopy.

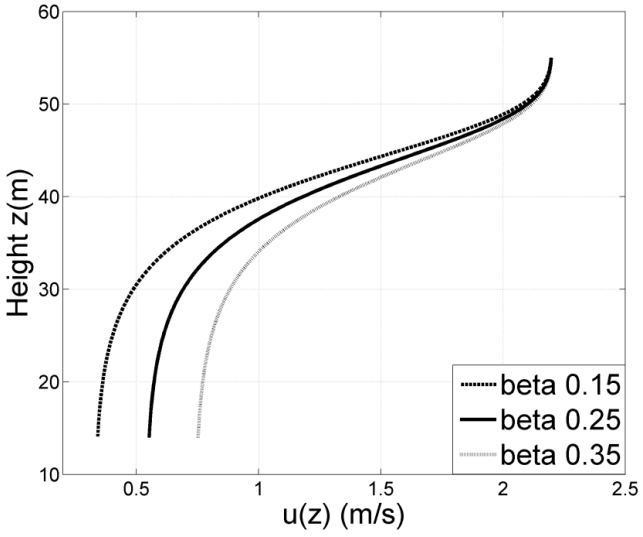

Figure 4. Modeled wind profiles for different values of the (β) parameter.

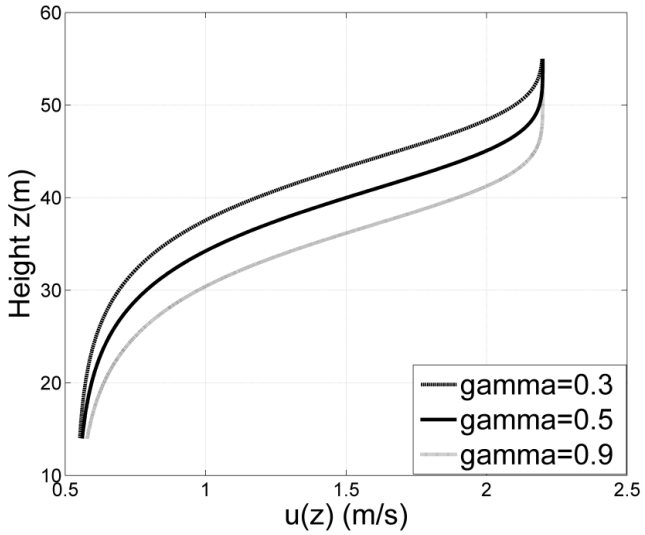

Figure 5. Modeled wind profiles for different values of the (γ) parameter.

Dias-Júnior *et al*. (2013) recently found that the z_i values observed above the Rebio-Jarú reserve varied over the day-time period. They found that z_i tends towards a maximum value of 41 m in the early morning and late afternoon. However, at noon, it falls to approximately 38 m, as shown in Figure 6.

These z_i values were used to test how well the modified HTF model fits $\overline{u}(z)$. Thus, the function for $\overline{u}(z)$ in Equation (4) was used to calculate the hourly wind profile data for 13 February 1999 under two conditions: i) z_i varied according to the Dias-Júnior procedure; and ii) fixed z_i.

These results indicate that the best fits for $\overline{u}(z)$ were obtained when: 1) β had a fixed value of 0.13 (which was obtained after many empirical tests); and 2) z_i and γ varied over the daytime period. z_i incorporates the asymmetrical effect in $\overline{u}(z)$. Physically, it expresses the influence of the canopy top forcing on a vortex centred on z_i. (Raupach *et al.*, 1996). In contrast, γ has a similar daytime trend to z_i, as shown in Figure 6.

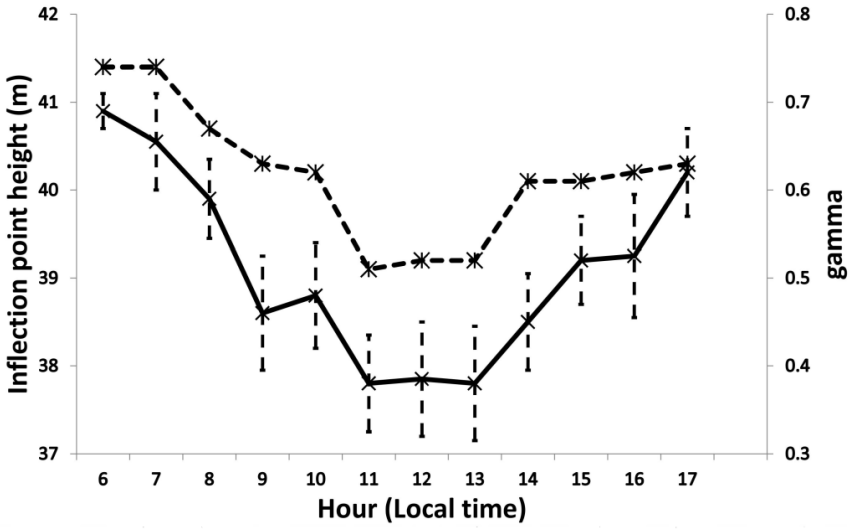

Figure 6. Daytime hourly variation of inflection point height (solid line) and gamma values (dashed line) for the Rebio-Jarú reserve.

To compare the observed and modelled profiles, i.e., $\overline{u}(z)$, data from 13 February 1999 was used to calculate the correlation coefficients for each z. These were then used to estimate a mean correlation coefficient, r (Table 1). The results were calculated for two conditions, to investigate variations to the wind profile shape over the daytime period. In condition r_1, the values of z_i varied; and in r_2 the values of z_i are held fixed (= 41 m). It is observed that $r_1 > r_2$, an indication that the wind speed profile was better modeled for the situations in which z_i was considered as being a variable parameter.

Table 1. Day-time hourly variation of the parameters γ, r_1 and r_2 measured in the Rebio-Jarú reserve for the Julian day 44, year 1999.

Hour	r_1 (z_i variable)	r_2 (z_i = *41 m*)
06:00	0.989	0.989
07:00	0.986	0.985
08:00	0.996	0.993
09:00	0.989	0.976
10:00	0.983	0.971
11:00	0.983	0.961
12:00	0.983	0.957
13:00	0.987	0.967
14:00	0.990	0.973
15:00	0.986	0.976
16:00	0.989	0.981
17:00	0.991	0.990

To investigate the physical role of each of these fit parameters, Figure 7 contains plots of $\overline{u}(z)$ versus z, where only one parameter was varied in each subplot. Figure 7a shows the wind profiles for different values of α. It amplifies the wind speed values as a whole. Figure 7b shows the wind profiles for different values of β. These profiles have the same wind speed value at the highest measurement. The differences between the two groups of wind profiles are more pronounced in the region corresponding to the within canopy zone. Figure 7c shows wind profiles for different values of γ. There is same split in wind speed values as in Figure 7b. However, unlike the previous figure, this split is more pronounced in the higher part of the profile. Figure 7d presents wind profiles for different values of μ. The wind profile shapes in Figure 7a and d are quite similar, except in the region immediately above the ground, where the profiles in Figure 7d slowly converge to the same curve (unlike in Figure 7a). The wind profile is very sensitive to changes in ω. Small variations can generate significant distortions in the wind profile, as shown in Figure 7e. The LAI parameter has a marked influence on the wind profile shape. When LAI is relatively small, the wind profile loses its s shape, as shown in Figure 7f.

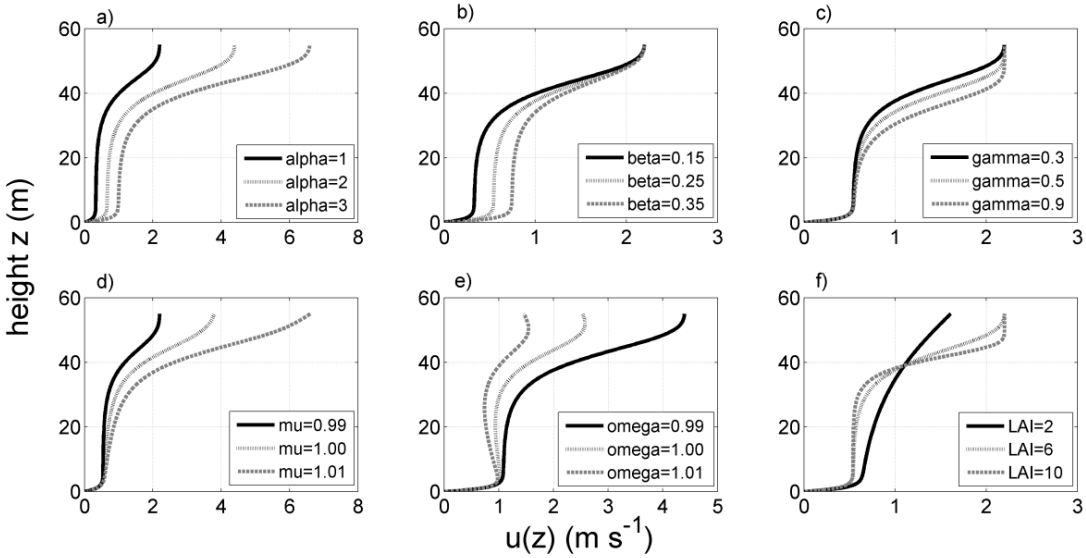

Figure 7. Modelled wind profiles for different parameter values: a) alpha; b) beta; c) gamma; d) mu; e) omega; and e) LAI

According to Doughty and Goulden (2008), the information provided by Equation (4) and the seasonal variability of LAI suggest that the vertical wind profile also undergoes seasonal changes. This can be seen in Figure 8, which contains two modelled profiles generated using the $\overline{u}(z)$ function, one for LAI=4.2 and the other for LAI=5.8. In this figure $\overline{u_h}$=2.2 m s^{-1}, β=0.25, γ=0.5 and z_i=39 m. These values are similar to those found by Doughty and Goulden

(2008) for the minimum and maximum LAI in the Amazon forest. Figure 8 shows the differences between the $\partial\bar{u}/\partial z$ values at level z_i for the curves representing dry and wet periods. In the wet period, $\partial\bar{u}/\partial z$ in the region immediately above the canopy is greater than during the dry season. Consequently, it is more difficult for the atmospheric flow to transfer momentum into the canopy during the wet season than during the dry season, as expected.

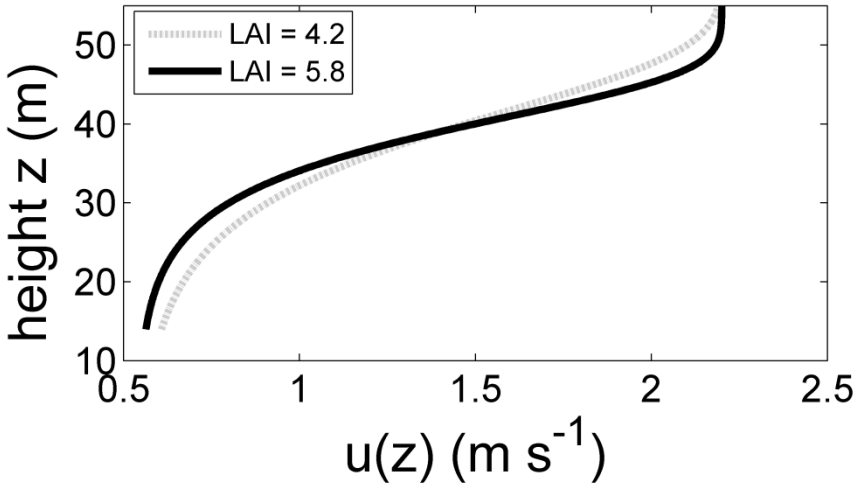

Figure 8. Modelled wind profiles for two different values of LAI (4.2: dashed grey line and 5.8: black solid line), which correspond to the seasonal extreme values in the Amazon forest.

There is another indication of a possible seasonal LAI variability in the Amazon forest, and of its consequences concerning the surface drag imposed by the plant canopy on the immediately above atmospheric flow. Mafra (2014) analysed the seasonal variability of nocturnal turbulent regimes above the Amazon forest in the Uatumã experimental site (central Amazon), using the methodology proposed by Sun *et al.* (2012). She found different values for the threshold value (V_L) of the average wind speed above the forest canopy that separates the weak and strong turbulence regimes. Note that the physical processes behind this threshold have recently received much attention (Martins *et al*., 2013; Mafra, 2014; Andreae *et al*., 2015), and the associated physical transition process was designated as a 'HOST' (hockey-stick transition) by Sun *et al*. (2015).

The β and γ parameters inside the HTF argument are linked to physical effects, which occur at the inflection point zone and above. They are probably associated to the existence of the roughness sublayer, and the so called 'mixing-layer analogy' (Raupach *et al*., 1996), which states that the wind speed profile above tall vegetation has an inflection point. This suggests that the region separates into two flow layers with distinct velocities, in which we expect a turbulent vortex, or, in the words of Cava and Katul (2008), a 'dominant eddy'. This

vortex could also be associated with the organization of ‘rolls‘ in the atmospheric flow with respect to rotation axes transverse to the mean stream direction (Robinson, 1991). However, according to Dias-Júnior *et al*. (2013), the height of the wind profile inflection point varies throughout the day. During the night, when the wind speed is sufficiently strong above the Rebio-Jarú, z_i increases creating conditions that allow the dominant eddy to penetrate more strongly and deeply into the canopy (higher torque associated with the vortex). This generates a more effective exchange of energy and mass between the regions above and within the forest canopy (Dias-Júnior *et al.*, 2015). At night, this process is associated with situations where the average wind speed exceeds the threshold value (V_L) for a ‘HOST‘ phenomenon (Sun *et al*., 2015). This increases the effectiveness of the mixture in the forest-atmosphere interface, challenging the traditional flux-profile relationships of HOST (Sun *et al*., 2015).

Figure 9 shows an abstract generalization of Figure 3, incorporating the features of a hypothetical secondary maximum in the wind profile. This secondary maximum is sometimes found in the trunk spaces of forests (Baldocchi and Meyers, 1988; Kaimal and Finnigan, 1994, pp. 77–79). Thus, the lower part of Figure 9 refers to a hypothetical analytical form for the function $\overline{u}(z)/\overline{u_h}$(z) near the forest floor. This, when incorporated into Equation (4) (the HTF) results in Equation (5) (the so called ‘modified HTF’). Figure 9 shows that the mean wind speed profile fits very well with the data.

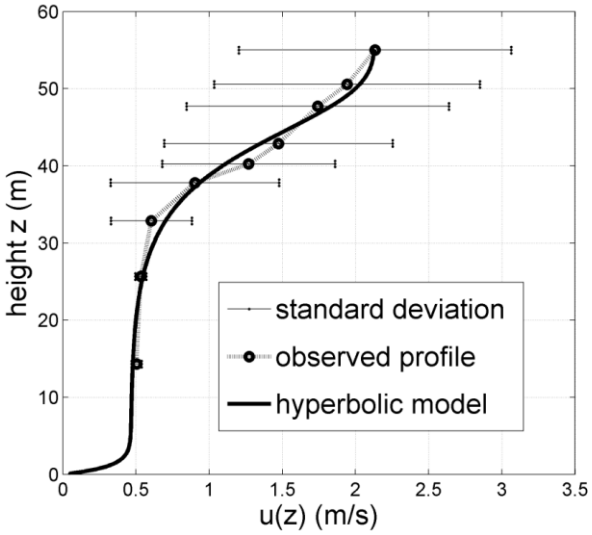

Figure 9. Observed mean wind profile and associated standard deviation compared with hyperbolic tangent function fitted data (second version).

4. Conclusions

This paper proposes an empirical-analytic model for describing the vertical wind speed profile above and within an Amazon forest, and provides a general non-dimensional relationship. The HTF was modified to obtain a better fit to experimental data collected above and within the Amazon forest. This function provides a good fit in many experimental situations, where there is variation in the height of the inflection point of the wind speed's vertical profile. These results are mainly useful for two reasons. First, they can be used to obtain a realistic estimate of the vertical wind profile when there is a limited amount of data. Second, they provide useful information regarding modifications to the wind profile shape, which were introduced by several distinct conditions. These include changes to the LAI values and changes to the height of the vertical profile's inflectional point. This formulation provides a better fit to the experimental data measured above and within the Amazon forest canopy.

Acknowledgments

The authors would like to thank all people which directly or indirectly contributed to the fulfillment of the1999 LBA - Intensive wet Campaign, and the support of the university in Ji-Paraná (UNIR), Instituto Brasileiro do Meio Ambiente e dos Recursos Naturais Renováveis (IBAMA) and Instituto Nacional de Colonização e Reforma Agrária (INCRA). This work was done under the LBA project framework, sponsored by the European Union, NASA, and Brazilian Agencies as the Conselho Nacional de Pesquisa e Desenvolvimento Tecnológico (CNPq) and the Fundação de Amparo a Pesquisa do Estado de São Paulo (FAPESP, process 01/06908-7). Leonardo Sá is particularly grateful to CNPq for his research grant (process303.728/2010-8).

References

Andreae MO et al. 2015. The Amazon Tall Tower Observation (ATTO): Overview of pilot measurements on ecosystem ecology, meteorology, trace gases, and aerosols. *Atmospheric Chemistry and Physics Discussions.* **15:** 11599-11726.

Andreae MO, Artaxo P, Brandão C, Carswell FE, Ciccioli P, Costa AL, Culf AD, Esteves JL, Gash JHC, Grace J, Kabat P, Lelieveld J, Malhi Y, Manzi AO, Meixner FX, Nobre AD, Nobre C, Ruivo MLP, Silva Dias MA, Stefani P , Valentini R, von Jouanne J, Waterloo

MJ. 2002. Biogeochemical cycling of carbon, water, energy, trace gases, and aerosols in Amazonia: the LBA-EUSTACH experiments. *J. Geophys. Res.* **33:** 1–25.

Araújo AC, Dolman AJ, Waterloo MJ, Gash JHC, Kruijt B, Zanchi FB, Lange JME, Stoevelaar R, Manzi AO, Nobre AD, Lootens RN, Backer J. 2010. The spatial variability of CO_2 storage and the interpretation of eddy covariance fluxes in central Amazonia. *Agric. For. Meteorol*. **150:** 226-237.

Baldocchi, DD, Meyers TP. 1988. Turbulence structure in a deciduous forest. *Boundary-Layer Meteorol.* **43(4):** 345-364.

Campanharo ASLO, Ramos FM, Macau EEN, Rosa RR, Bolzan MJA, Sa LDA. 2008. Searching chaos and coherent structures in the atmospheric turbulence above Amazon forest. *Phil. Trans. R. Soc. A* **366:** 579–589.

Cava D, Katul GG. 2008. Spectral Short-circuiting and Wake Production within the Canopy Trunc Space of an Alpine Hardwood Forest. *Boundary-Layer Meteorol.* **126:** 415-431.

Cellier P, Brunet Y. 1992. Flux-gradient relationships above tall plant canopies. *Agric. For. Meteorol.* **58:** 93-117.

Culf AD, Esteves JL, Marques Filho AO, Rocha, HR. 1996. Radiation, temperature and humidity over forest and pasture in Amazonia. In *Amazonian Deforestation and Climate*. Gash JHC, Nobre CA, Roberts JM and Victoria RL. Eds., Wiley, 175-191, Chichester.

Dias Júnior CQ, Sá LDA, Pachêco VB, Souza CM. 2013. Coherent structures detected in the unstable atmospheric surface layer above the Amazon Forest. *J. Wind Eng. Ind. Aerodyn.* **115:** 1–8

Doughty CE, Goulden ML. 2008. Seasonal patterns of tropical forest leaf area index and CO_2 exchange. *J. Geophys. Res.* **113:** G00B06.

Finnigan JJ. 2000. Turbulence in plant canopies. *Ann. Rev. Fluid Mec*. **32:** 519-571.

Fitzjarrald DR, Moore KE, Cabral OMR, Scolar J, Manzi AO, Sá LDA. 1990. Daytime Turbulent Exchange Between the Amazon Forest and the Atmosphere. *J. Geophys. Res.* **95:** 16825-16838.

Kaimal JC, Finnigan JJ. 1994. Atmospheric Boundary Layer Flows. Their Structure and Measurement. Oxford University Press, New York, 289 pp.

Kruijt B, Malhi Y, Lloyd J, Norbre AD, Miranda AC, Pereira MGP, Culf A, Grace J. 2000. Turbulence Statistics Above and Within Two Amazon Rain Forest Canopies. *Boundary-Layer Meteorol.* **94:** 297-331.

Mafra ACB. 2014. Características das trocas turbulentas noturnas de CO_2 entre a floresta de Uatumã, Amazonas, e a atmosfera. *Dissertação de Mestrado em Ciências Ambientais, Universidade Federal do Pará, Belém, Pará*.

Mahrt L, Vickers D, Sun J, Jensen NO, Jorgensen H, Pardyjak E, Fernando H. 2001. Determination of the Surface Drag Coefficient. *Boundary-Layer Meteorol.* **99:** 249-276

Mahrt L. 2010. Computing turbulent fluxes near the surface: Needed improvements. *Agric. For. Meteorol.* **150:** 501-509.

Marques Filho AO, Dallarosa RG, Pachêco, VB. 2005. Radiação solar e distribuição vertical de área foliar em floresta – Reserva Biológica do Cuieiras – ZF2, Manaus, Acta Amazonica, **35(4):** 427-436.

Marshall BJ, Wood CJ, Gardiner BA, Belcher BE. 2002. Conditional Sampling of Forest Canopy Gusts. *Boundary-Layer Meteorol* **102:** 225-251.

Martins HS, Sá LDA, Moraes OLL. 2013. Low level jets in the Pantanal wetland nocturnal boundary layer – Case studies. *American Journal of Environmental Energy,* **3(1):** 32-47.

Mc William ALC, Cabral OMR, Gomes BM, Esteves JL, Roberts JM. 1996. Forest and pasture leaf-gas exchange in south-west Amazonia. In *Amazonian Deforestation and Climate.* Gash JHC, Nobre CA, Roberts JM and Victoria RL Eds., Wiley, 265-285.

Moura RG. 2001. A study of the solar and terrestrial radiation above and inside a tropical rain forest. MSc thesis in Meteorology, National Institute of Space Research, Brazil (INPE-14015-TDI/1194).

Py C, de Langre E, Moulia B. 2004. The mixing layer instability of wind over a flexible crop canopy. *Comptes Rendus Mecanique,* **332:** 613-618.

Raupach MR, Finnigan JJ, Brunet Y. 1996. Coherent Eddies and Turbulence in Vegetation Canopies: The Mixing-layer Analogy. *Boundary-Layer Meteorol*. **78:** 351-382.

Raupach MR, Thom AS. 1981. Turbulence in and above Plant Canopies. *Ann. Rev. Fluid Mec*. **13:** 97-129.

Roberts JM, Cabral OMR, Costa JP, McWilliam A-LC Sa TDdA. 1996. An overview of the leaf area index and physiological measurements during ABRACOS, In *Amazonian Deforestation and Climate.* Gash JHC, Nobre CA, Roberts JM and Victoria RL Eds., Wiley, 287-306, Chichester.

Robinson SK. 1991. Coherent Motions in the Turbulent Boundary Layer. *Ann. Rev. Fluid Mec*. **23:** 601-639.

Sá LDA, Pachêco VB. 2006. Wind Velocity above and inside Amazonian Rain Forest in Rondonia. *Revista Brasileira de Meteorologia*. **21:** 50-58.

Sakai RK, Fitzjarrald DR, Moore KE. 2001. Importance of Low-Frequency Contributions to Eddy Fluxes Observed over Rough Surfaces. *J. Appl. Meteorol.* **40:** 2178-2192.

Silva Dias MAFS, Rutledge S, Kabat P, Silva Dias P, Nobre C, Fisch G, Dolman H, Zipser E, Garstang M, Manzi A, Fuentes J, Rocha H, Marengo J, Plana-Fattori A, Sá LDA, Avalá RCS, Andreae M, Artaxo P, Gielow R, Gatti L. 2002. Clouds and rain processes in a biosphere atmosphere interaction context in the Amazon Region. *J. Geophys. Res.* 107, 8072.

Sun J, Mahrt L, Nappo C, Lenschow DH. 2015. Wind and Temperature Oscillations Generated by Wave-Turbulence Interactions in the Stably Stratified Boundary Layer. *J. Atmos. Sci.*, **72:** 1484-1503.

Thom AS, Stewart JB, Oliver HR, Gash JHC. 1975. Comparison of aerodynamic and energy budget estimates of fluxes over a pine forest. *Q. J. R. Meteorol. Soc.* **101:** 93-105.

Tóta J, Fitzjarrald DR, Silva Dias MAF. 2012. Amazon Rainforest Exchange of Carbon and Subcanopy Air Flow: Manaus LBA Site – A Complex Terrain Condition. *The Scientific World Journal*. 165067. doi:10.1100/2012/165067

Vickers D, Mahrt L. 1997. Quality Control and Flux Sampling Problems for Tower and Aircraft Data. *J. Atmos. Oceanic Technol.* **14(3):** 512-526.

Viswanadham Y, Molion LCB, Manzi AO, Sá, LDA, Silva Filho VP, André RGB, Nogueira JLM, dos Santos RC. 1990. Micrometeorological Measurements in Amazon Forest during GTE-ABLE-2A Mission. *J. Geophys. Res.***95:**13,669-13,682.

von Randow C, Sá LDA, Gannabathula PS, Manzi AO, Arlino PR, Kruijt B. 2002. Scale variability of atmospheric surface layer fluxes of energy and carbon over a tropical rain forest in southwest Amazonia 1. Diurnal conditions. *J. Geophys. Res*: *Atmospheres* (1984–2012), **107(D20)**: LBA-29.

Yi C. 2008. Momentum Transfer within Canopies. *J. Appl. Meteorol. Climatol*. **47:** 262-275.

Zeri M, Sá LDA, Nobre CA. 2013. Estimating buoyancy heat flux using the surface renewal technique over four Amazonian forest sites in Brazil. *Boundary-layer meteorol.* **149(2):** 179-196.

Zeri M, Sa LDA. 2010. The impact of data gaps and quality control filtering on the balances of energy and carbon for a South west Amazon forest. *Agric. For. Meteorol*.**150:** 1543–1552.

Capítulo 3

Dias-Junior, C.Q. Sá, L.D.A. Marque Filho, E.P. Mauder, M. Manzi, A.O. 2015. Turbulence regimes in the stable boundary layer above and within the Amazon forest. *Submetido para Boundary Layer Meteorology*.

Turbulence regimes in the stable boundary layer above and within the Amazon forest

Cléo Q. Dias-Junior • Leonardo D. A. Sá • Edson. P. Marques Filho • Matthias Mauder • Antonio. O. Manzi

Abstract The structure of atmospheric turbulence is analyzed based on the existence of three different night-time turbulent regimes observed in the Amazon forest, classified according to criteria proposed by Sun et al. (Journal of the Atmospheric Sciences, 2012, Vol. 69, 338-351): regime 1) weak turbulence, low wind speed; regime 2) strong turbulence, with high wind speed, and regime 3) intermittent turbulence events. Therefore, we have investigated some of the main statistical characteristics of turbulent regimes. In situations with strong winds and high values of turbulent kinetic energy (4% of cases) sensible heat fluxes are about 40 times higher than the ones under light winds and low turbulent kinetic energy values (95% of cases). Furthermore, the inflection point height in the wind profile and shear length scale $L_h = \frac{u_h}{du/dz}$ (where u_h is the mean wind velocity at canopy top) increases with the regime 2, with the occurrence of strong mixing in the atmospheric boundary layer. In addition the coherent structure time scale in the regime 2 is greater than regime 1. It is suggested that, when the wind is strong enough, the forest-atmosphere exchanges are strongly influenced by a vortex whose center of symmetry is located just above the top of the forest canopy. Regime 3 is essentially nonstationary according with a criterion in the literature.

Keywords: Amazon forest · Coherent structures · Inflection-point instability · Nocturnal boundary layer · Turbulent regime

1 Introduction

The characteristics of the nocturnal boundary layer (NBL) have received considerable attention from a number of researchers, and significant scientific progress has been achieved based on high-quality data obtained during large-scale experimental campaigns such as the SABLES-98 (Cuxart et al. 2000), CASES-99 (Poulos et al. 2002), and LBA (Silva-Dias et al. 2002) projects, undertaken in the late 1990s. Despite several interesting investigations of

biosphere–atmosphere exchanges in the tropics (e.g., Shuttleworth et al. 1985, Fitzjarrald and Moore 1990, Viswanadham et al. 1990), a number of important aspects of the turbulent processes that occur above and within forests during the night have not been addressed, e.g.: i) the existence of different classes and/or regimes of nocturnal turbulence, as proposed by Van de Wiel et al. (2003), Cava et al. (2004), Sun et al. (2012) for experimental sites in the mid-latitudes; ii) the existence of instability of the inflection point in the wind profile and occurrence of mixed-layer similarity, and the characteristics of turbulent exchanges under these conditions (Högström and Bergström 1996, Raupach et al. 1996, Finnigan 2000); and iii) the importance of considering nonstationary flow as a subject of scientific interest, in addition to the need for classifying the characteristics of flows in the atmospheric surface layer (ASL), according to the stationarity indices discussed by Mahrt (1998, 2007), Van de Wiel et al. (2003), Zeri et al. (2013, 2014), Cava et al. (2014), among others.

The intention of this study was to combine the three objectives listed above, i.e., to attempt to understand how the instability of the inflection point, associated dominant turbulent eddy (DTE) near the forest–atmosphere interface, and consequent occurrence of the mixed-layer similarity are manifested under different turbulent regimes and different conditions of stationarity. The method of Sun et al. (2012) was used (hereafter, SUN12) for the detection of the distinct types of nighttime turbulence regimes. This method takes into account the possibility of external agents such as convective clouds acting on the ASL and disturbing its turbulent fields (Garstang et al. 1998, Garstang and Fitzjarrald 1999, Betts et al. 2002, 2009).

During turbulent events under a typical humid scenario of the tropics, particularly with the presence of convergence zones above the regions where the turbulence is studied (with the consequent increase in the incidence of convective clouds, storms, updrafts, and downdrafts), the nonstationarity of turbulent fields often occurs. Such situations are important regarding the generation of peculiar turbulence field patterns in the NBL (Mahrt 2007), and the aim of this study was to show that one of the turbulent regimes proposed by SUN12 corresponds to situations in which the nonstationarity indices are very high.

Robinson (1991), Raupach et al. (1996), Finnigan (2000) have discussed the importance of the role played by the DTE in the dynamics of the transfer process at the forest–atmosphere interface. Understanding how the dominant vortex (as named by Cava and Katul 2008) operates at the forest–atmosphere interface, and determining its effects both on the vertical profiles of scalar and vector quantities above and within the canopy and on the variability of turbulent flows, are of great interest for several reasons. One reason is related to

better understanding of the variability of trace gas concentrations in regions surrounded by forest (Andreae et al. 2015), including the residence time associated with the existence of certain chemical compounds within the forest canopy (Foken at al. 2012). Furthermore, it is interesting to expand comprehension of the biogeochemical processes that occur within forest environments in order to provide more realistic and appropriate parametrizations for use in ecophysiological models (Costa et al. 2010, Von Randow et al. 2013). Another reason concerns the need to better understand the processes involving extreme climatic events in tropical regions (Nepstad et al. 2004, Zeri et al. 2014), which would help improve public policies aimed at mitigating the socioeconomic effects of adverse meteorological phenomena, as well as providing grounds for financial support for the improvement of meteorological and climate models. Finally, better understanding is required of the theoretical aspects related to the organization of turbulence in the forest–atmosphere interface under different regimes, such as on scales associated with the occurrence of coherent structures (CS) (Collineau and Brunet 1993, Dias-Júnior et al. 2013), in addition to the deepening of the understanding of the genesis of some nonlinear phenomena in the NBL, as reported by Fitzjarrald and Moore (1990), Costa et al. (2011), among others.

2 Experimental Setup and dataset

The data were collected above the Rebio Jarú forest reserve in the south-western Amazon (Andreae et al. 2002). Detailed descriptions of the meteorological tower instrumentation and aspects of the regional climate may be found in Dias-Junior et al. (2013).

Briefly, the data were collected by instruments arranged on a 60-m-high meteorological tower (Fig. 1), as part of the LBA wet season intensive campaign in the western Amazon (Silva-Dias et al. 2002). As mentioned by von Randow et al. (2002), at the top of the tower, a 3-D sonic anemometer was installed on a vertical beam, 67 m above the forest floor. This instrument provided measurements of the three wind components (u, v, w) and the sonic virtual air temperature (T_v) at 16 Hz. In addition, vertical profiles of the wind speed, temperature, and relative humidity were measured with a sampling rate of 0.1 Hz. The wind speed data were measured by 10 cup anemometers (Low Power A100L2, Vector Instruments Inc.) arranged at heights to provide information with suitably accurate resolution for determining the inflection point height (z_i).

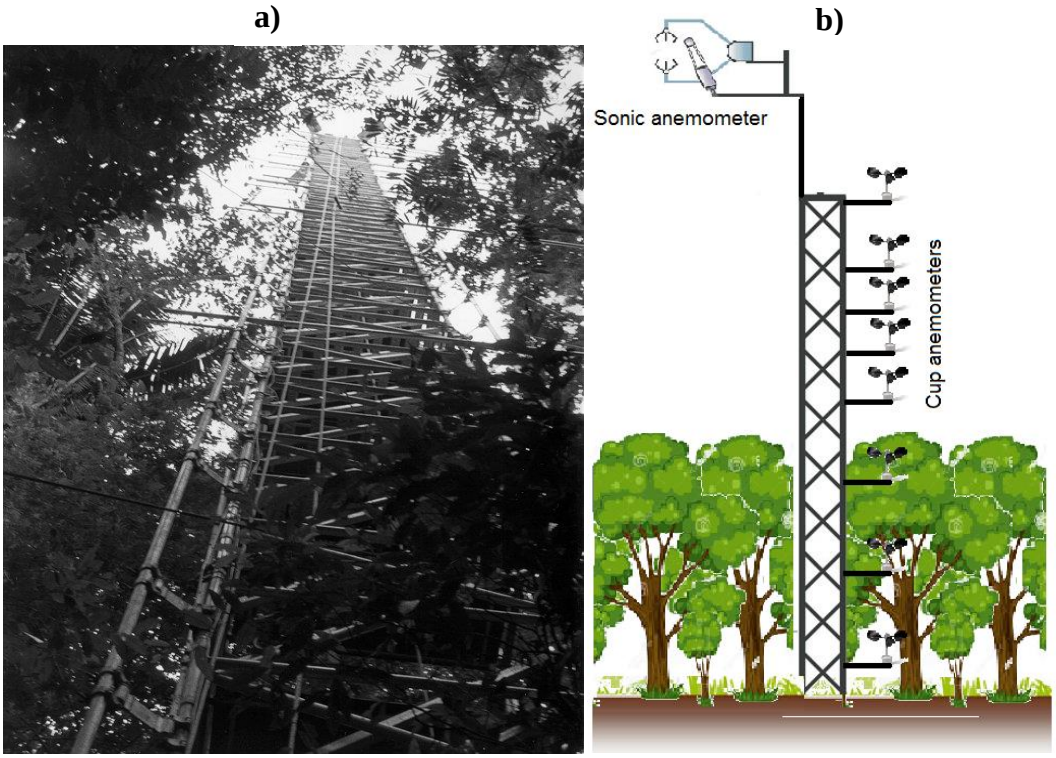

Fig 1 a) Photograph of the meteorological tower erected in the Rebio-Jarú forest reserve; b) schematic diagram showing the sonic and cup anemometers arranged on the tower and their relationship to the forest canopy.

In addition, data from 11 thermometers and hygrometers (model HMP45C-L150 Väisälä), installed in aspirated weather shelters (model RM Young 43408), were available for obtaining the vertical temperature and moisture profiles, respectively, both above and within the canopy. The location of each instrument is shown in Table 1.

Instruments	Height (m)
$T1, q1, A1$	58.35, 58.45
$T2, q2, A2$	54.90, 55.00
$T3, q3, A3$	50.45, 50.55
$T4, q4, A4$	47.60, 47.70
$T5, q5, A5$	42.80, 42.90
$T6, q6, A6$	37.65, 40.25
$T7, q7, A7$	32.75, 37.80
$T8, q8, A8$	30.95, 32.85
$T9, q9, A9$	25.45, 25.65
$T10, q10, A10$	14.30, 14.30
$T11, q11$	5.00

Table 1 Meteorological instruments location at the Rebio-Jarú reserve's tower: thermometers (T), hygrometers (q) and anemometers (A). The thermometers and hygrometers are at the same heights.

Data obtained on 14 typical nights were analysed (Julian days 38, 40–45, and 50–56, 1999). The time series were partitioned into 5-min datasets, according to the suggestions of Sun et al. (2002) and and Vickers et al. (2010), to improve the statistical analyses of the NBL turbulence regimes. Thus, from the investigated 14 nights, 1490 datasets were available. To verify the quality of the fast-response turbulent data and in order to perform subsequent analyses, the following procedures were implemented: i) spikes within the time series were removed according to the methodology of Vickers and Mahrt (1997); ii) the sampling rate of the data was reduced from 16 to 1 Hz to reduce computation time (Thomas and Foken 2007); and iii) linear trends were removed from the turbulent time series prior to performing the CS-detection procedure.

3 Methods

We used turbulent data measured at a fast-response sampling rate to calculate the average horizontal wind speed ($\overline{U} = u^2 + v^2)^{1/2}$. This methodology is similar to that used by SUN12 to characterize nocturnal turbulent regimes above the Rebio Jarú forest reserve. However, while that work used $V_{TKE} = \sqrt{TKE}$ as the characteristic scale of the turbulent velocity (TKE is the turbulent kinetic energy), in this paper, the characteristic scale is defined as the standard deviation of w (σ_w). This was adopted because according to Acevedo et al. (2009), σ_w is more appropriate than V_{TKE} because it is less affected by the submeso processes (Mahrt et al. 2008) that are very active in the Amazon (von Randow et al. 2002, Acevedo et al. 2014). After this procedure, it is possible to classify the available datasets into three turbulent regimes (which will be explained later).

3.1 Inflection point height in the wind profile and wind shear's length-scale (L_h)

This section is based mainly on the work of Dias-Júnior et al. (2013), who developed code to estimate the value of z_i . Thus, a third degree polynomial function was developed for the nine available measurements of the wind profile and a least square numerical best fit performed. Once the best-fitting function was determined, it was possible to calculate the z_i value, based on which a length scale associated with the wind shear (L_h) could be calculated (Raupach et al. 1996, Sá and Pachêco 2006):

$$L_h = \frac{\overline{u_h}}{\left(\overline{du}/dz\right)\Big|_h}, \qquad (1)$$

where u_h is wind speed at the canopy-height (h), and $\left(\overline{du}/_{dz}\right)\Big|_h$ is the vertical gradient of the mean wind speed over h.

It is noteworthy that both Raupach et al. (1996) and Brunet and Irvine (2000) had relative success using the shear length scale to express some universal characteristics of the atmospheric flow over various types of vegetation canopy.

3.2 Turbulent kinetic energy dissipation

The TKE dissipation rate per unit mass (ε) expresses quantitatively the conversion of turbulent mechanical energy into heat when the near-surface atmospheric flow acts against viscous shear forces (Kaimal and Finnigan 1994, pp 26-27). A process widely used to estimate the value of ε is based on the validity of Taylor's hypothesis (Stull 1988, pp 5-6) and on the relationship established by Kolmogorov (Stull 1988, pp.390) for the inertial subrange part of the turbulence spectrum regarding the x-component of the wind (Stull 1988, 390 pp):

$$S_x(k) = \alpha_x \varepsilon^{2/3} k^{-5/3} \qquad (2)$$

where $S_x(k)$ is the power spectral density corresponding to the wave number k and α_x is Kolmogorov's constant, the value of which depends on the wind speed component studied.

Here, the longitudinal component of the wind speed u was used, which yielded S_u values from an inertial subrange with edges between 1.0 and 2.5 Hz. This is entirely within the range of occurrence of the inertial subrange according to Bolzan and Vieira (2006), whose obtained results based on the same experimental data used here. We adopted a value of α_u = 12.52 (Kaimal and Finnigan 1994, pp 64).

3.3 Time Scale of Coherent Structures (CS)

According to Gao and Li (1993), the scale of occurrence of CS in a time series may be determined using the scale variance of the wavelet coefficients of the available data. The description of the wavelet methodology applied here can be found in Thomas and Foken (2005).

After preparation of the 5-min files, a continuous 1-D wavelet transform was used, which is defined when applied to a given signal $f(t)$ as:

$$W_\psi f(a,b) = \frac{1}{\sqrt{a}} \int_{-\infty}^{+\infty} f(t) \psi\left(\frac{t-b}{a}\right) dt \qquad (3)$$

where $a \in \mathcal{R}+$ and $b \in \mathcal{R}$.

The scale decomposition was performed by translation and dilatation of only one "mother wavelet", which was stretched or compressed and displaced along the time line to generate a family of "daughter wavelets". These can be expressed as the function of two parameters: one for their scale (a) and other for their time position (b).

The Morlet complex function (Eq. 4) was used because it is more suitable for the time scale analysis of CS, as discussed in depth by Thomas and Foken (2005):

$$\psi(\eta) = \pi^{1/4}\, e^{i\omega_0\eta}\, e^{-\eta^2/2} \tag{4}$$

where η is the dimensionless time parameter and ω_0 is the dimensionless frequency.

The CS time scale corresponds to the one for which the wavelet coefficient variance $\sigma(a,b)$ reaches its maximum value:

$$\sigma(a,b) = \int \left|T_\psi f(a,b)\right|^2 db \tag{5}$$

where $T_\psi f(a,b)$ is the Morlet wavelet transform.

Thus, if atmospheric transport is dominated by coherent eddies of a certain scale, as appears to be the case concerning the atmospheric flow above the Amazonian forest (Zeri et al. 2013, 2014), the corresponding power spectrum should exhibit a distinct peak at that scale. Accordingly, the event duration of CS (D_e) was inferred from the scale a_e of the clearly expressed maximum in the wavelet spectrum, the peak frequency of the mother wavelet $\omega^0_{\psi_{p,1,0}}$, and the time resolution of the time series (Thomas and Foken 2005),

$$D_e = \frac{a_e \Delta t \pi}{\omega^{\,0}_{\psi_{p,1,0}}} \tag{6}$$

3.4 Stationary conditions

Time series are considered stationary when the associated statistical moments (e.g., mean, variance, skewness, and curtosis) do not depend on the initial time of the analysed series (Panofsky and Dutton 1984, pp 39). These tests were undertaken because it is known that in the NBL, many phenomena such as gravity waves, density currents, low-level jets, cloud passage, and katabatic winds occur (Mahrt 1998, Poulos et al. 2002, Sun et al. 2002, 2004, Mahrt 2007, Zeri and Sá 2011). These commonly alter the mean flow and can cause it to become nonstationary, which can hinder robust estimation of the statistical moments under such conditions (Mahrt 2007, Zeri et al. 2014).

In this work, the methodology proposed by Mahrt (1998) was used to classify the time series according to its stationary or nonstationary characteristics. The process undertaken was as follows:

i) The 5-min time series were divided into five 1-min intervals (I records);

ii) Each 1-min interval was divided into five 12-s subintervals (J subrecords);

iii) Turbulent fluxes were calculated for all I and J intervals. Here, the sensible heat flux (H) was calculated because the analysis of the buoyancy effect was of considerable interest in this study; and

iv) Finally, the standard deviation corresponding to the heat fluxes associated with segments J (σ_{wi}) and I (σ_{wtb}) were calculated.

The nonstationarity (NR) for each 5-min time series was defined by the index (Mahrt 1998):

$$NR = \frac{\sigma_{btw}}{\sigma_{wi}} \qquad (7)$$

For stationary conditions, NR approaches unity. In this work, for classification purposes, time series for which $0.5 < NR < 2.0$ were considered stationary. It should be remembered that although NR does not result from a statistically exact estimation, it is very useful for separating time series according to their characteristics toward stationarity.

4 Results

4.1 Turbulent Regimes

Figure 2 shows the relationship between σ_w and $\overline{U}$ for the fast-response data measured at a height of 67 m above the forest floor of the Rebio Jarú reserve. Each point shown in Fig. 2 corresponds to the calculations using perturbations from the 5-min means (Sun et al. 2004). A clear distinction between the point-clusters corresponding to turbulent regimes 1 and 2 can be seen with regard to their respective fitted straight lines. The slope of the straight line corresponding to regime 1 (α_I), is clearly less than that corresponding to regime 2 (α_{II}). It is also noticeable that the point cluster corresponding to regime 3, for the same $\overline{U}$ values of regime 1, show higher σ_w values than regime 1.

The value of the threshold wind speed (V_L) that separates the regions in which regimes 1 and 2 are dominant was estimated visually. Regime 1, represented by the black circles, presents weak σ_w values, which increase slightly with $\overline{U}$ to reach V_L (≈3.0 m s^{-1}). In regime 2,

represented by the blue circles, values of σ_w increase quickly with $\overline{U}$ starting from V_L. For improved visualization of the data clusters of the turbulent regimes, least squares best fits were applied to obtain the straight lines corresponding to the data under regimes 1 and 2.

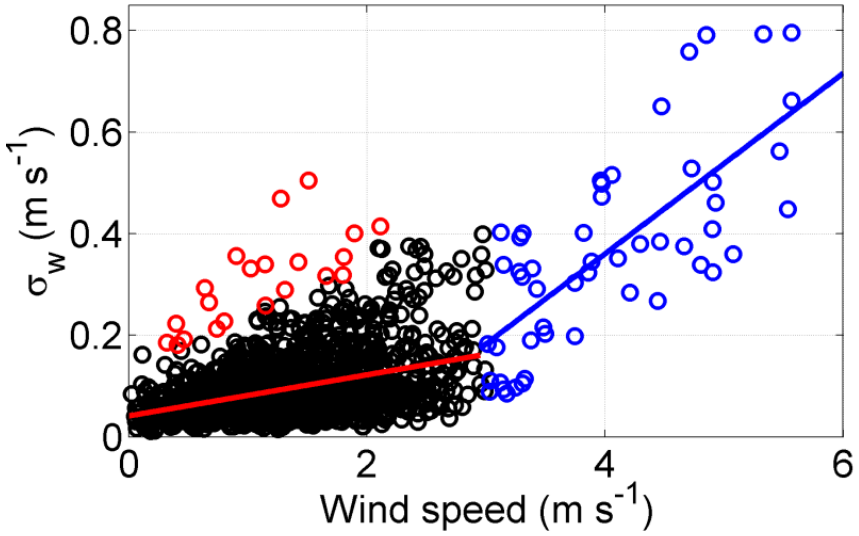

Fig 2 Standard deviation of the vertical velocity (σ_w), a characteristic turbulent velocity scale as a function of the wind speed measured at 67 m height, corresponding at 14 nights. Black, blue and red circles correspond respectively to regime 1 (low wind and weak turbulence), regime 2 (high wind and strong turbulence) and regime 3 (intermittent turbulence events).

According to SUN12, turbulent regime 3 (red circles) could be associated with turbulent events generated by intermittent top-down movements, characterized by strong downward movements of air. This objective of this work was to contribute to the physical interpretation of SUN12's turbulent regimes above tropical forests, including regime 3 with its nonstationary characteristics.

To determine the value of V_L, estimations of σ_w were plotted against U for each interval of 0.5 m s^{-1} over the entire available dataset. It was observed that in the region of V_L = 3.0 m s^{-1}, an abrupt change in the variation of σ_w occurred with respect to $\overline{U}$. All situations in which the wind speed was above the threshold of 3.0 ms^{-1} were associated with turbulent regime 2.

To separate the data belonging to regime 3 from those belonging to regime 1, the standard deviation of σ_w was determined for various intervals from $\overline{U}$ = 0 to $\overline{U} = V_L$. Based on these calculations, all data for which σ_w > 4.5 were defined as belonging to regime 3, i.e., the remaining data were considered as belonging to turbulent regime 1.

After identifying the nighttime turbulent regimes from the 1490 analysed time series, 95.1% of them were associated with regime 1, 3.4% with regime 2, and only 1.5% with

regime 3 (Table 2). Therefore, it is clear that the NBL of the Amazon is largely characterized by a regime of light winds and low TKE, although the total contributions to the global H from regime 2 exceed those provided by regime 1, as is shown later in this paper.

	Regime 1	**Regime 2**	**Regime 3**
Number of events	1417	51	22
$\bar{U}$ **(m s^{-1})**	1.39	4.53	1.10
σ_w **(m s^{-1})**	0.10	0.50	0.31

Table 2 Some characteristics of the nocturnal turbulent regimes above the Rebio-Jarú reserve.

Stationarity tests were performed for the available time series datasets. Figure 3 shows those situations where the time series were classified according to the NR index (represented by green dots). It can be seen that the degree of NR of regime 3 is considerably larger than regimes 1 and 2.

As can be seen in Fig. 3, the data of regime 3 are associated with time series that do not satisfy the stationarity condition well. These data also deviate from the data clusters related to regimes 1 and 2. This appears associated with the physical conditions in which the predominate interaction of the atmospheric flow with the underlying vegetation cover, is in the presence of strong vertical wind shear induced by surface roughness associated with the presence of the forest canopy. However, in situations associated with regime 3, factors unrelated to local forest–atmosphere interaction processes seem to play a dominant role.

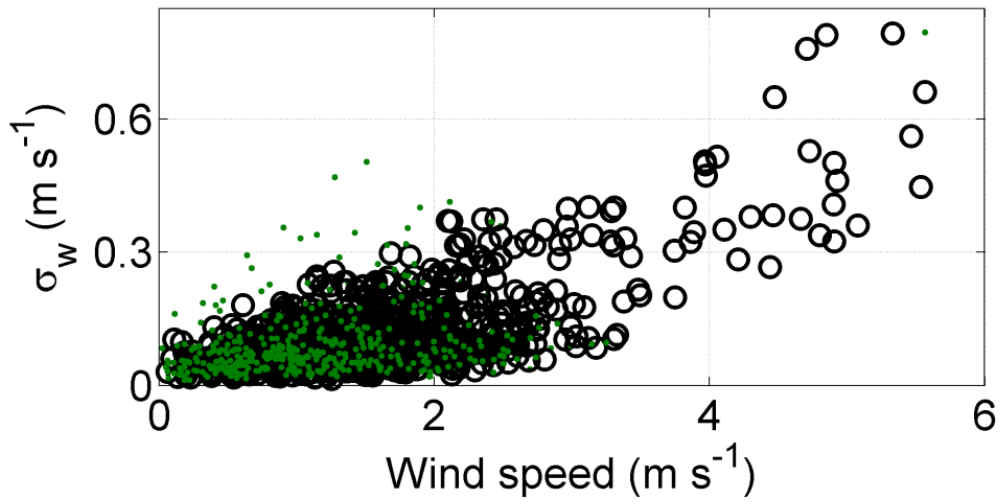

Fig 3 Similar to Fig 2. Black circles and green dots correspond, respectively to stationary 5min periods and non-stationary 5min period.

The next section shows that the turbulent fluxes of scalars are considerably higher during regime 2 compared with those observed during regime 1.

4.2 Sensible Heat Flux

Data from a typical evening during the 1999 rainy season (Julian days 45/46) were used to investigate the differences between H during the occurrence of regimes 1 and 2. Thus, 132 time series of 5-min datasets were available, but only 106 time series met the stationarity criteria and were used in the following analyses.

That night, there was a total H of approximately -2.35×10^5 J m^{-2}, integrated throughout the entire nighttime period. Regime 1 persisted for 81% of the reporting period and accounted for 28% of H (Table 3). Conversely, regime 2 persisted for 19% of the studied period and accounted for 72% of the total H.

Turbulent regimes	Full H (J m^{-2})	Average H (W m^{-2})
Regime 1	-0.65×10^5	-1.82
Regime 2	-1.7×10^5	-43.62

Table 3 Full H integrated throughout the entire night-time period and average values of H for both regime 1 and regime 2.

The number of occurrences of regime 1 is far greater than the instances of regime 2. However, when regime 2 does occur, it contributes more significantly to H in comparison with regime 1. This will become clearer in Sect. 4.5, where a case study of regime 2 revealed that the forest canopy is heated and has a considerable fall in its relative humidity over a period of about 20 min.

It should be noted that Fitzjarrald and Moore (1990) used data from the Ducke reserve, located in the central Amazon, to characterize the forest–atmosphere nocturnal sensible heat exchanges. They found that in conditions of relatively strong winds, H was >10 times its average value throughout the analysed period. They also found that the situations of strong wind and considerable H were intermittent, occurring for only 3% of the entire period analysed. However, they did not conduct their analysis based on different turbulent regimes, which is why they could not specify the conditions under which the phenomenon of the considerable increase in H occurred.

According to Raupach et al. (1996) the DTE would present a centre of symmetry at the inflection point location. Therefore, a variation in the value of z_i should have important dynamical consequences at the forest–atmosphere interface, where eddies centred at the inflection point could possibly penetrate into the canopy, which might result in a buildup in the values of H in the region of occurrence of the DTE.

4.3 Inflection Point Height, Wind Shear, and Dissipation Length Scale

Several researchers have shown that the atmospheric turbulent flow above high vegetation is dominated by strong vertical wind shear, which is generated mainly at the forest–atmosphere interface (Paw U et al. 1992, Raupach et al. 1996, Brunet and Irvine 2000, Finnigan 2000, Thomas and Foken 2007). It exhibits high efficiency in the absorption of the horizontal momentum of the flow, which results in the generation of an inflection point in the wind profile (Raupach et al. 1996, Brunet and Irvine 2000, Sá and Pachêco 2006, Thomas and Foken 2007, Dias-Junior et al. 2013). The depth of the wind shear layer might be associated with length scale L_h (Dupont and Brunet 2009).

This absorption of momentum by the canopy occurs because of the impact of the flow against the vegetation structure, which generates turbulent wakes behind the bluff bodies and dissipates TKE by converting it into heat. Therefore, it is interesting to obtain the rate at which TKE is lost by calculating the TKE dissipation rate (ε). Therefore, the value of ε was estimated above the treetops (67 m), because fast-response turbulent data were available at this level from the sonic anemometer. However, as discussed above, it was not possible to estimate the value of ε in the region closest to the forest–atmosphere interface, where it would be expected that the action of the DTE would be most intense. Nevertheless, the variation of ε associated with the change of turbulent regime should provide interesting insights regarding the characteristics of each regime.

Figures 4a–c show the probability density functions for the values of the parameters z_i, L_h, and ε respectively, under turbulent regimes 1 (dashed line) and 2 (solid line). It can be seen from Fig. 4a that values of z_i are clustered approximately around 37 and 39.5 m for regimes 1 and 2, respectively. Figure 4b shows that the mean values of L_h are 7.5 and 14 m for regimes 1 and 2, respectively. Figure 4c shows that there is a clear difference between the ε values found for regimes 1 and 2. Thus, it may be concluded that for regime 2, the ε values are at least one order of magnitude greater than for regime 1.

It should be noted that the z_i values under regimes 1 and 2 appear to present a distinct but relatively small difference. This difference might result in a considerable increase in the radius of the DTE for regime 2 in comparison with regime 1 (the centre of the DTE should be in z_i). Thus, such a difference has important implications regarding both the capability of the DTE to penetrate downwards (regime 2) or not (regime 1) deep into the canopy and the associated forest–atmosphere exchange processes.

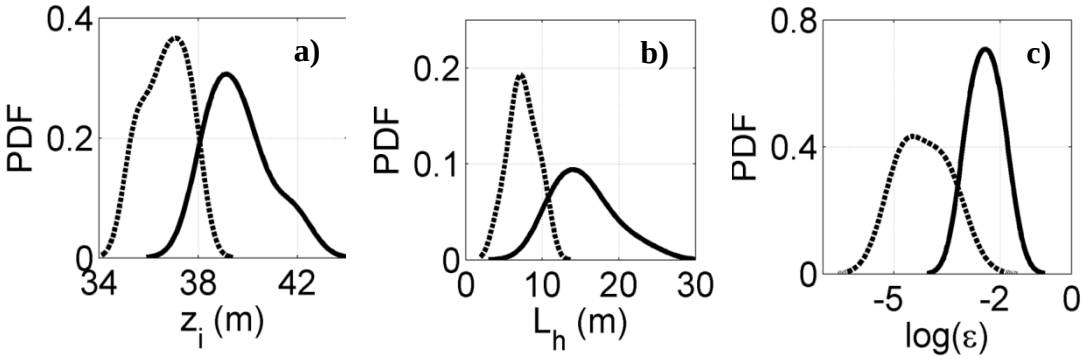

Fig 4 Probability Density Functions (PDFs) for: a) Inflection point height, z_i, (m); b) Wind shear length-scale, L_h, (m); c) logarithm of the viscous dissipation, ε, (m^2 s^{-3}). Dashed lines correspond to regime 1's occurrences and full lines correspond to regime's 2 ones.

When interpreting the above findings, it is important to consider the results of other researchers who also found variations in the height of the inflection point (z_i), above tall vegetation. For example, Thomas and Foken (2007), using data from a boreal forest in Germany, found that the z_i value varies as the direction of the average wind changes. However, Dupont and Patton (2012), using data obtained from a deciduous forest in California, found that the z_i value changes depending on whether the trees are in leaf.

Other results that deserve attention are those of Poggi et al. (2004). They used flow simulations in a wind tunnel to study the turbulent flow over canopies with different degrees of roughness. They noted clear inflection points in the vertical wind profiles of simulations of dense canopies; however, for sparse canopies, they were unable to observe such inflection points clearly. Nevertheless, according to Poggi et al. (2004), the intensity of the inflection in the wind profile influences the organization of turbulence above forest canopies. Moreover, the existence of strong vertical wind shear at the forest–atmosphere interface (and the consequent existence of z_i) is also a necessary condition for the emergence of Kelvin–Helmholtz instabilities, as discussed by Cheng et al. (2005) in their study regarding the performance of the Monin–Obukhov Similarity Theory in each of the four types of physical transient phenomena during the nights of the CASES-99 experiment. In addition, Finnigan (2000) states that inflection points in the vertical wind profile are typical characteristics of an atmospheric flow above tall vegetation and that their presence suggests the validity of the mixing-layer analogy, with flow layers that have different average speeds above and below z_i; thus, reinforcing the findings presented by Raupach et al. (1996).

4.4 Time Scale of Coherent Structures (CS)

CS are critical in the transfer of momentum and scalars at the forest–atmosphere interface (Thomas and Foken 2007, Steiner et al. 2011). Next to the treetops, such structures appear associated with an intense wind shear that is generated by the impact of the atmospheric flow on the canopy (Finnigan 2000, Dias-Júnior et al. 2013).

In this study, the time scales (D_e) of CS of u, w, and T were identified as shown in Figs. 5a–c, respectively. The dashed and continuous lines in Figs. 5a–c correspond to events in regimes 1 and 2, respectively. It can be seen that the values of D_e are significantly higher for regime 2 in comparison with regime 1, particularly for variables u and T. It is clear that the values of D_e in regime 1 for u, w, and T are about 68, 47, and 64 s, respectively, whereas they are about 87, 54, and 76 s, respectively, for regime 2.

According to Thomas and Foken (2005), the spectra of scalars are closer to the spectra of the horizontal velocity in the low-frequency region, in comparison to the vertical velocity. This leads to the conclusion that transport through low-frequency processes, such as the CS, is generally related more to horizontal transport. This behaviour could explain the similarities between the D_e values of u and T. Gao and Li (1993) offered another interesting explanation that used the time series of T and w to compare the time scales of the CS for different levels above and within a deciduous forest at Camp Borde, Canada. They observed that w-structures were shorter-lived than those of T. They explained such a result as a consequence of temperature changes caused primarily by nonlocal transport associated with movements induced by updrafts and downdrafts. However, changes in w can result both from organized movements and from atmospheric flow disturbances linked to turbulence generated by local interactions.

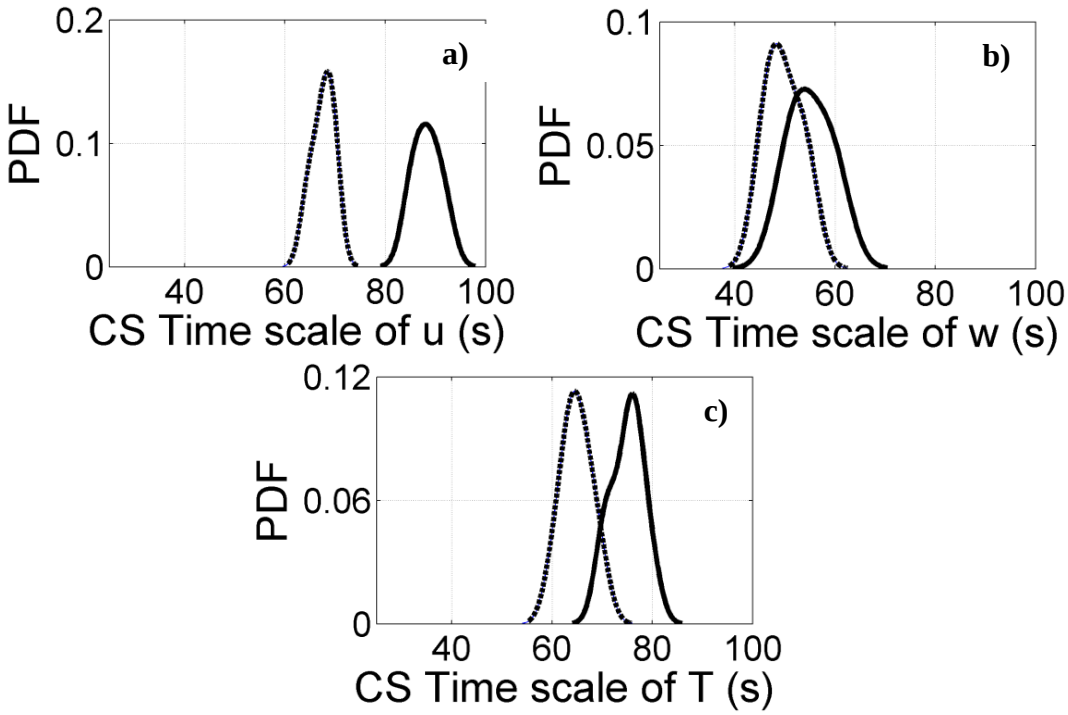

Fig 5 The same of the Fig. 4 but for the coherent strucuture time scale correspond to: a) horizontal wind velocity streamwise componente, u; b) vertical wind velocity component, w; c) temperature, T. Dashed lines correspond to regime 1's occurrences and full lines correspond to regime's 2 ones.

4.5. Case Study

In this section, special attention is given to an example of turbulent regime 2 (Julian day 45, from 2130 to 2150 local time) in which the vertical profiles of U (wind speed), T (temperature), and q (humidity) are shown for a long-lasting event (20 min) of turbulent-regime 2. This is based on data obtained at 10-s intervals, from above and within the forest canopy, using the meteorological tower in the Rebio Jarú forest reserve (see Table 1). It should be noted that less attention is given to the occurrence of regime 1 because it is the dominant state of the Amazonian nighttime period, and thus it has already been studied often (Fitzjarrald and Moore 1990, Kruijt et al. 2000).

4.5.1. Continuous Profiles of Temperature, Relative Humidity, and Wind Speed

Figures 6a–c show the continuous vertical profiles of temperature, relative humidity, and wind speed, respectively. A number of features can be observed during the occurrence of a regime-2 event: i) heating of the air within the canopy (Fig. 6a); ii) a decrease of relative humidity within the canopy (Fig. 6b); and iii) an increase in wind speed both above and within the forest canopy (Fig. 6c).

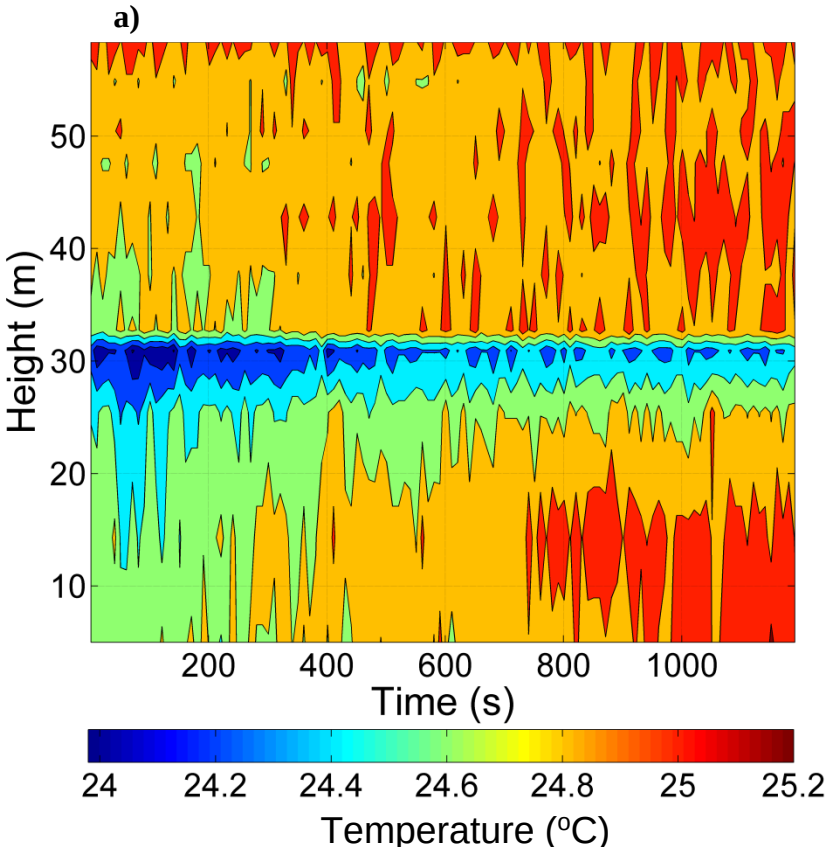
a)
Height (m)
50
40
30
20
10
200
400
600
800
1000
Time (s)
24
24.2
24.4
24.6
24.8
25
25.2
Temperature (°C)

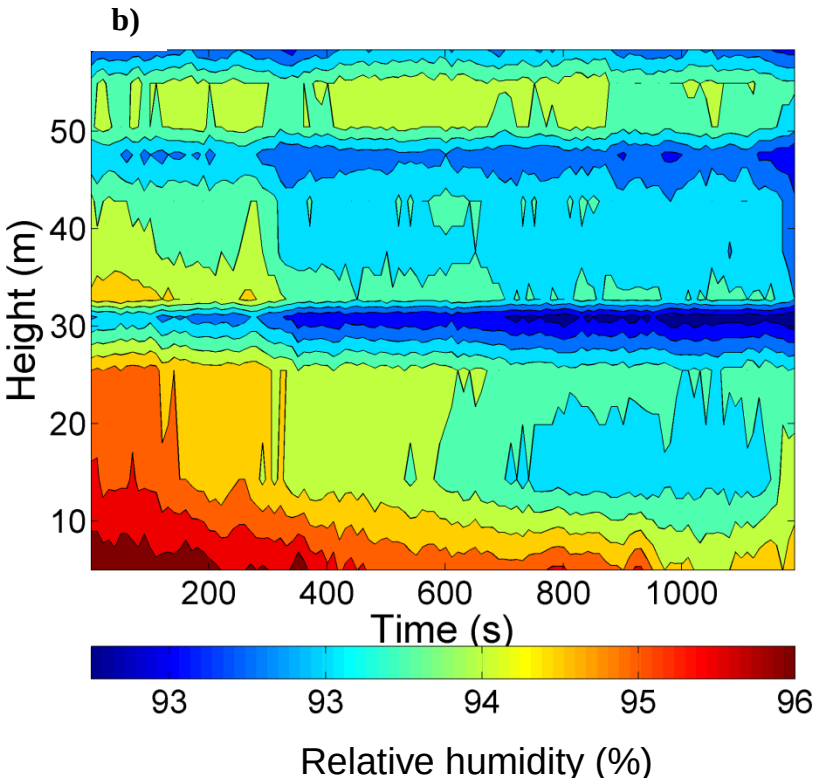
b)
Height (m)
50
40
30
20
10
200
400
600
800
1000
Time (s)
93
93
94
95
96
Relative humidity (%)

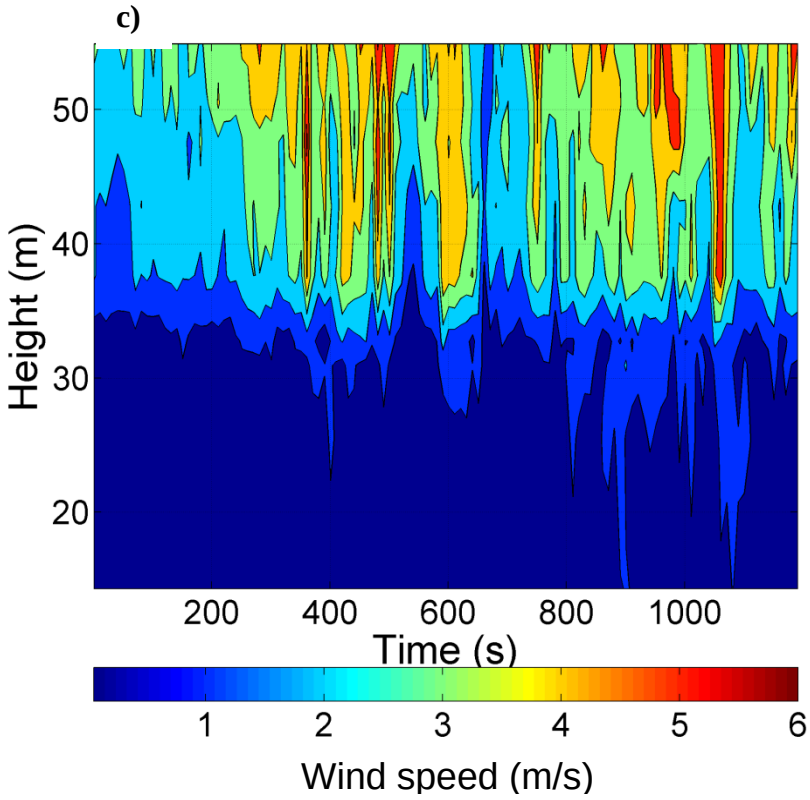

Fig 6 Contour plots regarding the evolution of: a) Temperature; b) relative humidity and c) wind speed for a case study concerning the turbulent regime 2 (Julian day 45 from 21:30 to 21:50 local time).

There are a number of noteworthy results discernible in Figs. 6a and b. For example, the height of approximately 32 m denotes the clear separation between the processes above and below the forest canopy. This level probably corresponds to what was called the "thermodynamic height" of the forest (h_t) by Cava and Katul (2008). Figure 6a shows a clear decrease and Fig. 6b shows a gradual increase in the thicknesses of the "blue bands", indicating temperatures between 24.0 and 24.4 °C and relative humidity values between 92% and 93.5%, respectively. Within the forest canopy, there is a tendency for this environment in warm and dry at all the observed levels. In Fig. 6b, in addition to the blue band at h_t, there is also another distinct line at the height of approximately 47 m. The blue band at approximately 32-m height is linked to the average height of the forest canopy and its interface with the atmosphere.

It is easy to understand why the minimum value of the vertical temperature profile is found at the canopy top, i.e., it is a consequence of the negative local radiation balance. Clearly, there is a net loss of energy in the treetop region through radiative processes, in which the upward longwave radiation component is not completely offset by the downward longwave component. Molion (1987), in his analysis of the diurnal variability of the energy

budget over the Amazon rainforest in the Ducke reserve (central Amazon), has shown that the deficit in the energy balance due to longwave radiation is of the order of 40 W m^{-2} at virtually all times of a typical day.

It should be noted that Shuttleworth et al. (1985) were among the first to analyse the evolution of temperature profiles above and within the Amazon rainforest. For this, they used data from a 45-m-high tower installed in the Ducke reserve in the central Amazon. According to them, in the absence of convective storms and episodes of rain, i.e., under dry conditions, the profiles of temperature, humidity, and moisture deficit have similar behaviours in two layers that are commonly decoupled during the night: "in the lower 2/3 of the canopy is partially decoupled from that at higher levels". This decoupling between the two layers is associated with a decrease in turbulent activity above the canopy, such that the radiative processes in the near-surface lower layer, among the internal layers of the vegetation, are responsible for the equilibrium of the heat balance. This would be the prevailing situation for those periods during which turbulent regime 1 is dominant. However, in turbulent regimes 2 and 3, such a situation does not hold. In regime 2, the strong winds and action of the DTEs penetrate into the canopy and disturb the thermal equilibrium, whereas in regime 3, top-down air movements, which could be associated with convective clouds and downdraughts, similarly disturb the thermal equilibrium.

The above analysis of Shuttleworth et al. (1985) regarding the nighttime period was focused mainly on hourly averages and there has been no attempt to separate them according to the characteristics of the turbulent regime. However, Fitzjarrald and Moore (1990) have studied nocturnal data obtained from the same location of the Ducke reserve and observed an alternation between periods of intense turbulent exchanges and weak turbulent transfers, but they did not expand their study into a quantitative analysis concerning the differences between these two processes. Mafra (2014) used data from an 80-m-high tower erected in the Uatumã reserve in the central Amazon (ATTO Project) and applied the SUN12 methodology to study the seasonal variability of CO_2 fluxes in each of the three turbulent regimes; substantial differences were found between the turbulent fluxes in regimes 1 and 2.

4.5.2. Temperature, Relative Humidity, and Wind Speed Profiles

For better visualization of the vertical profiles discussed above and their variations over a period of about 20 min (related to the studied case concerning the occurrence of turbulent regime 2), Figs. 7a and b present the average temperature profiles for the first 5 min (T_1) and last 5 min (T_2), respectively (shown in Fig. 6a, too); Fig. 7c shows their difference ($T_2 - T_1$).

Figures 7d and e are similar to Figs. 7a and b, but for profiles of relative humidity, providing (q_1) and (q_2) values, respectively, instead of (T_1) and (T_1); Fig. 7f shows their difference ($q_2 - q_1$).

It can be seen from Figs. 6a and 7a–c that at the origin of the time series (where the regime-2 episode starts), there is a greater T-gradient between the regions located above and below the forest canopy (Fig. 7a). However, it decreases considerably along the time line during the occurrence of regime 2, which is particularly true for the vertical T-gradient just above the forest canopy. Furthermore, during this episode, the vertical T-gradient within the canopy (between 15 and 25 m) appears to increase, and the vertical T-profile, observed between the heights of Z_2 = 47.5 m and Z_1 = 14.5 m ($T_2 - T_1$), is approximately linear between 15 and 50 m; this difference increases downwards until the 15-m level.

The vertical profile of relative humidity between the heights of Z_1 and Z_2, ($q_2 - q_1$) (Fig. 7e) also shows an approximately linear function between the heights of 15 and 50 m. However, unlike the temperature, it can be seen that relative humidity decreases (above and within the canopy) to the extent that the regime-2 episode evolves. Based on these considerations, it is possible to suggest that the DTEs are capable of bringing warmer and drier air from above into the region within the vegetation canopy.

Figures 7c and f show the positions of points $P1 \approx 14.5$ m, $PC \approx 31$ m, and $P2 \approx 47.5$ m. It is assumed that these points correspond to the inferior edge of the DTE, forest–atmosphere interface, and upper edge of the DTE, respectively. In the edge regions of the DTE, greater local shear would be expected, the existence of which would be reflected in the variables measured there. This assumption is based on the conspicuous discontinuity observed in the T-profile (exactly at points $P1$, PC, and $P2$), but less evident in the q-profiles at the same points ($P1$, PC, and $P2$). Cava and Katul (2008) have shown the existence of short-circuiting spectral effects on the atmospheric flow at the forest–atmosphere interface. Our assumption is that a similar effect should exist in the edge regions of the DTE.

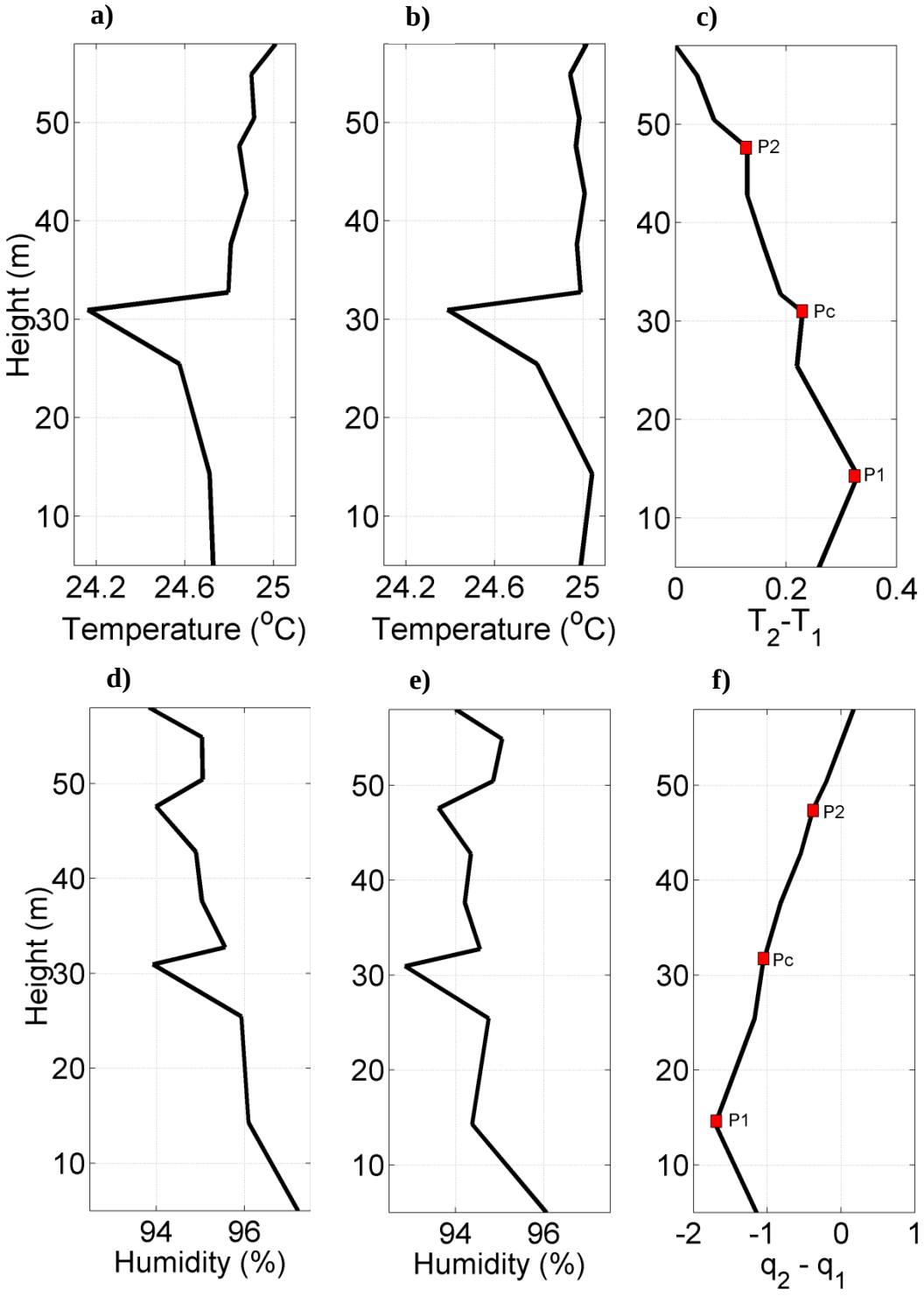

Fig 7 5 min-vertical profiles of a) mean temperature (T_1) for the earliest 5 min of the regime 2's event; b) the same but the latest 5 min mean temperature (T_2) of the same event. $T_2 - T_1$ values; d, e and f) the same for the a, b and c graphics, but for the relative humidity.

5 Discussion

Little attention has been given to the existence of an inflection point in a wind profile near vegetated surfaces. Consequently, a comprehensive theory that incorporates the

differences among the distinct nighttime turbulent regimes, and the physical consequences of their existence in the surface–atmosphere exchange processes, particularly above and within tall vegetation, is lacking. Robinson (1991) and Raupach et al. (1996) are among those authors who have associated the existence of the inflection point to a particular instability, which generates less-dissipative CS. Furthermore, according to Robinson (1991), there are different types of CS: some with an axis of symmetry arranged longitudinally along the atmospheric flow (more dissipative structures) and others with an axis of symmetry disposed transversely to the direction of dominant atmospheric flow, which are organized like rolls (less dissipative). It is possible that the latter are associated with the occurrence of instability, such as that of the inflection point, or even with the presence of Kelvin–Helmholtz instability (Starkenburg et al. 2013), possibly representing the turbulent conditions found in regime 2.

Furthermore, it has been observed that the different nocturnal turbulent regimes presented here are related to distinct conditions of the location of z_i. Based on Figs. 5–7, it is possible to suggest that one of the differences between turbulent regimes 1 and 2 is that the atmospheric flow associated with regime 2 presents greater inertia against surface drag forces, in such way that the value of z_i is higher, i.e., in regime 2, the upper part of the flow below z_i is shifted up (see observation Stull 1988, pp 534-535, regarding the formation of small nocturnal jets above sloping terrain). Thus, we suggest the following interpretation regarding regime 2: the locations of the DTEs are linked to the location of z_i, i.e., their structures present the centre of symmetry at the z_i level, as suggested by both Robinson (1991) and Raupach et al. (1996).

The existence of z_i determines specific features of the wind shear stress at level h (Raupach et al. 1996, Sá and Pachêco 2006, Dias-Júnior et al. 2013). This tension could be expressed by the L_h length scale (length associated with the depth of penetration of the flow into the canopy), which is closely linked with the mechanical action of the present DTE near the top of the forest's canopy. Thus, it is to be expected that in regime 2, the value of L_h, which is associated with a greater capability of penetration of a flow into the canopy, is higher when compared with conditions in which there is a smaller value of L_h (i.e., turbulent regime 1).

Moreover, it is observed that the temperature, relative humidity, and wind speed profiles (Figs. 6 and 7) corroborate the physical information contained in the values of z_i and L_h, and in accordance with this, the greater speed of the atmospheric flow in regime 2 might penetrate more deeply inside the canopy (greater L_h), with a downward transfer of warmer and drier air into the forest canopy during nighttime periods.

6 Conclusions

This study used data obtained from instruments on a 67-m-high tower, erected as part of the LBA project, in Rondônia in the west of the Brazilian Amazon. The arrangement of instruments on the tower favours research into the variability of the inflection point height in wind profiles. The possibility of estimating the inflection point height (z_i) facilitated an investigation into the effects of the existence of DTEs immediately above the forest canopy. Under certain circumstances, these DTEs play an active role in forest–atmosphere exchanges. The results obtained from the analysed situations confirm the validity of the so-called "mixing-layer analogy". A fundamental result is the existence of nocturnal turbulent regimes with different characteristics (action of the DTE, TKE dissipation rate, wind shear scale L_h, among others), which influence the height of z_i. The variations of these characteristics from one regime to another were investigated, and it was established that low wind regimes occur throughout much of the night, whereas regimes with high wind and/or situations of marked nonstationarity seldom occur and only for short periods. However, these are periods during which turbulent fluxes show values that are approximately one order of magnitude larger than during the regime of weak winds. Finally, it was observed that regime 3 was predominantly nonstationary, probably because of phenomena that originate far from the surface, such as convective clouds.

Acknowledgements This work is part of the Large-scale Biosphere-Atmosphere Experiment in Amazonia (LBA), and was supported by the Fundação de Amparo a Pesquisa do Estado de São-Paulo (FAPESP)/process 1997/9926-9. We would like to thank the Instituto Nacional de Colonização e Reforma Agrária (INCRA) and the Instituto Brasileiro do Meio Ambiente (IBAMA). Cléo Dias-Junior would like to acknowledge the support from IMK-IFU, Karlsruhe Institute of Technology (Garmisch-Partenkirchen, Germany) and is grateful to the Coordenação de Aperfeiçoamento de Pessoal de Nível Superior (CAPES) for his PhD's grant and to the Brazilian Government's Program "Ciência sem Fronteiras" grant (process 99999.002233/2014-02). Leonardo Sá and Edson Marques Filho are grateful to Conselho Nacional de Desenvolvimento Científico e Tecnológico (CNPq) for their research grants, (respectively, processes 303.728/2010-8 and 308597/2012-5).

References

Acevedo OC, Costa FD, Oliveira PE, Puhales FS, Degrazia GA, Roberti DR (2014) The Influence of Submeso Processes on Stable Boundary Layer Similarity Relationships. J Atmos Sci 71:207-225

Acevedo OC, Moraes OLL, Degrazia GA, Fitzjarrald DR, Manzi AO, Campos JG (2009) Is friction velocity the most appropriate scale for correcting nocturnal carbon dioxide fluxes? Agric For Meteorol 149:1-10

Andreae MO, Acevedo OC, Araùjo A, Artaxo P, Barbosa CGG, Barbosa HMJ, Brito J, Carbone S, Chi1 X, Cintra BBL, da Silva NF, Dias NL, Dias-Júnior CQ, Ditas F, Ditz R, Godoi AFL, Godoi RHM, Heimann M, Hoffmann T, Kesselmeier J, Könemann1 T, Krüger ML, Lavric JV, Manzi AO, Moran-Zuloaga D, Nölscher AC, Santos Nogueira D, Piedade MTF, Pöhlker C, Pösch U, Rizzo LV, Ro CU, Ruckteschler N, Sá LDA, Sá MDO, Sales CB, Santos RMND, Saturno1 J, Schöngart J, Sörgel M, de Souza CM, de Souza RAF, Su H, Targhetta N, Tóta J, Trebs I, Trumbore S, van Eijck A, Walter D, Wang Z, Weber B, Williams J, Winderlich J, Wittmann F, Wolff1 S, Yáñez-Serrano AM (2015) The Amazon Tall Tower Observatory (ATTO) in the remote Amazon Basin: overview of first results from ecosystem ecology, meteorology, trace gas, and aerosol measurements. Atmos Chem Phys Discuss 15:11599-11726

Andreae MO, Artaxo P, Brandão C, Carswell FE, Ciccioli P, Costa AL, Culf AD, Esteves JL, Gash JHC, Grace J, Kabat P, Lelieveld J, Malhi Y, Manzi AO, Meixner FX, Nobre AD, Nobre C, Ruivo MLP, Silva-Dias MA, Stefani P, Valentini R, von Jouanne J, Waterloo MJ (2002) Biogeochemical cycling of carbon, water, energy, trace gases, and aerosols in Amazonia: The LBA-EUSTACH experiments. J Geophys Res 107:D20 8066

Betts AK, Fisch G, von Randow C, Silva Dias MAF, Cohen JCP, da Silva R, Fitzjarrald DR (2009) The Amazonian boundary layer and mesoscale circulations. In: Keller M et al. Amazonia and Global Change, Geophysical Monograph Series. Washington, D. C, pp 163-181

Betts AK, Fuentes JD, Garstang M, Ball JH (2002) Surface diurnal cycle and Boundary Layer structure over Rondonia during the rainy season. J Geophys Res D: Atmos, 107:LBA 32

Bolzan MJA, Vieira PC (2006) Wavelet Analysis of the Wind Velocity and Temperature Variability in the Amazon Forest. Braz J Phys 36:1217-1222

Brunet Y, Irvine MR (2000) The Control of Coherent Eddies in Vegetation Canopies: Streamwise Structure Spacing, Canopy Shear Scale and Atmospheric Stability. Boundary-Layer Meteorol 94:139-163

Cava D, Donateo A, Contini D (2014) Combined stationary index for the estimation of turbulent fluxes of scalars and particles in the atmospheric surface layer. Agric For Meteorol 194:88-103

Cava D, Giostra U, Siqueira M, Katul G (2004) Organised Motion and Radiative Properties in the Nocturnal Canopy Sublayer above an Even-aged Pine Forest. Boundary-Layer Meteorol 112:129-157

Cava D, Katul GG (2008) Spectral Short-circuiting and Wake Production within the Canopy Trunc Space of an Alpine Hardwood Forest. Boundary-Layer Meteorol 126:415-431

Cheng Y, Parlange MB, Brutsaert W (2005) Pathology of Monin-Obukhov similarity in the stable boundary layer. J Geophys Res 110: 1-10

Collineau S, Brunet Y (1993) Detection of Turbulent Coherent Motions in a Forest Canopy. Part II: Time-scales and Conditional Averages. Boundary-Layer Meteorol 66:49-73

Costa FD, Acevedo OC, Mombach JCM Degrazia GA (2011) A Simplified Model for Intermittent Turbulence in the Nocturnal Boundary Layer. J Atmos Sci 68:1714-1729

Costa MH, Biajoli MC, Sanches L, Malhado ACM, Hutyra LR, Rocha HR, Aguiar RG Araújo AC (2010) Atmospheric versus vegetation controls of Amazonian tropical rain forest evapotranspiration: Are the wet and seasonally dry rain forests any different? J Geophys Res Biogeosci 115(G4)

Cuxart J, Yagüe C, Morales G, Terradellas E, Orbe J, Calvo J, Fernández A, Soler MR, Infante C, Buenestado P, Espinalt A, Joergensen HE, Rees JM, Vilà J, Redondo JM, Cantalapiedra IR, Conangla L (2000) Stable Atmospheric Boundary-Layer Experiment in Spain (SABLES 98): A Report. Boundary Layer Meteorol 96, 3: 337-370

Dias Júnior CQ, Sá LDA, Pachêco VB, de Souza CM (2013) Coherent structures detected in the unstable atmospheric surface layer above the Amazon forest. J Wind Eng Ind Aerodyn 115: 1-8

Dupont S, Brunet Y (2009) Coherent structures in canopy edge flow: a large-eddy simulation study. J Fluid Mech 630:93-128

Dupont S, Patton EG (2012) Influence of stability and seasonal canopy changes on micrometeorology within and above an orchard canopy: The CHATS experiment. Agric For Meteorol 157:11-29

Finnigan JJ (2000) Turbulence in plant canopies. Annu Rev Fluid Mech 32:519-571

Fitzjarrald DR, Moore KE (1990) Mechanisms of Nocturnal Exchange between the Rain Forest and the Atmosphere. J Geophys Res D: Atmos 95: 16839-16850

Foken T, Meixner FX, Falge E, Zetzsch C, Serafimovich A, Bargsten A, Behrendt T, Biermann T, Breuninger C, Dix S, Gerken T, Hunner M, Lehmann-Pape L, Hens K, Jocher G, Kesselmeier J, Lüers J, Mayer JS, Moravek A, Plake D, Riederer M, Rütz F, Scheibe M, Siebicke L, Sörgel M, Staudt K, Trebs I, Tsokankunku A, Welling M, Wolff

V Zhu Z (2012) Coupling processes and exchange of energy and reactive and non-reactive trace gases at a forest site – results of the EGER experiment. Atmos Chem Phys 12:1923-1950

Gao W, Li BL, (1993) Wavelet Analysis of Coherent Structures at the Atmosphere-Forest Interface. J Appl Meteorol 32:1717-1725

Garstang M, Fitzjarrald DR (1999) Observations of Surface to Atmosphere Interactions in the Tropics. Oxford University Press, New York, 405 pp

Garstang M, White S, Shugart HH, Halverson J (1998) Convective Cloud Downdrafts as the Cause of Large Blowdowns in the Amazon Rainforest. Meteorol Atmos Phys 67:199-212

Högström U, Bergström H (1996) Organized Turbulence in the Near-Neutral Atmospheric Surface Layer. J Atmos Sci 53:2452-2464

Kaimal JC, Finnigan JJ (1994) Atmospheric Boundary Layer Flows. Their Structure and Measurement. Oxford University Press, New York, 289 pp

Kruijt B, Malhi Y, Lloyd J, Nobre AD, Miranda AC, Pereira MGP, Culf A Grace J (2000) Turbulence Statistics Above and Within Two Amazon Rain Forest Canopies. Boundary-Layer Meteorol 94: 297-331

Mafra ACB (2014) Características das trocas turbulentas noturnas de CO2 entre a floresta de Uatumã, Amazonas, e a atmosfera. Master thesis, Universidade Federal do Pará, Brazil

Mahrt L (1998) Stratified Atmospheric Boundary Layers and Breakdown of Models. Theor Comput Fluid Dyn 11: 263-279

Mahrt L (2007) The influence of nonstationarity on the turbulent flux-gradient relationship for stable stratification. Boundary-Layer Meteorol 125:245-264

Mahrt L (2008) Mesoscale wind direction shifts in the stable boundary-layer. Tellus 60A:700-705

Molion LCB (1987) Micrometeorology of an Amazonian Rain Forest. In: The Geophysiology of Amazonia - Vegetation and Climate Interactions, Dickinson RE, Wiley-The United Nations University, New York, pp 255-272

Nepstad D, Lefebvre P, d. Silva UL, Tomasella J, Schlesinger P, Solorzano L, Moutinho P, Ray D, Benito JG (2004) Amazon drought and its implications for forest flammability and tree growth - a basin-wide analysis. Global Change Biol 10:704-717

Panofsky HA, Dutton JA (1984) Atmospheric Turbulence. Wiley, New York, 397 pp

Paw U KT, Brunet Y, Collineau S, Shaw RH, Maitani T, Qiu J, Hipps L (1992) On coherent structures in turbulence above and within agricultural plant canopies. Agric For Meteorol 61:55-68

Poggi D, Porporato A, Ridolfi L, Albertson JD, Katul GG (2004) The effect of vegetation density on canopy sub-layer turbulence. Boundary-Layer Meteorol 111:565-587

Poulos GS, Blumen W, Fritts DC, Lundquist JK, Sun J, Burns SP, Nappo C, Banta R, Newsom R, Cuxart J, Terradellas E, Balsley B, Jensen M (2002) CASES-99: A comprehensive investigation of the stable nocturnal boundary layer. Bull Am Meteorol Soc 83, 4: 555-581

Raupach MR, Finnigan JJ, Brunet Y (1996) Coherent Eddies and Turbulence in Vegetation Canopies: The Mixing-layer Analogy. Boundary-Layer Meteorol 78: 351-382

Robinson SK (1991) Coherent Motions in the Turbulent Boundary Layer. Annu Rev Fluid Mech 23:601-639

Sá LDA, Pachêco VB (2006) Wind Velocity above and inside Amazonian Rain Forest in Rondonia. Revista Brasileira de Meteorologia 21:50-58

Shuttleworth JW, Gash JHC, Lloyd CR, Moore CJ, Roberts J, Marques Filho AO, Fisch GF, Silva Filho VP, Ribeiro MNG, Molion LCB, Sá LDA, Nobre CA, Cabral OMR, Patel SR, Moraes JC (1985) Daily Variations of Temperature and Humidity within and above Amazonian Forest. Weather, 40.4: 102-108

Silva Dias MAFS, Rutledge S, Kabat P, Silva Dias P, Nobre C, Fisch G, Dolman H, Zipser E, Garstang M, Manzi A, Fuentes J, Rocha H, Marengo J, Plana-Fattori A, Sá LDA, Avalá RCS, Andreae M, Artaxo P, Gielow R, Gatti L (2002) Clouds and rain processes in a biosphere atmosphere interaction context in the Amazon Region. J Geophys Res D: Atmos 1984–2012 107(D20), LBA-39

Starkenburg D, Fochesatto GJ, Prakash A, Cristóbal J, Gens R, Kane DL (2013) The role of coherent flow structures in the sensible heat fluxes of an Alaskan boreal forest. J Geophys Res D: Atmos 118:8140-8155

Steiner AL, Pressley SN, Botros A, Jones E, Chung SH, Edburg SL (2011) Analysis of coherent structures and atmosphere-canopy coupling strength during the CABINEX field campaign: implications for atmospheric chemistry. Atmos Chem Phys Discuss 11:21013-21054

Stull RB (1988) An Introduction to Boundary Layer Meteorology. Kluwer, Dordrecht, 666 pp

Sun J, Burns SP, Lenschow DH, Banta R, Newsom B, Coulter R, Frasier S, Ince T, Nappo C, Cuxart J, Blumen W, Delany AC, Lee X, Hu XZ (2002) Intermittent Turbulence

Associated with a Density Current Passage in the Stable Boundary Layer. Boundary-Layer Meteorol 105:199-219

Sun J, Lenschow DH, Burns SP, Banta R, Newsom BK, Coulter R, Frasier S, Ince T, Nappo C, Balsley BB, Jensen M, Mahrt L, Miller D, Skelly B (2004) Atmospheric Disturbances that Generate Intermittent Turbulence in Nocturnal Boundary Layers. Boundary-Layer Meteorol 110:255-279

Sun J, Mahrt L, Banta RM, Pichugina YL (2012) Turbulence Regimes and Turbulence Intermittency in the Stable Boundary Layer during CASES-99. J Atmos Sci 69: 338-351

Thomas C, Foken T (2005) Detection of long-term coherent exchange over spruceforest using wavelet analysis. Theor Appl Climatol 80:91-104

Thomas C, Foken T (2007) Flux contribution of coherent structures and its implications for the exchange of energy and matter in a tall spruce canopy. Boundary-Layer Meteorol 123:317-337

Van de Wiel BJH, Moene AF, Hartogensis OK, De Bruin HAR, Holtslag AAM (2003) Intermittent Turbulence in the Stable Boundary Layer over Land.Part III. A Classification for Observations during CASES-99. J Atmos Sci 60:2509-2522

Vickers D, Göckede M, Law BE (2010) Uncertainty estimates for 1-hour averaged turbulence fluxes of carbon dioxide, latent heat and sensible heat. Tellus B 62:87-99

Vickers D, Mahrt L (1997) Quality Control and Flux Sampling Problems for Tower and Aircraft Data. J Atmos Oceanic Technol 14:512-526

Viswanadham Y, Molion LCB, Manzi AO, Sá LDA, Silva Filho VP, André RGB, Nogueira JLM, Dos Santos RC (1990) Micrometeorological Measurements in Amazon Forest during GTE/ABLE-2A Mission. J Geophys Res 95:13669-13682

Von Randow C, Sá LDA, Prasad GSSD, Manzi AO, Arlino PRA, Kruijt B (2002) Scale Variability of Atmospheric Surface Layer Fluxes of Energy and Carbon over a Tropical Rain Forest in Southwest Amazonia. I. Diurnal Conditions. J Geophys Res D: Atmos 107:D20 8062

von Randow C, Zeri M, Restrepo-Coupe N, Muza M. N, Gonçalves LGG, Costa MH, Araújo AC, Manzi AO, Rocha HR, Saleska SR, Alaf Arain M, Baker IT, Cestaro BP, Christoffersen B, Ciais P, Fisher JB, Galbraith D, Guan X, van der Hurk B, Ichii K, Imbuzeiro H, Jain A, Levine N, Miguez-Macho G, Poulter B, Roberti DR, Sahoo A, Schaefer K, Shi M, Tian H, Verbeeck H Yang Z.-L (2013) Inter-annual variability of carbon and water fluxes in Amazonian forest, Cerrado and pasture sites, as simulated by terrestrial biosphere models. Agric For Meteorol 182-183:145-155

Zeri M, Sá LDA (2011) Horizontal and Vertical Turbulent Fluxes Forced by a Gravity Wave Event in the Nocturnal Atmospheric Surface Layer over the Amazon Forest. Boundary-Layer Meteorol 138:413-431

Zeri M, Sá LDA, Manzi AO, Araújo AC, Aguiar RG, von Randow C, Sampaio G, Cardoso FL, Nobre CA (2014) Variability of Carbon and Water Fluxes Following Climate Extremes over a Tropical Forest in Southwestern Amazonia. PLoS One 9. 2: e88130

Zeri M, Sá LDA, Nobre CA (2013) Estimating Buoyancy Heat Flux Using the Surface Renewal Technique over Four Amazonian Forest Sites in Brazil. Boundary-Layer Meteorol 149:179-196

Capítulo 4

Dias-Junior, C.Q. Marques Filho, E.P. Sá, L.D.A. 2015. LES applied to analyze the turbulent flow organization above amazon forest. *Submetido para Journal of Wind Engineering and Industrial Aerodynamics.*

LES applied to analyze the turbulent flow organization above amazon forest

Cleo Q. Dias-Junior[1,2]; Edson P. Marques Filho[3]; Leonardo D. A. Sá[4].

1 - Federal Institute of Education Science and Technology of Pará/Bragança, Brazil

2 - National Institute of Amazonian Research / CLIAMB, Manaus, Brazil

3 - Federal University of Bahia, Salvador, Brazil

4 - National Institute for Space Research/CRA, Belém, Brazil

Corresponding author: cleo.quaresma@ifpa.edu.br

Abstract The occurrence of coherent structures (CSs) above the Amazon forest is analyzed. To perform this study, Large Eddy Simulation is used, which has been improved by the introduction of a drag force which is representative of a typical Amazon forest canopy. The simulation's results show that the flow is sensitive to the presence of canopy and an inflexion point is simulated in wind profiles. In addition, the profiles of momentum flux and turbulent kinetic energy are similar to those obtained experimentally. On the region between *1h* and *4h* several CSs features associated with turbulent flow regarding pressure, momentum fluxes, skewness and vorticity fields are detected suggesting that "roll" structures arranged perpendicularly to the mean wind direction populate this region. It is interesting to mention that: i) the skewness of the wind velocity has also a maximum value on the region, what indicates an asymmetric distribution of the wind velocity relatively to its mean value, fact that might be associated to the generation process of the "roll" structures; ii) the horizontal vorticity component transversal to the mean wind direction is greater than the vorticity components on the other orthogonal directions suggesting that "roll" structures move perpendicularly to the mean wind direction.

Keywords: LES; Rougness sublayer; Reynolds stress; Coherent strucuture; Amazon forest.

1. Introduction

It is well known that forests play an important role in the mass, energy and momentum exchange processes between vegetation and the atmosphere (Fitzjarrald et al., 1990; Kruijt et al., 2000; von Randow et al., 2004). Tropical forests, such as the Amazonian, require special attention, since are characterized by an energy balance at the forest canopy in which the latent heat fluxes are greater than the sensible heat fluxes, with very low values of the Bowen ratio

(in general, less than 0.4), what strongly contributes to the warming of the tropical troposphere (Silva Dias et al., 2002;. von Randow et al., 2002; Betts et al., 2009). Furthermore, the availability of water for evaporation processes directly affects several feedback processes spanning clouds generation, turbulent transport, radiative exchanges, hydrological processes and ecophysiological issues (Betts, 2004; Betts et al., 2009; Restrepo-Coupe et al., 2013; Zeri et al., 2014). In recent decades many researchers performed a lot of effort for a better understanding of exchanges between the Amazon forest and the atmosphere, particularly the turbulent processes (Fitzjarrald et al., 1990; Kuijt et al., 2000; Silva Dias et al, 2002; von Randow et al, 2002; Zeri and Sá, 2011; Dias-Junior et al., 2013; Zeri et al., 2014). With this objective, large experimental projects such as Amazonian Region Micrometeorological Experiment (ARME), Global Troposphere experiments/*Amazon* Boundary Layer Experiment (GTE-ABLE), Brazilian *Amazonian* Climate Observation Study (ABRACOS), The large-scale Biosphere-Atmosphere Experiment in *Amazonia* (LBA) were carried out in order to have a more systematic view of the processes that occur in the Amazon forest's environment. One of the latest, LBA, was a multinational and interdisciplinary research program, whose main objective was to better understand climatological, ecological, biogeochemical and hydrological issues of Amazonia, as a regional entity, in a scenario with perspective of global climate change (Avissar and Nobre, 2002).

However, studies with experimental data still present certain restrictions, such as: i) difficulties in accurately determining the height of the rough sublayer and its diurnal and seasonal variability; ii) understand the aspects of the turbulence structure at different heights above the canopy, particularly as regards the characteristics of the existing eddies within the inner, outer and transition layers (McNaughton and Laubach, 2000; Malhi et al., 2004) and what are the possible relationships they have among themselves; iii) the difficulty in understanding why, under certain conditions, there may be cases involving active turbulence or non-active turbulence (Högström, 1990).

An alternative to overcome this problem is through the use of Large Eddy Simulation (LES), a three-dimensional modeling procedure which: i) directly resolved the major turbulent flow structures, which contain most of the flow energy and occurs at the atmospheric boundary layer larger scales; ii) is intended for parameterize only the smallest turbulent structures, generally associated with the inertial subdomain region of the turbulence spectrum (Sagaut et al., 2006). LES is based on the assumption that the flow's structures in the smaller scales, such as those in the inertial subrange of developed turbulence, tend to be more homogeneous and isotropic and therefore less affected by the actual boundary conditions

(Smagorinsky, 1984). Thus, it can be expected that the modeling with respect to these scales have a universal character, i.e., less dependency on the type of flow being simulated (Maruyama et al., 1999; Pope, 2004).

Few studies using LES have been published in the international literature concerning the Amazon region. Among the few can be mentioned da Silva et al. (2011) who used the LES to investigate the role of latent heat flux and the consequent formation of clouds above a fluvial bay in the eastern Amazon and Vilà-Guerau de Arellano et al. (2011) who investigated the diurnal variability of the concentration of some chemical species in the Amazon region. However, practically have not studies that used LES to characterize the organization of the turbulent flow above the Amazon forest in order to obtain suitable information regarding some features of the turbulent flow within the roughness sublayer above the vegetation.

This work started with the entering a vertical profile of the leaf area index (LAI) into the LES model. This in order to validate the LES simulations against available experimental data of the LBA's "Rebio Jarú" reserve, in western Amazon, and also to obtain a better understanding of the organization of turbulence, its statistical moments, wind velocity and vorticity fields and vertical variability above and within the forest environment. In addition, CSs, in its sweep and ejection phases, are investigated for predominantly neutral conditions. In general the wind velocity fields generated by LES agree quite well with the available experimental data.

2. Experimental data

First a brief description will be made of Rebio Jarú forest reserve, since some of the parameters that were entered in the model (sensible heat flux, latent heat flux, the virtual potential temperature, specific humidity, height of the boundary layer, the Coriolis parameter) are experimental data collected there. This was performed to enter these parameters in order to make the simulations as realistic as possible.

The Jarú forest reserve (Rebio Jarú), located southwest of the Amazon, has an area of approximately 268,150 hectares between $10^0$05'S and $10^0$19'S and $61^0$35'W and 61°57'W, with altitude ranging from 100 m to 150 m above sea level. For more information on its climatology see Dias-Junior. et al. (2013). According Andreae et al. (2002) this forest reserve is characterized by area of native vegetation of tropical forest with an average height ranging between 30 m and 35 m, with some species reaching up to 45 m high. Marques Filho et al. (2005) reported LAI equal to 5.0 in the reserve. Fig. 1 shows the 60 m height aluminum

micrometeorlogical tower ($10^0$4.706'S and $61^0$56.027'W) which was provided with micrometeorological instruments, whose descriptions can be found in Zeri and Sá (2010).

Fig. 1. Picture showing the meteorological tower built at Rebio Jarú forest reserve and the surrounding vegetation.

3 Numerical methods

In this work we used the LES code originally developed by Moeng (1984) and modified by Moeng and Sullivan (1994). We simulated the turbulent flow within and above the Amazon forest. For this work be presented in a didactic way we will perform some basic descriptions of the LES's version used here and the modifications contained therein.

3.1. Numerical implementation

In LES models the separation between the solved scale and the subgrade one is obtained by applying a low-pass filter on the variables of the Navier-Stokes (N-S) equations (Eq 1, 2 and 3) for an incompressible fluid (Leonard, 1974; Sagaut et al., 2006, pp. 31). Thus, the variables filtered correspond to a volumetric average and describe the turbulent motions in the solved scale (Deardorff, 1972). Scales not explicitly solved by LES are parameterized. In

this work we shall use the symbols $\bar{x}$ and x'' to represent a variable x in any solved scale and subgride, respectively.

$$\frac{\partial \bar{u}}{\partial t} = \overline{\bar{u}\bar{\xi}_z} - \overline{\bar{w}\bar{\xi}_y} + f\bar{v} - \frac{\partial P^*}{\partial x} - \frac{\partial \langle \bar{P} \rangle}{\partial x} - \frac{\partial \tau_{xx}}{\partial x} - \frac{\partial \tau_{xy}}{\partial y} - \frac{\partial \tau_{xz}}{\partial z} \quad (1)$$

$$\frac{\partial \bar{v}}{\partial t} = \overline{\bar{w}\bar{\xi}_x} - \overline{\bar{v}\bar{\xi}_z} + f\bar{u} - \frac{\partial P^*}{\partial y} - \frac{\partial \langle \bar{P} \rangle}{\partial y} - \frac{\partial \tau_{xy}}{\partial x} - \frac{\partial \tau_{yy}}{\partial y} - \frac{\partial \tau_{yz}}{\partial z} \quad (2)$$

$$\frac{\partial \bar{w}}{\partial t} = \overline{\bar{u}\bar{\xi}_y} - \overline{\bar{v}\bar{\xi}_z} + \frac{g\bar{\theta}}{\theta_0} - \frac{\partial P^*}{\partial z} - \frac{\partial \tau_{xz}}{\partial x} - \frac{\partial \tau_{yz}}{\partial y} - \frac{\partial \tau_{zz}}{\partial z} - \langle \frac{\partial \bar{w}}{\partial t} \rangle \quad (3)$$

Here brackets denote horizontal averages ξ_x, ξ_y, ξ_z are the vorticity components in *x*, *y* and *z*, respectively. ρ_0 is the mass density of air, *P* is the grid average pressure, g is the gravitational acceleration. τ_{ij} are the subgrid-scale Reynolds stresses. θ is the potential temperature, and θ_0 is the reference potential temperature (304 K in our simulations)

The equations of motion are solved numerically using a pseudoespectral method in horizontal directions and finite difference scheme of second order centered in space in the vertical direction. The temporal derivatives are discretized using the 2nd order Adams-Bashforth scheme, stable for small time steps (Mesinger and Arakawa, 1982). The numerical stability of the system is determined by calculating the number of Courant in each time step (Δt) (Courant et al., 1967). The lateral boundary conditions are assumed to be cyclic. The Monin-Obukhov similarity theory is used to estimate the momentum turbulent fluxes on the surface. This boundary is considered rigid, and with zero vertical velocity. The upper boundary condition is radiative, with zero vertical gradients for the horizontal components of wind speed and subgrid turbulent fluxes. For consistency, in LES model the vertical velocity is also zero at the grid top.

A numerical grid of 128 x 128 x 256 points distributed in an equally spaced way over an area of 2 x 2 Km^2 in the horizontal plane and up to 1 Km in the vertical direction was used, resulting in cells of 15.62 m on the horizontal direction and 3.9 m on the vertical direction. This resolution is large enough to capture numerous surface flow structures which often have length scales of the order of the canopy height on the horizontal direction, and of the order of one third of the canopy height on the vertical direction (Raupach et al., 1996; Finnigan, 2000).

It is important to mention that LES relies on directly resolving the large scales of turbulent motion. Furthermore subgrid scales have a little contribution to the total turbulent

momentum flux and energy (Edburg et al., 2012). For this reason in this present simulation we used only resolved scales.

3.2. Canopy structure

The drag imposed by the forest canopy upon the atmospheric flow was introduced in the model by an additional force in the N-S equations. Such a force is expressed by the product of the drag coefficient (c_d), the leaf area density (LAD) and the square of the instantaneous velocity, as proposed by Patton et al. (2003). The drag force generated by the canopy ($\bar{F}$) is three-dimensional and time-dependent and can be written as follows (Shaw and Schumann, 1992; Patton et al., 2003; Dupont and Brunet, 2009):

$$\bar{\boldsymbol{F}} = -c_d LAD|\bar{\boldsymbol{u}}|\bar{\boldsymbol{u}} \quad (4)$$

where $|\bar{\boldsymbol{u}}|$ is the current resolved scalar wind speed and $\bar{\boldsymbol{u}}$ is the resolved velocity vector $(\bar{\boldsymbol{u}}, \bar{\boldsymbol{v}}, \bar{\boldsymbol{w}})$ in the (x, y, z) directions, where x refers to the downstream, y to the spanwise an z to the upward directions. Since the goal is to simulate the turbulent flow above the Rebio Jarú is important to use some parameters that incorporate the roughness of the Amazon forest into the model. Given that some researchers found parameters such as: i) LAI equal to 5.0, obtained by Marques Filho et al. (2005); ii) the average canopy height (h) equal to 35 m as mentioned by Andreae et al. (2002). These parameters were introduced into the LES model. In addition, was used LAD similar to that found by Marques Filho et al. (2005) in order to allow simulations to reproduce the turbulent flow in the Rebio Jarú forest reserve the most realistic way possible. Fig. 2 shows the vertical profile of the LAD encountered by Marques Filho et al. (2005) for the Rebio Jarú (gray area) and introduced into LES in this study (black line).

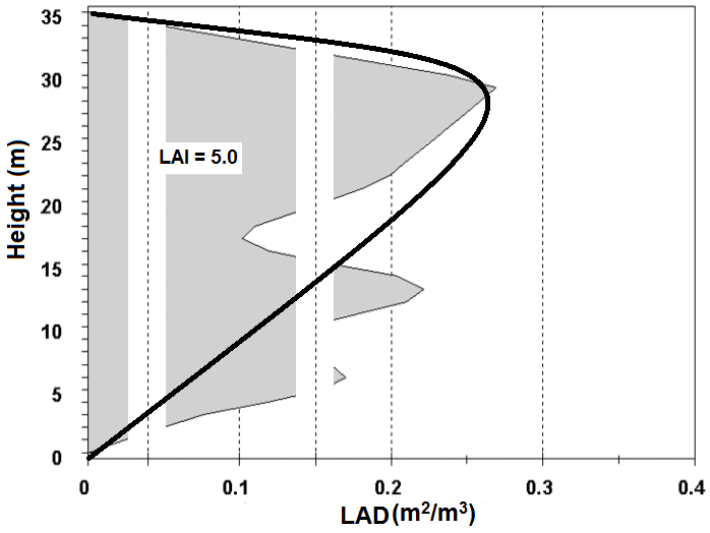

Fig. 2. Vertical Profile of leaf area density of the Rebio Jarú forest reserve (for LAI = 5.0): Found by Marques Filho et at. (2005) (gray region) and modifications inserted in the LES used in this work (black line).

3.3. Initial and boundary conditions

The initial objective of this study is to simulate the turbulent flow above and within the forest canopy for approximately neutral conditions (*h/L = -0.15*, where *L* is the Obukhov length). Therefore, the initial and boundary conditions, as well as external forcing, were chosen so as to generate a planetary boundary layer corresponding to an early morning convective period of (between *09 H* and *10 H*, local time). At this time the sensible heat flux is still low and the conditions of stability are still approaching to neutrality. Therefore, we used experimental data corresponding to the local time between 09 H and 10 H, for the Julian days between 40-45 of 1999. These data were entered into the model as initial condition (Table 1).

Table 1. simulations parameters and bulk statistics

Mean horizontal wind speed (*U*)	*3.5* $\boldsymbol{m/s}$
heat flux *(Q)*	*0.05* K/s
Coriolis parameter *(f)*	- 2.55 $x\ 10^{-5}\ s^{-1}$
Drag coeficiente $\boldsymbol{(c_d)}$	*0.30*
Inversion height $\boldsymbol{(z_i)}$	*500 m*
Obukhov length, *(L)*	*- 227 m*
Friction velocity $\boldsymbol{(u_*)}$	*0.52 m/s*

The initial vertical profiles of horizontal components of wind speed are assumed to be equal to the values of the components of the geostrophic wind (Fig. 3c). The initial vertical profiles of potential temperature and water vapor were established to play a mixed layer (ML) role with a potential temperature of 304 K (Fig. 3a) and specific humidity of 20 g/kg (Fig. 3b). This has been done in order to enter the humidity's buoyancy into the model, as a part of the virtual potential temperature θ_v (Stull, 1988, pp 275). These values are averages obtained with the experimental data. The depth of the ML was 500 m (Garstang and Fitzjarrald, 1999; Oliveira and Fisch, 2000). In the heat exchange in the ML, the θ_v value ranges from 3 K along a vertical length of 24 m (6 grid points) (Oliveira and Fisch, 2000). In the free atmosphere above the inversion layer, θ_v varies at a rate of approximately 4 K/ Km (Garstang and Fitzjarrald, 1999, pp. 261).

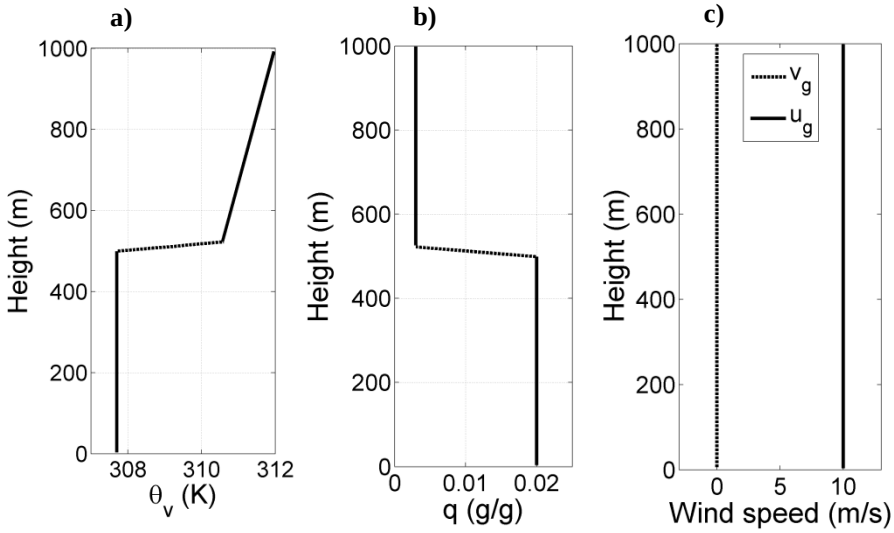

Fig. 3. Vertical profiles of (a) virtual potential temperature (θ_v); (b) specific humidity (q); (c) horizontal velocity components; used as initial condition in the LES.

4. Results

This paper aims to characterize the turbulent flow at the interface Amazon rainforest-atmosphere. For this, statistical moments of first, second and third order were calculated from the vertical profiles of wind speed found as results of LES modeling. These profiles correspond to the horizontally averaged statistics of the resolved flow field (streamwise and spanwise) for a given *z* (vertical location) as performed by Shen and Leclerc, 1997. 10,000 time steps (Δt) for all runs have been integrated, and the 4,000 initial Δt were needed to arrive at a computational equilibrium. Thus, temporal statistical analyzes were carried out based on the average field generated by LES after initial 4000 Δt, that is, when the turbulent fields exhibited a near-equilibrium condition. The mean fields were saved every 2000 Δt. It should be noted that throughout the simulation, a time step of 1s was kept fixed.

4.1. Mean statistical fields above the Amazon rainforest

Initially some vertical profiles of simulated variables are analyzed for: i) wind speed; ii) turbulent kinetic energy (TKE); iii) momentum flux; and iv) standard deviation of *u* and *w*. This is performed in order to compare our findings with those of other studies, both experimental as modeling ones, which also analyzed the turbulent flow over rough surfaces, like forests. This comparison is important as it will assess the ability of the LES model used in this work in simulating the turbulent flow over a forest with LAD similar to that found in the Amazonian rainforest.

Figs. 4a and 4b show vertical sections of the horizontal wind speed ($U = [u^2 + v^2]^{1/2}$) and of the TKE, respectively, both being normalized with the friction velocity, u_*, calculated at canopy top. Observing Fig. 3a, is detectable an inflection point on the vertical wind profile next the top of the canopy. This result is similar to those already obtained both experimentally above the Amazon rainforest (Sá and Pacheco 2006; Dias-Junior et al., 2013; de Souza et al., 2015) and in other forested regions (Raupach et al., 1996; Finnigan, 2000) as well as to the ones provided by LES modeling regarding several experimental fields (Shaw and Schumann, 1992; Patton et al. 2003; Finnigan et al., 2009; Edburg et al., 2012; Schlegel et al., 2014; and others) and also by wind tunnel experiments (Raupach, 1981; Marshall et al., 2002).

By observing the TKE profile of Fig. 4b it is possible to note that the turbulent energy is maximum near the top of the tree canopy and its value falls down rapidly within the forest canopy. This occurs as a consequence the action of the drag force imposed by the forest canopy (Raupach and Thom 1981; Meyers and Baldocchi, 1990; Shen and Leclerc, 1996; Dupont and Brunet, 2009). Above the vegetation is observed that TKE shows a gradual decay. Experimental studies (Shaw et al., 1988; Su et al., 1998) and modeling (Shen and Leclerc, 1996; Su et al., 1998; Dupont and Brunet, 2009; Edburg et al., 2012) also showed that TKE decreases rapidly inside the canopy, changing slowly or remaining constant above the treetops as obtained by LES simulation.

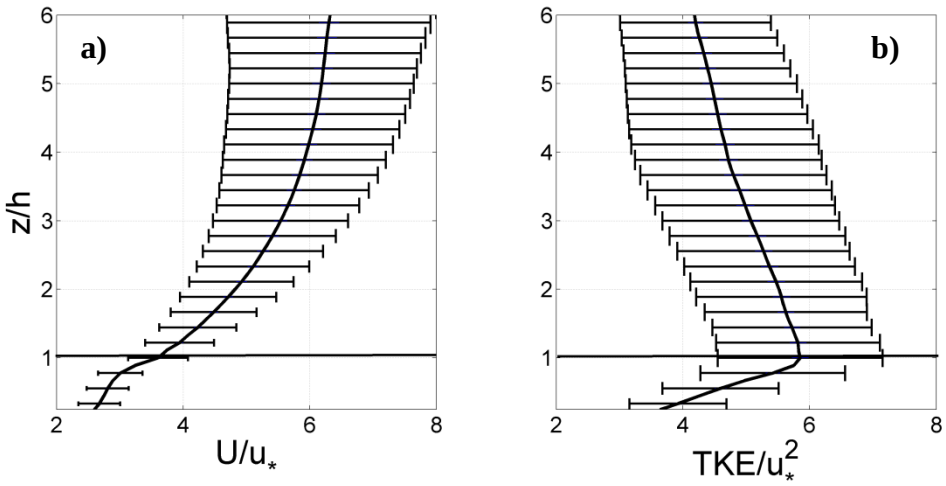

Fig. 4. Vertical profile: a) of horizontal wind speed and b) of turbulent kinetic energy. Both normalized by the fiction velocity calculated at canopy top.

Fig. 5a shows the vertical profiles of the standard deviations of u and w (σ_u and σ_w, respectively). It could be observed that both σ_u and σ_w, decrease with the decline of the

measurement height. However, above the trees σ_w practically does not change value, while σ_u decreases slightly with the height. Incidentally, Fitzjarrald et al. (1990) analyzed data from the Duke forest reserve, located in the central Amazon. They used three different measurement heights; one within the canopy (*0.67 h*) and the other two above the canopy (*1.12 h* and *1.27 h*). They showed that the σ_w values presented gentle variations above the canopy. However, within the vegetation, they observed that the σ_w value fell by half, compared with values above the canopy. Besides, Su et al. (1998) used data from a deciduous forest located in Canada with LAI equal to 2. For this forest they found a profile σ_u/u_* similar to the one obtained with our LES modeling. Several other studies have used the LES (Patton et al., 2003; Finnigan et al., 2009; Edburg et al., 2012) or wind tunnel (Raupach, 1981; Brunet et al., 1994; Marshall et al., 2002) to investigate the vertical profile of the behavior of σ_u/u_* and σ_w/u_*. The results in these other works closely approximate the results found here.

Fig. 5b shows the vertical profile of the normalized momentum flux $< w'u' >/u_*^2$. Note that there is a rapid decrease of $\langle w'u' \rangle/u_*^2$ with depth inside the canopy. On the other hand, above the forest canopy $\langle w'u' \rangle/u_*^2$ is practically constant. Is convenient to mention that Raupach et al. (1996) in their investigation about momentum absorption by several kind of vegetation canopies also noted that above the canopy $\langle w'u' \rangle/u_*^2$ is approximately constant with height, but declines rapidly within the crown's vegetation.

As observed by Raupach et al. (1996) $\langle w'u' \rangle/u_*^2$ tends to zero close to the ground, indicating that almost all the horizontal momentum was absorbed by the canopy.

Other studies using the LES to model the turbulent flow over forests, also reached similar results for $\langle w'u' \rangle/u_*^2$ (Su et al., 1998; Patton et al., 2003). Nevertheless some results with LES investigation suggest that $\langle w'u' \rangle/u_*^2$ is practically zero from the half of the canopy down (Finnigan et al., 2009; Edburg et al., 2012). However, these results were found for simulations where the LAI was less than 5.0, in which possibly the momentum flux between the regions above and within the forest canopy is quite different from that of the terra firme Amazonian forest, which is the goal of this investigation.

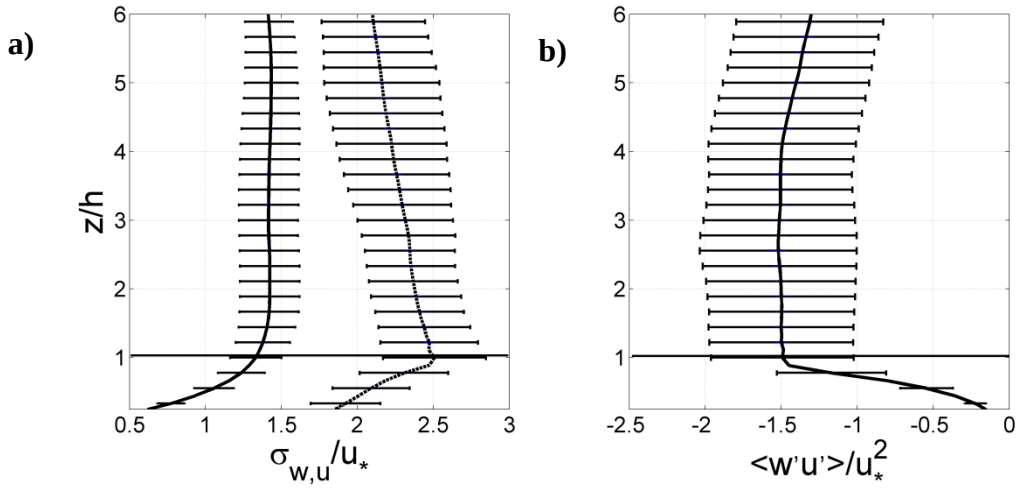

Fig. 5. Vertical profile: a) standard deviation of the streamwise velocity (dashed line) and standard deviation of the vertical velocity (solid line) and b) of momentum flux. Both normalized by the fiction velocity calculated at canopy top.

Based on the vertical profiles of *U, TKE,* σ_u, σ_w e $\langle w'u' \rangle$ it is possible to suggest that the turbulent flow above a vegetated surface with characteristics similar to the Amazon rainforest's ones, is being simulated quite well. As a next step, other profiles are analyzed, such as: i) sweep and ejection phases of CSs; ii) the correlation coefficient between the horizontal and vertical wind speed (r_{wu}); iii) skewness of the horizontal (Sk_u) and vertical (Sk_w) components of wind velocity; iv) standard deviation of pressure; v) vorticity field. Proceeding in such way is possible to obtain a more accurate picture of the turbulent flow organization over extremely rough surfaces, such as the Amazonian rainforest.

4.2. Sweeps and ejections.

It is expected that the momentum flux near the surface is negative, as momentum is always being transported downwards in order to be dissipated by friction in the regions closer to the surface. However, this negative value of momentum flux is associated with two physically quite different conditions, depending on the step of the CS's cycle above the canopy, namely: i) $u' > 0$ and $w' < 0$; ii) $u' < 0$ and $w' > 0$. In the first case, a flow's parcel with positive fluctuation of momentum is brought down into the canopy, and the second case, a flow's parcel with u-momentum's deficit is transferred upwards from the canopy.

Momentum flux $\langle w'u' \rangle$ can be partitioned into four associated quadrants in accordance with the signs of w' and u' (Raupach, 1981; Shaw et al., 1983). Several results from experimental data and from LES modeling have shown that the contributions from

ejections (quadrant 2: $w'> 0$ and $u' <0$) and sweeps (quadrant 4: $w'< 0$ and $u'> 0$) are the major constituents of the momentum fluxes, both above and within forest canopies (Raupach, 1981; Baldocchi and Meyers, 1988; Kanda and Hino, 1994; Finnigan, 2000; Dupont and Brunet, 2009; Finnigan et al., 2009; Dupont and Patton, 2012). In this work the sum of the sweep and ejection contributions for momentum fluxes corresponds approximately to 74% and 65% of the total flux above and within the canopy, respectively (not shown).

Fig. 6 shows the vertical profile of the ratio $R = \langle w'u' \rangle_4 / \langle w'u' \rangle_2$ between momentum flux for the sweep and ejection phases. It can be observed that within the vegetation, the sweeps contribute more significantly for $\langle w'u' \rangle$ than the ejections. A maximum *R* value is observed at the level $z \approx 0.7\ h$ (Sign I on the figure). According to Silva Dias et al. (2002), in the Rebio Jarú reserve this level approximately coincides with the zero-plane displacement height (*d*), the mean level of momentum absorption within the canopy (Jackson, 1981). Besides, Shen and Leclerc (1997) based on their LES results found that approximately at this $z \approx 0.7\ h$ level the pressure forces present its maximum intensity within canopy.

The situation above the canopy is exactly the opposite, i.e. ejections are more important than sweeps for the total flux of momentum. *R* depicts a minimum value, slightly less than 0.5, at the height $z \approx 3h$ (Sign II on the figure), and from this point upwards the value *R* decreases with height. It can also be noted that in the treetop $(z = h)$ the ejections and sweeps occur in approximately equal proportions.

Several experimental and simulation results have shown that sweep's intensity exceeds ejection's intensity within the vegetation (Raupach, 1981; Baldocchi and Meyers, 1988; Gao et al., 1989; Kanda and Hino, 1994; Shen and Leclerc, 1997; Su et al., 1998; Launiainen et al., 2007; Poggi and Katul, 2007; Dupont et al., 2008). However, in the forest-atmosphere interface and above the canopy there is some divergence between the results found in the literature. Several researchers, using experimental and LES data, found results similar to those obtained here, i.e. sweeps and ejections occur in approximately equal intensities in the forest-atmosphere interface. According with our results, from the treetop upwards the ejections start to dominate the total flux of momentum (Baldocchi and Meyers, 1988; Lee and Black, 1993a; Shen and Leclerc, 1997; Katul and Albertson, 1998; Su et al., 1998; Launiainen et al., 2007). However, other results showed that, at canopy top, the sweeps are primarily responsible for the generation of momentum flux (Raupach and Thom, 1981; Gao et al., 1989; Kanda and Hino, 1994; Poggi and Katul, 2007; Dupont et al., 2008).

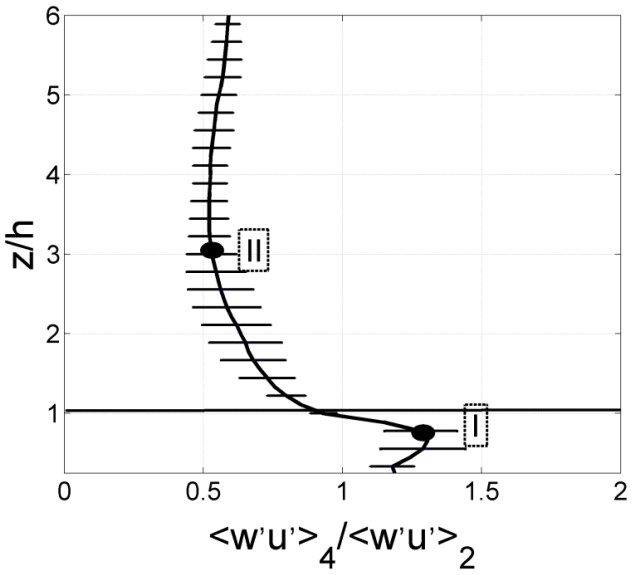

Fig. 6. Flux ratio: momentum flux by sweep ($w' < 0\ e\ u' > 0$) to that by ejection ($w' > 0\ e\ u' < 0$).

4.3. Efficiency of momentum transport.

An interesting feature of turbulent flow near the ground surface is that TKE generated near the inferior boundary is not always fully used to generate turbulent flux, that is, for the same values of $\overline{u'^2}$, $\overline{v'^2}$ and $\overline{w'^2}$ may be generated distinct values of $\overline{u'w'}$ e $\overline{v'w'}$, depending on specific environmental conditions (Högström, 1990; Katul et al., 1996). The understanding the causes of these differences provides information for a better understanding of the genesis of the turbulence structure near the surface.

The correlation coefficient $r_{wu} = \langle w'u' \rangle / \sigma_w \sigma_u$ might be interpreted as a measure of the efficiency of the turbulent field be able to generate turbulent flux. In order to illustrate this proposition, we present the Fig. 7, in which r_{wu} is plotted as a function of the normalized height. It is observed that r_{wu} decreased dramatically downward into the canopy (starting from sign I). In the region between *1 h* and *4 h* (between the signs I and II) r_{wu} practically does not change its value (r_{wu} varies between 0.42 and 0.43). Similar results was found by Raupach et al. (1996), using data from wind tunnel and from different vegetation cover, shown that immediately above the canopy r_{wu} has values around -0.5 with its intensity decreasing downward. Researchers such as Launiainen et al. (2007), using data from a pine forest located in Finland, showed that r_{wu} has maximum intensity near the top of the canopy (r_{wu} ranging between -0.4 and -0.5). Results applying LES above forest canopies also corroborate the results found here (Su et al., 1998; Dupont and Brunet, 2009). This reinforces

the conviction that our LES modeling results agree quite well with the main results presented in the literature.

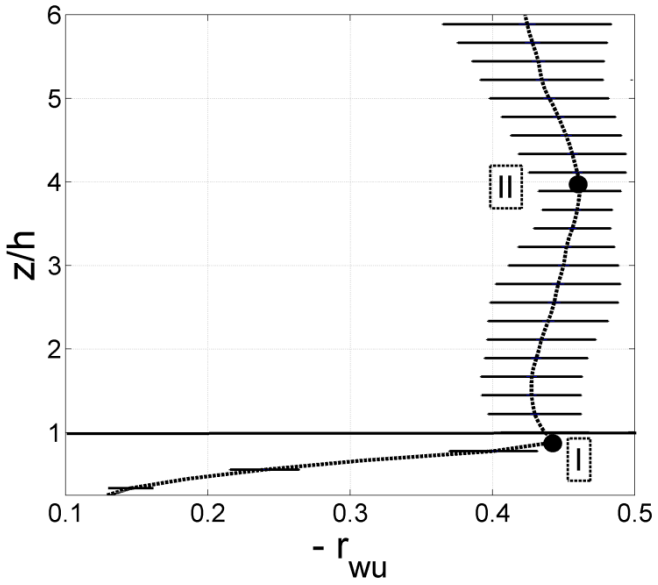

Fig. 7. Vertical profile of correlation coeficiente between *u* e *w* (r_{wu}).

4.4 Moments of third order for the wind speed.

(Sk_u) and (Sk_w), respectively, the skewnesses of *u* and *w*, are related to the degree of asymmetry of the probability distribution of *u* and *w* around their respective average values. The values of these parameters provide useful information about some features of momentum vertical transport in the forest-atmosphere interface in its various steps. Non-zero values of (Sk_u) and (Sk_w) are typical manifestations of the existence of heterogeneous turbulence (Lumley and Panofsky, 1964, pp. 94), since under turbulent conditions homogenous expected that the velocity distribution is Gaussian, with equal skewness to zero and kurtosis equal to 3 (Sorbjan, 1989, pp.41). Skewed processes are fundamental for the consolidation of an inhomogeneous turbulent field at the forest environment, even in the situations in which the roughness elements introduced in the simulation are horizontally homogeneous (as in the case of this simulation). Fig. 8 shows the vertical profile of Sk_u and Sk_w simulated for Rebio Jarú. It is possible to see that: i) in the forest-atmosphere interface (sign I) Sk_u and Sk_w show values close to zero; ii) Within the canopy Sk_u is positive and Sk_w is negative, as found also by several other researchers using experimental data (Baldocchi and Meyers, 1988a; Katul and Albertson, 1998; Su et al., 1998; Katul and Chang, 1999; Finnigan, 2000; 2000; Launiainen et al., 2007). According to Poggi and Katul (2004) there is a general trend of Sk_u be positive and Sk_w be negative within the canopy, which according to Baldocchi and Meyers

(1988) can be attributed to the greater intensity of turbulence at the canopy top, which is carried down by the negative fluctuations of *w'*. Poggi and Katul (2004) point out that in denser canopies there is a predominance of sweeps comparatively to ejections. This tendency will reflect on the signs of the skewnesses of u and w. iii) Above the forest canopy $Sk_u < 0$ and $Sk_w > 0$ and they change sign at the level *z/h = 1*, which corresponds to the mean tree height. From this level downwards Sk_u becomes negative and Sk_w becomes positive, what should be explained by the third order momentum budget at the Amazonian forest-atmosphere interface discussed by Fitzjarrald et al. (1990). Poggi and Katul (2004) point out those changes in sign of Sk_u and Sk_w, above the canopy, may be related to the fact that ejections dominate the turbulent changes of momentum there, as found in this simulation

It is important to mention that Fitzjarrald et al. (1990) are among the first researchers which used experimental data to calculate the Sk_w above and within the Amazonian forest (Ducke Reserve, in central Amazonia). They showed that Sk_w is positive above the canopy and becomes negative within the forest canopy during the day. At the canopy top Sk_w tends to zero. This findings corroborate the results presented here and those of other authors (Kruijt et al., 2000; Poggi and Katul, 2004; Dupont and Brunet, 2009).

Another interesting issue to be mentioned refers to the difference in the values of Sk_u and Sk_w as calculated on regions with distinct LAI values (Su et al., 1998; Katul and Poggi, 2004; Dupont and Brunet, 2009). According to Poggi and Katul (2004) these differences in the skewness values are a consequence of the fact that within canopies with greater LAI, sweeps and ejections are the main agents responsible for the generation of momentum flux within and above the canopy, respectively, as mentioned above. However, for less dense canopies, sweeps and ejections play similar roles concerning flux production.

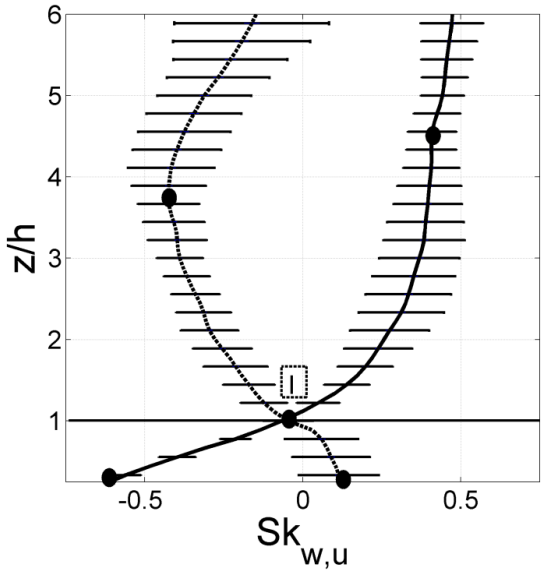

Fig. 8. Vertical profiles of skewness of *u* (dotted line) and *w* (solid line).

4.5. Standard deviation of pressure.

To start the analysis of the pressure in turbulent fields, it is important to take into account that the pressure action at a given point of the flow derives not only from local forcings, but depends on the integrated effect of velocity and temperature fields as a whole (Townsend, 1976, pp 43-44). According to the authors the pressure fluctuation in a turbulent flow results from the combined action of three main factors: i) the interaction between the mean velocity gradients and turbulent fluctuation gradients; ii) the fluctuations in the Reynolds stress acting on its average value; iii) the influence of buoyancy forces in inducing pressure fluctuations in the flow.

Obtaining of pressure fluctuations measurements in turbulent field is not an easely performed task, especially on works using experimental data, even the pressure fluctuation forces playing a very important role in the turbulent processes, particularly with regard to the return to isotropy term (Townsend, 1976, pp 165-166; Stull, 1988, pp 123). However, pressure fluctuations profiles are often used in work such as wind tunnel and LES (Su et al., 1998; Shen and Leclerc, 1997; Dupont and Brunet, 2009; Finnigan et al., 2009).

In this research the vertical profile of σ_p normalized by u_*, is showed in Fig. 9. It is possible to observe that σ_p decreased from the canopy top downward to the ground. From the canopy top upwards, σ_p increases until approximately *2.5 h* (sign II); above *2.5 h* σ_p practically does not change value reflecting the fact that at this level, the individual non homogeneities of the turbulent flow generated near the canopy top are no more capable to

influence the pressure field of the turbulence heterogeneous bottom boundary, with its impact objects and turbulent wakes (Griffin, 1981).

Another interesting feature of σ_p is that it presents an inflection point near the canopy top (sing I), almost at the same height in which an inflection point was detected on the wind profile, which seems to support the assumption of Raupach et al. (1996) regarding the existence of two superimposed layers in this region and the consequent presence of a like "mixing - layer" organization of the turbulence there.

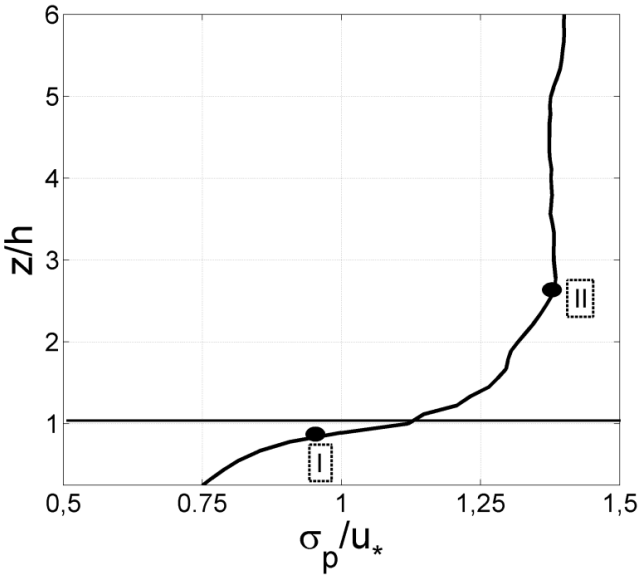

Fig. 9. Vertical profile of standard deviation of pressure normalized by u_*.

4.6. Vorticity.

Turbulent flows are essentially rotational since they present zones with considerable vorticity in a wide range of scales, which is expressed by the existence of vortex (regions in which the vorticity is concentrated) in a wide range of sizes (Abry, 1997, pp. 220). The vorticity at each point of the flow is defined as $\boldsymbol{\omega} = 1/2\ (\boldsymbol{\nabla}\ x\ \boldsymbol{u})$ (Feynman et al., 1964, Chap 40.5; Frisch, 1995, pp. 16). Authors such as Gerz et al. (1994) discussed the importance of the existence of a vorticity field in turbulent flow and its ability to generate CSs and vortex tubes, which can be better understood by analyzing the terms of the tendency of vorticity equation (Tennekes, 1985), particularly its term $\omega_j\ (\partial u_i/\partial x_j)$ entitled "stretching" and "twisting", where u_i is the velocity fluctuation in the *i*-direction, and $(\partial u_i/\partial x_j)$ is the gradient u_i in the *j*-direction (Aris, 1990, pp.88).

Thus, the vorticity field arranged in vortex tubes evolves over time in such way that the regions with high concentration of ω_j are stretched in the direction *j* and compressed in other directions, and ω_j may also have its rotation axis direction modified by the action of the

twisting term (Gerz et al., 1994; Abry, 1997, pp 221). According to these authors, this process is indirectly associated with a tendency of larger structures give rise to smaller ones.

It is important to note that the calculation of vorticity from experimental data, it is not a trivial task, since to carry out such procedure would request an experimental design quite sophisticated which is beyond the scope of this study. However, the calculation of vorticity with data from numerical simulations is often found in the literature (Gerz et al., 1994; Kanda and Hino, 1994; Dupont et al., 2008; Finnigan et al., 2009; Dupont and Brunet, 2009).

That said, is presented the Fig 10 which shows the vertical profile of vorticity in its three axes, which are arranged: i) along the mean flow direction (ω_x); ii) perpendicular to the mean flow direction (ω_y); and iii) vertical direction (ω_z). It is possible to see that ω_x, ω_y and ω_z are larger in the canopy top region, reducing its values upwards and downwards from this region. Similar results have been found by researchers using LES to simulate the turbulent flow over forests (Kanda and Hino, 1994; Finnigan et al., 2009; Dupont and Brunet, 2009). Moreover, it is noted that at the treetop ω_y vorticity is greater than the ones in the other two directions, suggesting that the dominant features present vortex rotation axis perpendicular to the direction of the dominant flow.

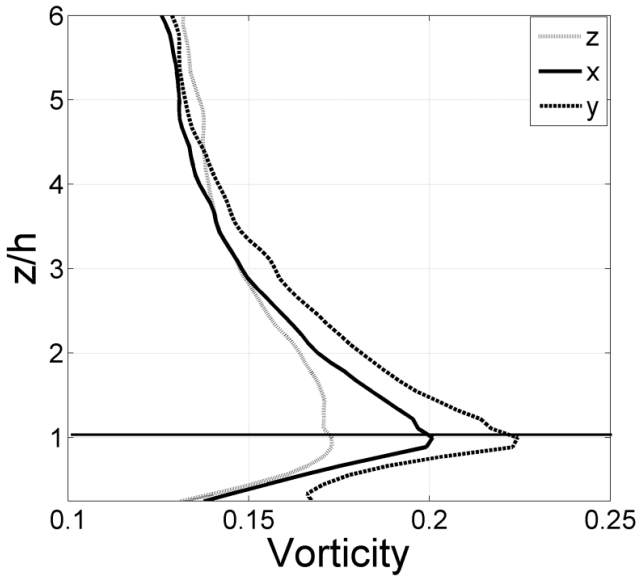

Fig. 10. Vertical profile of vorticity in the *x, y* and *z* directions.

4.7. Discussion.

In this work we used the LES to simulate the main features of turbulent flow, under neutral conditions, in a region with characteristics similar to those of the Amazonian rainforest. It is observed that in such situation, numerical flow simulation is capable to creating an inflection point in the vertical wind profile located at canopy top (Fig. 4a).

According to Kanda and Hino (1994), near the canopy top the inflection points in vertical profiles of wind velocity are continuously present on the flow due to the existing balance between pressure gradient and the drag generated by the canopy. Dupont and Brunet (2009) report that the development of an inflection point at canopy top leads to the Kelvin-Helmholtz instability, and as result, the presence of predominantly two-dimensional eddies in the form of rolls with axes of symmetry perpendicular the direction of the mean flow. As a consequence, they start to populate the flow near the treetop, in the so-called roughness sub-layer. In this research, in addition to obtaining realistic simulation of vertical profile of wind speed above and within the canopy, also has been researched the vorticity field in the region near the canopy top. The three components of the vorticity (ω) have been simulated. ω_x, ω_y and ω_z are the components of ω in the direction of the mean flow (U), transverse to U and vertical, respectively. As a result, there is the interesting fact that ω_y at canopy top is greater than ω_x and ω_z (Fig. 10). This greater ω_y value suggests that the vortices above the Amazonian rainforest are arranged in a way perpendicular to the mean flow (Robinson, 1991; Raupach et al., 1996; Finnigan et al., 2009). Furthermore, the maximum values found for the momentum flux (Fig. 5a), the values of r_{wu} (Fig. 7) and the turbulent intensities (σ_u and σ_w) in the region close to the canopy top (Fig 5b) would be connected among them generating rolls in forest-atmosphere interface in a similar way, as obtained by different authors in their studies concerning the flow over different types of tall vegetation (Kanda and Hino, 1994; Dupont et al.; 2008; Dupont and Brunet, 2009; Finnigan et al., 2009). It is also observed that near the canopy top, the occurrence of sweeps and ejections are practically equal in number (Fig. 6). This result confirms the findings of Kanda and Hino (1994), which found that in regions in which the like-roll structures occur, the generated sweeps and ejections have similar intensities.

Some researchers suggest that eddies generated above the canopy have a tilted elliptical shape (Ho and Huerre, 1984; Kanda and Hino, 1994; Dupont and Brunet 2009), as well shown by Dupont and Brunet (2009), pp 122, this tilted shape should help to explain the spatial distribution of sweep and ejection along the flow, while the elliptical shape of the eddies would be responsible for the existence of a momentum flux balance in this region. Ho and Huerre (1984) report that if the existing eddies would present circular shapes, there would be no dynamic conditions for the existence of momentum flux.

5. Conclusions

In this work we used the LES to simulate the turbulent flow within and above a forested region with surface roughness characteristics similar to those of the Amazonian rainforest. It was decided to simulate the flow under near neutral conditions. Unlike other studies that have used several parameterizations for represent turbulent exchanges in the LES in order to simulate the flow above a forest, in this study it is used only a drag force associated to a vertical profile of LAI to represent the Amazonian rainforest canopy. Such choice is based on the experimental evidence that in the roughness sublayer above the Amazonian rainforest, mechanical forces are the main generator of turbulent kinetic energy. As interesting results to mention, it is shown that the model used in this work represented fairly well the characteristics of turbulent flow within and above the Amazonian rainforest, what is presented in several analyses. It is observed that the modeled vertical profiles of statistical moments of first, second and third order are quite close to those found with experimental data. Furthermore, it was shown that the turbulent flow immediately above the canopy is populated by structures which are organized with symmetry axis perpendicular to the mean flow, known in the literature as *rolls*.

Acknowledgements

The authors would like to thank all people which directly or indirectly contributed to the fulfillment of the 1999 LBA-Intensive wet Campaign, and the support of the university in Ji-Paraná (UNIR), Instituto Brasileiro do Meio Ambiente e dos Recursos Naturais Renováveis (IBAMA) and Instituto Nacional de Colonização e Reforma Agrária (INCRA). This work was done under the LBA project framework, sponsered by the European Union, NASA, and Brazilian Agencies as the Conselho Nacional de Pesquisa e Desenvolvimento Tecnológico (CNPq) and the Fundação de Amparo à Pesquisa do Estado de São Paulo (FAPESP, process 01/06908-7). Cléo Dias-Junior is particularly grateful to CAPES for his PhD grant. Leonardo Sá is particularly grateful to CNPq for his research grant (process 303.728/2010-8). Edson Marques Filho is particularly grateful to CNPq for his research grant (process 308597/2012-5).

References

Abry, P., 1997. Ondelettes et turbulences: multirésolutions, algorithmes de décomposition, invariance d'échelle et signaux de pression, ed. Diderot, Paris.

Andreae, M.O., Artaxo, P., Brandão, C., Carswell, F.E., Ciccioli, P., Costa, A.L., Culf, A.D., Esteves, J.L, Gash, J.H.C., Grace, J., Kabat, P., Lelieveld, J., Malhi, Y., Manzi, A.O., Meixner, F.X., Nobre, A.D., Nobre, C., Ruivo, M.L.P., Silva Dias, M.A., Stefani, P., Valentini, R., von Jouanne, J., Waterloo, M.J., 2002. Biogeochemical cycling ofcarbon, water, energy, trace gases, and aerosols in Amazonia: the LBA-EUSTACH experiments. *Journal of Geophysical Research*. 33,1–25.

Aris, R., 1989. Vectors, Tensors and the Basic Equations of Fluid Mechanics, ed. Dover, New York.

Avissar, R., Nobre, C.A., 2002. Preface to special issue on the Large-Scale Biosphere-Atmosphere Experiment in Amazonia (LBA). *Journal of Geophysical Research: Atmospheres (1984–2012)*, *107*(D20), LBA-1.

Baldocchi, D.D., Meyers, T.P., 1988. Turbulence structure in a deciduous forest. *Boundary-Layer Meteorology*, *43*(4), 345-364.

Betts, A. K., 2004. Understanding hydrometeorology using global models. *Bulletin of the American Meteorological Society*, 85: 1673-1688.

Betts, A.K., Fisch, G., Von Randow, C., Silva Dias, M.A.F., Cohen, J.C.P., Da Silva, R., Fitzjarrald, D.R., 2009. The Amazonian boundary layer and mesoscale circulations. *Amazonia and Global Change*, 163-181.

Brunet, Y., Finnigan, J.J., Raupach, M.R., 1994. A wind tunnel study of air flow in waving wheat: single-point velocity statistics. *Boundary-Layer Meteorology*, *70*(1-2), 95-132.

Courant, R., Friedrichs, K., Lewy, H., 1967. On the partial difference equations of mathematical physics. *IBM journal of Research and Development*,11 (2), 215-234.

da Silva, R.R., Gandu, A.W., Sá, L.D., Dias, M.A.S., 2011. Cloud streets and land–water interactions in the Amazon. *Biogeochemistry*, *105*(1-3), 201-211.

de Souza, C.M., Dias-Junior, C.Q., Tóta, J., Sá, L.D.A., 2015. An empirical-analytic model to describe the vertical wind speed profile above and within amazon forest. *Meteorological Applications*. Submeted article.

Deardorff, J.W., 1972. Numerical investigation of neutral and unstable planetary boundary layers. *Journal of the Atmospheric Sciences*, 29:91-115.

Dias-Junior, C.Q., Sá, L.D.A., Pachêco, V.B., de Souza, C.M., 2013. Coherent structures detected in the unstable atmospheric surface layer above the Amazon forest. *Journal of Wind Engineering and Industrial Aerodynamics*, *115*, 1-8.

Dupont, S., Brunet, Y., 2009. Coherent structures in canopy edge flow: a large-eddy simulation study. *Journal of Fluid Mechanics*, *630*, 93-128.

Dupont, S., Brunet, Y., Finnigan, J.J., 2008. Large-eddy simulation of turbulent flow over a forested hill: Validation and coherent structure identification. *Quarterly Journal of the Royal Meteorological Society*, *134*(636), 1911-1929.

Dupont, S., Patton, E.G., 2012. Influence of stability and seasonal canopy changes on micrometeorology within and above an orchard canopy: The CHATS experiment. *Agricultural and Forest Meteorology*, *157*, 11-29.

Edburg, S.L., Stock, D., Lamb, B.K., Patton, E.G., 2012. The effect of the vertical source distribution on scalar statistics within and above a forest canopy. *Boundary-layer meteorology*, *142* (3), 365-382.

Feynman R.P., Leighton R.B., Sands M., 1964. *Lectures on Physics* I. Addison - Wesley.

Finnigan, J., 2000. Turbulence in plant canopies. *Annual Review of Fluid Mechanics*, *32*(1), 519-571.

Finnigan, J.J., Shaw, R.H., Patton, E.G., 2009. Turbulence structure above a vegetation canopy. *Journal of Fluid Mechanics*, *637*, 387-424.

Fitzjarrald, D.R., Moore, K.E., Cabral, O.M., Scolar, J., Manzi, A.O., Sá, L.D.A., 1990. Daytime turbulent exchange between the Amazon forest and the atmosphere. *Journal of Geophysical Research: Atmospheres (1984–2012)*, *95*(D10), 16825-16838.

Gao, W., Shaw, R.H., 1989. Observation of organized structure in turbulent flow within and above a forest canopy. *In Boundary Layer Studies and Applications* (pp. 349-377). Springer Netherlands.

Garstang, M., Fitzjarrald, D.R., 1999. Observations of surface to atmosphere interactions in the tropics. Oxford University Press.

Gerz, T., Howell, J., Mahrt, L., 1994. Vortex structures and microfronts. *Physics of Fluids* 3 1242-151.

Griffin, O.M., 1981. Universal Similarity in the Wakes and Vibrating Bluff Structures. *Journal of Fluids Engineering*, 103, 1: 52-58.

Ho, C. M., & Huerre, P. (1984). Perturbed free shear layers. *Annual Review of Fluid Mechanics*, *16*(1), 365-422.

Högström, U., 1990. Analysis of turbulence structure in the surface layer with a modified similarity formulation for near neutral conditions. *Journal of the atmospheric sciences*, *47*(16), 1949-1972.

Jackson, P.S., 1981. On the displacement height in the logarithmic velocity profile. *Journal of Fluid Mechanics*, 111, pp 15-25 doi:10.1017/S0022112081002279.

Kanda, M., Hino, M., 1994. Organized structures in developing turbulent flow within and above a plant canopy, using a large eddy simulation. *Boundary-Layer Meteorology*, *68*(3), 237-257.

Katul, G.G., Albertson, J.D., 1998. An Investigation of Higher-Order Closure Models for a Forested Canopy. *Boundary-Layer Meteorology*, 89, 1: 47-74.

Katul, G.G., Albertson, J.D., Parlange, M.B., Hsieh, C.I., Conklin, P.S., Sigmon, J.T., Knoerr, K.R., 1996. The "inactive" eddy motion and the large-scale turbulent pressure fluctuations in the dynamic sublayer. *Journal of the atmospheric sciences*. *53*(17), 2512-2524.

Katul, G.G., Chang, W.H., 1999. Principal length scales in second-order closure models for canopy turbulence. *Journal of Applied Meteorology*, *38*(11), 1631-1643.

Kruijt, B., Malhi, Y., Lloyd, J., Norbre, A.D., Miranda, A.C., Pereira, M.G.P., Grace, J. 2000. Turbulence statistics above and within two Amazon rain forest canopies. *Boundary-Layer Meteorology*, *94*(2), 297-331.

Launiainen, S., Vesala, T., Mölder, M., Mammarella, I., Smolander, S., Rannik, Ü., Katul, G.G., 2007. Vertical variability and effect of stability on turbulence characteristics down to the floor of a pine forest. *Tellus B*, *59* (5), 919-936.

Lee, X., Black, T.A., 1993. Atmospheric turbulence within and above a Douglas-fir stand. Part I: statistical properties of the velocity field. *Boundary-Layer Meteorology*, *64*(1-2), 149-174.

Leonard, A., 1974. Energy cascade in large-eddy simulations of turbulent fluid flows. In *Turbulent Diffusion in Environmental Pollution* (Vol. 1, pp. 237-248).

Lumley, J. L., Panofsky, H. A., 1964. *The Structure of Atmospheric Turbulence*. Wiley, 239 pp., New York.

Malhi, Y., Baker, T.R., Phillips, O.L., Almeida, S., Alvarez, E., Arroyo, L., ..., Lloyd, J., 2004. The above-ground coarse wood productivity of 104 Neotropical forest plots. *Global Change Biology*, *10*(5), 563-591.

Marques Filho, A.D.O., Dallarosa, R.G., Pachêco, V.B., 2005. Radiação solar e distribuição vertical de área foliar em floresta Reserva Biológica do Cuieiras ZF2, Manaus. *Acta Amazônica*, *35*(4), 427-436.

Marshall, B. J., Wood, C. J., Gardiner, B. A., & Belcher, R. E. (2002). Conditional sampling of forest canopy gusts. *Boundary-Layer Meteorology*, *102* (2), 225-251.

Maruyama, T., Rodi, W., Maruyama, Y., Hiraoka, H., 1999. Large eddy simulation of the turbulent boundary layer behind roughness elements using an artificially generated inflow. *Journal of Wind Engineering and Industrial Aerodynamics*, 83, 1–3, 381-392.

McNaughton, K.G., Laubach, J., 2000. Power spectra and cospectra for wind and scalars in a disturbed surface layer at the base of an advective inversion. *Boundary-layer meteorology*, *96*(1-2), 143-185.

Mesinger, F., Arakawa, A., 1976. Numerical Methods Used in Atmospheric Models. Volume I, Global Atmospheric Research Programme (GARP), WMO-ICSU Joint Organization Committee, GARP publications Series, Nº 17, 292 pp.

Meyers, T.P., Baldocchi, D.D., 1991. The budgets of turbulent kinetic energy and Reynolds stress within and above a deciduous forest. *Agricultural and forest meteorology*, *53*(3), 207-222.

Moeng, C.H., 1984. A large-eddy-simulation model for the study of planetary boundary-layer turbulence. *Journal of the Atmospheric Sciences*, *41*(13), 2052-2062.

Moeng, C.H., Sullivan, P.P., 1994. A comparison of shear-and buoyancy-driven planetary boundary layer flows. *Journal of the Atmospheric Sciences*, *51*(7), 999-1022.

Oliveira, P.J., Fisch, G., 2000. Efeitos da Turbulência na Camada Limite Atmosférica em áreas de Floresta e Pastagem na Amazônia. Revista Brasileira de Meteorologia, 15(2): 39–44.

Patton, E. G., Sullivan, P.P., Davis, K.J., 2003. The influence of a forest canopy on top-down and bottom-up diffusion in the planetary boundary layer. *Quarterly Journal of the Royal Meteorological Society*, *129* (590), 1415-1434.

Poggi, D., Katul,G.G., 2007. Turbulent flows on forested hilly terrain: the recirculation region. *Quarterly Journal of the Royal Meteorological Society*, *133*(625), 1027-1039.

Pope, S.B., 2004. Ten questions concerning the large-eddy simulation of turbulent flows. *New journal of Physics, 6* (1), 35.

Raupach, M.R., 1981. Conditional statistics of Reynolds stress in rough-wall and smooth-wall turbulent boundary layers. *Journal of Fluid Mechanics*, *108*, 363-382.

Raupach, M.R., Finnigan, J.J., Brunet, Y., 1996. Coherent Eddies and Turbulence in Vegetation Canopies: The Mixing-layer Analogy. *Boundary-Layer Meteorology,* 78,

Raupach, M.R., Thom, A.S., 1981. Turbulence in and above plant canopies. *Annual Review of Fluid Mechanics*, *13*(1), 97-129.

Restrepo-Coupe, N., da Rocha, H.R., Hutyra L.R., Alessandro C. Araujo, A.C., Borma, L.S., Christoffersen, B., Cabral, O.M.R., de Camargo, P.B., Cardoso, F.L., Lola da Costa,

A.C., Fitzjarrald, D.R., Goulden, M.L., Kruijt, B., Maia, J.M.F., Malhi, Y.S., Manzi, A.O., Miller, S.D., Nobre, A.D., von Randow, C., Sá, L.D.A., Sakai, R.K., Tota, J., Wofsy, S.C., Zanchi, F.B., Saleska, S.R., 2013. What drives the seasonality of photosynthesis across the Amazon basin? A cross-site analysis of eddy flux tower measurements from the Brasil flux network. *Agricultural and Forest Meteorology*, 182, 128-144.

Sá, L.D.A., Pachêco, V.B., 2006. Wind velocity above and inside Amazonian Rain Forest in Rondônia. *Revista Brasileira de Meteorologia*, *21*(3a), 50-58.

Sagaut, P., Deck, S., Terracol, M., 2006. *Multiscale and multiresolution approaches in turbulence (pp. 294-319)*. London: Imperial College Press.

Schlegel, F., Stiller, J., Bienert, A., Maas, H.G., Queck, R., Bernhofer, C., 2014. Large-eddy simulation study of the effects on flow of a heterogeneous forest at sub-tree resolution. *Boundary-Layer Meteorology*, 1-30.

Shaw, R.H., Den Hartog, G., Neumann, H.H., 1988. Influence of foliar density and thermal stability on profiles of Reynolds stress and turbulence intensity in a deciduous forest. *Boundary-Layer Meteorology*, *45*(4), 391-409.

Shaw, R.H., Schumann, U., 1992. Large-eddy simulation of turbulent flow above and within a forest. *Boundary-Layer Meteorology*, *61*(1-2), 47-64.

Shaw, R.H., Tavangar, J., Ward, D.P., 1983. Structure of the Reynolds stress in a canopy layer. *Journal of climate and applied meteorology*, *22*(11), 1922-1931.

Shen, S., Leclerc, M.Y., 1997. Modelling the turbulence structure in the canopy layer. *Agricultural and Forest Meteorology*, *87*(1), 3-25.

Silva Dias, M.A.F.S., Rutledge, S., Kabat, P., Silva Dias, P., Nobre, C., Fisch, G., Dolman, H., Zipser, E., Garstang, M., Manzi, A., Fuentes, J., Rocha, H., Marengo, J., Plana-Fattori, A., Sa, L.D.A., Avala, R.C.S., Andreae, M., Artaxo, P., Gielow, R., Gatti, L., 2002. Clouds and rain processes in a biosphere atmosphere interaction context in the Amazon region. *Journal of Geophysical Research*, 20, 1–46.

Smagorinsky, J., 1984: Some Historical Remarks on the Use of Nonlinear Viscosities. In: *Large Eddy Simulation of Complex Engineering and Geophysical Flows*.

Sorbjan Z., 1989. *Structure of the Atmospheric Boundary Layer*. Prentice-Hall, 317 pp., London.

Stull, R.B., 1988. *An Introduction to Boundary Layer Meteorology*, Kluwer, 666 pp., Dordrecht.

Su, H.B., Shaw, R.H., Paw, K.T., Moeng, C.H., Sullivan, P.P., 1998. Turbulent statistics of neutrally stratified flow within and above a sparse forest from large-eddy simulation and field observations. *Boundary-Layer Meteorology*, *88*(3), 363-397.

Tennekes, H., 1985. A Comparative Pathology of Atmospheric Turbulence in Two and Three Dimensions, In: Ghil, M., Benzi R., Parisi G., Turbulence and Predictability in Geophysical Fluid Dynamics and Climate Dynamics, Ed. North-Holland Physics Publishing, Amsterdam pp. 45-70.

Townsend, A.A., 1976. The Structure of Turbulent Shear Flow. ed. Cambridge University-Press, Cambridge.

Vilà-Guerau de Arellano, J., Patton, E.G., Karl, T., van den Dries, K., Barth, M.C., Orlando, J.J., 2011. The role of boundary layer dynamics on the diurnal evolution of isoprene and the hydroxyl radical over tropical forests. *Journal of Geophysical Research: Atmospheres (1984–2012)*, *116*(D7).

Von Randow, C., Manzi, A.O., Kruijt, B., De Oliveira, P.J., Zanchi, F.B., Silva, R.L., Kabat, P., 2004. Comparative measurements and seasonal variations in energy and carbon exchange over forest and pasture in South West Amazonia. *Theoretical and Applied Climatology*, *78*(1-3), 5-26.

von Randow, C., Sá, L.D., Gannabathula, P.S., Manzi, A.O., Arlino, P.R., Kruijt, B., 2002. Scale variability of atmospheric surface layer fluxes of energy and carbon over a tropical rain forest in southwest Amazonia 1. Diurnal conditions. *Journal of Geophysical Research: Atmospheres (1984–2012)*, *107*(D20), LBA-29.

Zeri M., Sá L.D.A., Manzi A.O., Araújo A.C., Aguiar R.G., von Randow C, Sampaio G., Cardoso F.L. Nobre C.A., 2014. Variability of Carbon and Water Fluxes Following Climate Extremes over a Tropical Forest in Southwestern Amazonia, *PLOS ONE*, 9, 2: e88130.

Zeri, M., Sá, L.D.A., 2010. The impact of data gaps and quality control filtering on the balances of energy and carbon for a Southwest Amazon forest. *Agricultural and forest meteorology*, *150*(12), 1543-1552.

Zeri, M., Sá, L.D.A., 2011. Horizontal and vertical turbulent fluxes forced by a gravity wave event in the nocturnal atmospheric surface layer over the Amazon forest. *Boundary-layer meteorology*, *138*(3), 413-431.

CONCLUSÕES

Foram usadas as facilidades oferecidas por uma torre de 67m de altura instalada na Amazônia ocidental, na reserva florestal Rebio-Jarú, em Rondônia. A organização dos instrumentos na torre favoreceu a investigação da variabilidade da altura do ponto de inflexão no perfil vertical do vento. Tal investigação facilitou a pesquisa de alguns aspectos da estrutura da turbulência atmosférica durante os períodos diurno e noturno acima da Rebio-Jarú.

Dentre os principais resultados do período diurno destacam-se: i) um modelo empírico-analítico capaz de descrever o perfil vertical de velocidade do vento acima e dentro da floresta amazônica. Esta formulação, fundamentada em parâmetros básicos tais como a altura do ponto de inflexão do perfil vertical do vento, o índice de área foliar, proporcionou um melhor ajuste para os dados experimentais medidos tanto acima quanto dentro do dossel; ii) uma correlação estatisticamente robusta entre a escala temporal de ocorrência das estruturas coerentes e a altura do ponto de inflexão. Tais resultados são importantes para melhorar o entendimento acerca da subcamada rugosa além de permitir parametrizações mais realistas dos processos de trocas entre a floresta e a atmosfera.

Para a camada limite noturna observou-se que os maiores valores da altura do ponto de inflexão estavam relacionados a situações em que era possível observar a existência de um vórtice turbulento dominante, imediatamente acima do dossel florestal. Tal vórtice, sob certas circunstâncias, desempenha um papel ativo nos processos de troca entre floresta-atmosfera. Outro resultado encontrado foi à existência de regimes turbulentos noturnos com características diferentes (taxa de dissipação de energia cinética turbulenta, escala de comprimento de cisalhamento do vento, escala temporal das estruturas coerentes, dentre outros), e que são influenciados pela altura do ponto de inflexão. Outro resultado importante foi: a) regimes de vento fraco são muito mais frequentes no período noturno; b) regimes de vento forte ou situações marcadamente não estacionárias ocorrem durante curtos intervalos de tempo. Entretanto, nestes regimes de ventos fracos os fluxos turbulentos são aproximadamente uma ordem de magnitudes maiores que aqueles onde os ventos são fracos.

Além dos resultados encontrados com dados experimentais, recorreu-se também a simulação dos grandes turbilhoes (Large eddy simulation - LES) para uma melhor compreensão de algumas características do escoamento turbulento acima de superfícies rugosas, tal como a floresta amazônica. Inseriu-se no LES uma força de arrasto representativa da Rebio-Jarú. Observou-se que o modelo simulou bem o escoamento turbulento acima e

dentro da floresta amazônica. Os perfis verticais modelados dos momentos estatísticos de primeira, segunda e terceira ordem foram muito próximos dos resultados mostrados na literatura, para dados experimentais. Além disso, mostrou-se que o escoamento turbulento imediatamente acima do dossel é povoado por estruturas que se organizam perpendicularmente a direção do escoamento médio, conhecidas, na literatura, como estruturas em forma de rolos.

REFERÊNCIAS BIBLIOGRÁFICAS

Acevedo, O. C.; Fitzjarrald, D. R. 2003. In the Core of the Night - Effects of Intermittent Mixing on a Horizontally Heterogeneous Surface. *Boundary-Layer Meteorology*, 106:1-33.

Acevedo, O. C.; Moraes, O. L. L.; Degrazia, G. A.; Fitzjarrald, D. R.; Manzi, A. O.; Campos, J. G. 2009. Is friction velocity the most appropriate scale for correcting nocturnal carbon dioxide fluxes? *Agricultural and Forest Meteorology*, 149:1-10.

Araújo, A. C.; Dolman, A. J.; Waterloo, M. J.; Gash, J. H. C.; Kruijt, B.; Zanchi, F. B.; Lange, J. M. E.; Stoevelaar, R.; Manzi, A. O.; Nobre, A. D.; Lootens R. N.; Backer, J. 2010. The spatial variability of CO_2 storage and the interpretation of eddy covariance fluxes in central Amazonia. *Agricultural and Forest Meteorology*, 150: 226-237.

Belušić, D.; Mahrt L. 2012. Is geometry more universal than physics in atmospheric boundary layer flow? *J. Geophys. Res*.,117, D09115.

Brunet Y.; Irvine, M. R. 2000. The Control of Coherent Eddies in Vegetation Canopies: Streamwise Structure Spacing, Canopy Shear Scale and Atmospheric Stability. *Boundary-Layer Meteorology*, 94(1): 139-163.

Campanharo, A. S. L. O.; Ramos, F. M.; Macau, E. E. N.; Rosa, R. R.; Bolzan M. J. A.; Sá, L. D. A. 2008. Searching Chaos and Coherent Structures in the Atmospheric Turbulence above Amazon Forest, *Philosophical Transactions of the Royal Society of London A, Mathematical and Physical Sciences*, 366 (1865): 579-589.

Cava, D.; Giostra, U.; Siqueira, M.; Katul, G. 2004. Organised Motion and Radiative Properties in the Nocturnal Canopy Sublayer above an Even-aged Pine Forest. *Boundary-Layer Meteorology*, 112:129-157.

Cava, D.; Katul, G. G. 2008. Spectral Short-circuiting and Wake Production within the Canopy Trunc Space of an Alpine Hardwood Forest. *Boundary-Layer Meteorology*, 126: 415-431.

Dias-Júnior, C. Q.; Sá, L. D. A.; Pachêco, V. B.; de Souza, C. M. 2013. Coherent structures detected in the unstable atmospheric surface layer above the Amazon forest. *Journal of Wind Engineering & Industrial Aerodynamics* 115: 1-8.

Doughty, C. E.; Goulden, M. L. 2008. Seasonal patterns of tropical forest leaf area index and CO_2 exchange. *Journal of Geophysical Research: Biogeosciences* (2005–2012), 113(G1).

Eder, F.; Serafimovich A.; Foken, T. 2013. Coherent Structures at a Forest Edge: Properties, Coupling and Impact of Secondary Circulations. *Boundary-Layer Meteorology*, 148: 285-308.

Finnigan, J. J. 2000. Turbulence in plant canopies. *Annual Review of Fluid Mechanics*, 32: 519-571.

Finnigan, J. J.; Shaw R. H.; Patton, E. G. 2009. Turbulence structure above a vegetation canopy, *Journal of Fluid Mechanics*, 637: 387-424.

Högström, U.; Bergström, H. 1996. Organized Turbulence in the Near-Neutral Atmospheric Surface Layer. *Journal of the Atmospheric Sciences*, 53(17): 2452-2464.

Kruijt, B.; Malhi, Y.; Lloyd, J.; Norbre, A.D.; Miranda, A.C.; Pereira, M.G.P.; Grace, J. 2000. Turbulence statistics above and within two Amazon rain forest canopies. *Boundary-Layer Meteorology*, 94(2), 297-331.

Mafra, A. C. B. 2014. *Características das trocas turbulentas noturnas de CO_2 entre a floresta de Uatumã, Amazonas, e a atmosfera*. Dissertação de Mestrado Universidade Federal do Pará, Belém, Pará.

Mahrt, L. 1998. Stratified Atmospheric Boundary Layers and Breakdown of Models. *Theoretical and Computational Fluid Dynamics*, 11: 263-279.

Mahrt, L. 1999. Stratified Atmospheric Boundary-Layers. *Boundary-Layer Meteorology*, 90: (3): 375-396.

Mahrt, L. 2000. Surface Heterogeneity and Vertical Structure of the Boundary Layer. *Boundary-Layer Meteorology*, 96 (1-2): 33-62.

Mahrt, L.; Sun, J.; Vickers, D.; MacPherson, J. I.; Pederson J. R.; Desjardins, R. L. 1994. Observations of Fluxes and Inland Breezes over Heterogeneous Surface. *Journal of the Atmospheric Sciences*, 51 (17): 2484-2499.

Marshall, B. J.; Wood, C. J.; Gardiner B. A.; Belcher, B. E. 2012. Conditional Sampling of Forest Canopy Gusts, *Boundary-Layer Meteorology*, 102: 225-251.

Pachêco, V. B. 2001. Algumas Características do Acoplamento entre o Escoamento Acima e Abaixo da Copa da Floresta Amazônica em Rondônia, INPE, São José dos Campos, SP, Dissertação de Mestrado em Meteorologia, 109 pp.

Paw U, K. T.; Brunet, Y.; Collineau, S.; Shaw, R. H.; Maitani, T.; Qiu J.; Hipps, L. 1992. On coherent structures in turbulence above and within agricultural plant canopies. *Agricultural and Forest Meteorology*, 61 (1-2): 55-68.

Poulos, G. S.; Blumen, W.; Fritts, D. C.; Lundquist, J. K.; Sun, J.; Burns, S. P.; Nappo, C.; Banta, R.; Newsom, R.; Cuxart, J.; Terradellas, E.; Balsley, B.; Jensen, M. 2002. CASES-99: A comprehensive investigation of the stable nocturnal boundary layer. *Bulletin of the American Meteorological Society*, 83(4): 555-581.

Princevac, M.; Hunt, J. C. R.; Fernando, H. J. S. 2008. Quasi-Steady Katabatic Winds on Slopes in Wide Valleys: Hydraulic Theory and Observations. *Journal of the Atmospheric Sciences*, 65: 627-643.

Raupach, M. R.; Finnigan, J. J.; Brunet, Y. 1996. Coherent Eddies and Turbulence in Vegetation Canopies: The Mixing-layer Analogy. *Boundary-Layer Meteorology*, 78(3-4): 351-382.

Robinson, S. K. 1991. Coherent Motions in the Turbulent Boundary Layer. *Annual Rev.of Fluid Mechanics*, 23: 601-639.

Sá L. D. A., Pachêco, V. B. 2006. Wind Velocity above and inside Amazonian Rain Forest in Rondonia., *Revista Brasileira de Meteorologia*, 21 (3a): 50-58.

Stewart R. W. 1969. Turbulence and waves in a stratified atmosphere, *Radio Science*, 4 (12): 1269-1278.

Sun, J.; Burns, S. P.; Lenschow, D. H.; Banta, R.; Newsom, B.; Coulter, R.; Frasier, S.; Ince, T.; Nappo, C.; Cuxart, J.; Blumen, W.; Delany, A. C.; Lee X.; Hu, X.-Z. 2002. Intermittent Turbulence Associated with a Density Current Passage in the Stable Boundary Layer, *Boundary-Layer Meteorology*, 105: 199-219.

Sun, J.; Mahrt, L.; Banta, R. M.; Pichugina, Y. L. 2012. Turbulence Regimes and Turbulence Intermittency in the Stable Boundary Layer during CASES-99. *Journal of the Atmospheric Sciences*, 69: 338-351.

Thomas, C.; Foken, T. 2007. Flux contribution of coherent structures and its implications for the exchange of energy and matter in a tall spruce canopy. *Boundary-Layer Meteorology*, 123: 317-337.

Turner, B. J.; Leclerc, M. Y.; Gauthier, M.; Moore K.; Fitzjarrald, D. R. 1994. Identification of turbulent structures above a forest canopy using a wavelet transform. *Journal of Geophysical Research*, 99 (D1): 1919-1926.

Van de Wiel, B. J. H.; Moene, A. F.; Hartogensis, O. K.; De Bruin H. A. R.; Holtslag, A. A. M. 2003. Intermittent Turbulence in the Stable Boundary Layer over Land.Part III. A Classification for Observations during CASES-99. *Journal of the Atmospheric Sciences*, 60: 2509-2522.

Van de Wiel, B. J. H.; Moene, A. F.; Ronda, R. J.; De Bruin H. A. R.; Holtslag, A. A. M. 2002b. Intermittent Turbulence and Oscillations in the Stable Boundary Layer over Land. Part II. A System Dynamica Approach. *Journal of the Atmospheric Sciences*, 59: 2567-2581.

Van de Wiel, B. J. H.; Ronda, R. J.; Moene, A. F.; De Bruin H. A. R.; Holtslag, A. A. M. 2002a. Intermittent Turbulence and Oscillations in the Stable Boundary Layer over Land. Part I. A Bulk Model. *Journal of the Atmospheric Sciences*, 59: 942-958.

Williams, C. A.; Scanlon, T. M.; Albertson, J. D. 2007. Influence of surface heterogeneity on scalar dissimilarity in the roughness sublayer. *Boundary-Layer Meteorology*, 122:149-165.

Yi, C. 2008. Momentum Transfer within Canopies. *Journal of Applied Meteorology and Climatology*. 47: 262-275.

Zeri, M.; Sá L. D. A., Nobre, C. A. 2014. Contribution of coherent structures to the buoyancy heat flux under different conditions of stationarity over Amazonian forest sites. *Atmospheric Science Letters, Doi: 10.1002/asl2.544.*

Zeri, M.; Sá, L. D. A. 2011.Scale dependence of coherent structures contribution to the daytime buoyancy heat flux over the Pantanal wetland, Brazil. *Atmospheric Science Letters*, 12 (2): 200-206.

Zhang, R.; He, X.; Doolen, G.; Chen, S. 2001. Surface tension effects on two-dimensional two-phase Kelvin-Helmholtz instabilities. *Advances in Water Resources*, 24(3-4): 461-478.